Thermodynamic Consistency of the currently used Beam Mathematical Models and Thermodynamically Consistent New Formulations for Bending of Thermoelastic, and Thermoviscoelastic Beams

By

Dhaval Mysore Krishna

Submitted to the graduate degree program in Mechanical Engineering and the Graduate Faculty of the University of Kansas in partial fulfillment of the requirements for the degree of Doctor of Philosophy

Committee members

Prof. Karan S. Surana, Chairperson

Prof. Peter TenPas

Prof. Robert Sorem

Prof. Ray Taghavi

Prof. Masoud Darabi

Date defended: _____

The Dissertation Committee for Dhaval Mysore Krishna certifies
that this is the approved version of the following dissertation :

Thermodynamic Consistency of the currently used Beam Mathematical Models and Thermodynamically Consistent New Formulations for Bending of Thermoelastic, and Thermoviscoelastic Beams

Prof. Karan S. Surana, Chairperson

Date approved: _____

Abstract

In order to enhance currently used beam mathematical models in $\mathbb{R}^2$ and $\mathbb{R}^3$ to include mechanisms of dissipation and memory, it is necessary to establish if the mathematical models for these theories can be derived using the conservation and the balance laws of continuum mechanics in conjunction with the corresponding kinematic assumptions. This is referred to as thermodynamic consistency of the beam mathematical models. Thermodynamic consistency of the currently used beam models will permit use of entropy inequality to establish constitutive theories in the presence of dissipation and memory mechanism for the currently used beam mathematical models. This is the main motivation for the work presented in this dissertation. The currently used beam mathematical models for homogeneous, isotropic matter and reversible deformation physics are derived based on kinematic assumptions related to the axial and transverse displacement fields. These are then used to derive strain measures followed by constitutive relations. For linear beam theories, strain measures are linear functions of displacement gradients and stresses are linear functions of strain measures. Using these stress and strain measures, energy functional is constructed over the volume of the beam consisting of kinetic energy, strain energy and potential energy of loads. The Euler's equation(s) extracted from the first variation of this energy functional set to zero yield the differential equations describing the evolution of the deforming beam. Alternatively, principle of virtual work can also be used to derive mathematical models for beams. For linear elastic behavior with small deformation and small strain these two approaches yield same mathematical models. The energy methods or the principle of virtual work cannot be used for irreversible process, thus precluding their use in the

presence of dissipation and memory mechanisms.

In this dissertation we examine whether the currently used beam mathematical models for reversible deformation physics and with the corresponding kinematic assumption (i) can be derived using the conservation and balance laws of classical continuum mechanics or (ii) are the conservation and balance laws of non-classical continuum mechanics necessary in their derivation. In order to ensure that the mathematical models for various beam theories result in deformation that is in thermodynamic equilibrium we must establish the consistency of the beam theories with regard to the conservation and the balance laws of continuum mechanics, classical or non-classical in conjunction with their corresponding kinematic assumptions. Currently used Euler-Bernoulli and Timoshenko beam mathematical models that are representative of most beam mathematical models are investigated. This is followed by details of general and higher order thermodynamically consistent beam mathematical models that is free of kinematic assumptions and other approximations and remains valid for slender as well as deep beams. Model problem studies are presented for slender as well as deep beams. The new formulation presented here ensures thermodynamic equilibrium as it is derived using the conservation and the balance laws of continuum mechanics and remains valid for slender as well as non-slender beams.

The new formulation presented for thermoelastic reversible mechanical deformation is extended for thermoviscoelastic beams with dissipation and for thermoviscoelastic beams with dissipation and memory. In each case model problem studies are presented using currently used mathematical models (when possible) and the results are compared with those obtained using the new thermodynamically consistent formulation presented here.

Acknowledgements

First and foremost I would like to thank my advisor Dr. Karan Surana, without whom it would have been impossible to get my PhD. When I was lost during the beginning of my PhD, he was the one who took me in as his student and helped me fulfill my dream of getting a PhD. The knowledge that I gained by taking his courses and having discussions are invaluable, and this gave me a new and improved perspective about mathematical modeling of the physical world. His financial support for conference travels and summer 209 is very much appreciated.

I would also like to thank Dr. Peter W. TenPas, Dr. Robert Sorem, Dr. Ray Taghavi, and Dr. Masoud Darabi for serving on my committee, and also for the valuable lessons I gained by taking their courses and/or through discussions.

Help from students of the Computational Mechanics Lab, both past and present, is very much appreciated, especially my friend Stephen Long.

The encouragement and support from my friends and well wishers since the beginning of this endeavor is appreciated, especially by Dr. M. N. Chandrashekar, Amool Raina and Vivek Ram.

I am thankful to the Dept. of Mechanical Engineering of the University of Kansas for providing me with financial support as a GTA and instructor during my time here as a PhD student.

I appreciate the love and support provided by Yvonne, my finance (my wife in three weeks) during the past two and a half years of my PhD. I appreciate her patience and

understanding while getting my degree. She also provided me with stability in my life which I didn't even know I lacked until I met her.

Last but not the least, my higher education would have been impossible without the support from my parents, especially my father for the hardships and sacrifices he made to get me to this level. I dedicate this dissertation to my father.

Contents

List of Figures

Chapter 1

Introduction

1.1 Introduction and Literature Review

Derivation of Euler-Bernoulli beam theory dates back to 1750 first presented by L. Euler and D. Bernoulli. Historical development and the details of the progression of this beam theory can be found in references [1–6]. In the Euler-Bernoulli beam theory, at a cross-section of the beam linear axial strain is established based on geometric consideration as a function of curvature, moment of the corresponding axial stress is integrated over the beam cross-section to obtain an expression for the bending moment in terms of curvature, modulus of elasticity and bending moment of inertia of the beam cross-section. It is shown in the later sections of this dissertation that this relationship is in fact constitutive theory. The mathematical models (or the equilibrium equations) for the deforming beam based on the kinematic assumptions used in Euler-Bernoulli and Timoshenko are derived:

(i) First by constructing a functional (I) consisting of kinetic energy, strain energy due to bending and potential energy of the loads.

(ii) The first variation of this functional is set to zero ($\delta I = 0$). This is a necessary condition for an extremum of the functional I in (i).

(iii) The Euler's equations derived from $\delta I = 0$ (using either fundamental lemma of the calculus

of variation or the fourth basic lemma [7–10]) constitute the equations of dynamic equilibrium of the deforming beam. In addition to Euler-Bernoulli beam and Timoshenko beam mathematical models other beam models can be derived using this approach.

The published works on beam theories such as [11–22] either follow the energy approach or the principle of virtual work or in some cases a slight variation of this approach described in a later section. The fundamental differences between the various current beam mathematical models arise due to:

(a) The kinematic assumption for axial displacement of a deforming cross section of the beam. This leads to a specific axial strain and axial stress field and a specific expression for the moment obtained by integrating moment of the axial stress over the beam cross-section.

(b) The second difference arises due to inclusion of specific chosen physics related to strain energy in the functional I.

Consideration in (a) and (b) leads to different beam theories. All currently used beam theories are essentially derived using (a) and (b) in conjunction with energy functional or principle of virtual work. Some writing on beam theories consider a slightly different approach [23] in which moment of forces is used to construct additional equilibrium equations.

Remarks

(1) This approach described above for deriving mathematical model of beam deformation is only valid for conservative systems in which the mechanical deformation is reversible. Thus, the beam mathematical models requiring considerations of dissipation and rheology cannot be derived using this approach.

(2) Dissipation and rheology mechanisms if needed in currently used beam mathematical models can only be addressed using phenomenological approaches employing springs and dash pots in $\mathbb{R}^1$. Short comings of this approach in extending it to $\mathbb{R}^2$ and $\mathbb{R}^3$ are well known [24].

(3) The consideration of kinetic energy and potential energy of loads in the energy functional I is rather straight forward. However, the strain energy consideration requires rate of work conjugate pairs which we only know for sure if we derive the energy equation (first law of thermodynamics). Since stress is a consequence of strain through material response, moment in the beam theory is the result of curvature through material response; thus, it is perhaps fitting to say the stress and strain rate, moment and curvature rate are rate of work conjugate pairs. This in fact is the basis for strain energy considerations in the functional I. It is rather obvious that this approach relies heavily on clear and precise understanding of physics and may work well in simple deformation physics, but in more complex situations this approach may not be as straight forward and may even lead to erroneous choices.

1.2 Conservation and the balance laws: classical and non-classical continuum mechanics

Since the derivation of the beam mathematical models presented in this dissertation always begins with the use of conservation and balance laws (necessary for thermodynamic consistency), we present these in the following. *In the following and the remainder of the dissertation we consider isotropic, homogeneous and continuous matter with small deformation and small strain*. Explicit forms of the conservation and the balance laws in x_1x_2 space are presented as these are needed in the derivations of the mathematical models for beam bending in $\mathbb{R}^2$.

1.2.1 Classical Continuum Mechanics

In classical continuum mechanics a material point has only three translational degrees of freedom. Each material point has mass hence linear momentum but no dimension, hence no angular momentum due to rotation rates in the solid matter. For solid continua it is beneficial to consider conservation and balance laws in Lagrangian description. Conservation of mass relates density in the reference configuration and the density in the current configurations through determinant of the

Jacobian of deformation or the deformation gradient tensor. Balance of linear momenta is a statement of the balance of rate of change of linear momenta with body forces and internal stress field (through Cauchy principle). In classical continuum mechanics this yields what are known as equilibrium equations, statements of force balance in fixed x-frame. Balance of angular momenta in classical continuum mechanics simply results in the symmetry of the Cauchy stress tensor. Thus, it adds no additional equations in the final mathematical model. First law of thermodynamics yields energy equation and the second law of thermodynamics (entropy inequality) expressed in Helmholtz free energy density is primarily instrumental in the derivation of the constitutive theories. Conjugate pairs in the first and the second laws of thermodynamics establish rate of work conjugate pairs.

In deforming solid matter with small deformation and small strain, the displacements $\boldsymbol{u}$ and the gradients of displacements (${}^{d}\boldsymbol{J}$) are complete measures of the deformation physics at a material point. Decomposition of ${}^{d}\boldsymbol{J}$ into symmetric (${}^{d}_{s}\boldsymbol{J}$) and skew symmetric (${}^{d}_{a}\boldsymbol{J}$) tensors

$$[\,{}^{d}J] = [\,{}^{d}_{s}J] + [\,{}^{d}_{a}J]\;;\; [\,{}^{d}_{s}J] = \frac{1}{2}\left([\,{}^{d}J] + [\,{}^{d}J]^{T}\right) = [\varepsilon]\;;\; [\,{}^{d}_{a}J] = \frac{1}{2}\left([\,{}^{d}J] - [\,{}^{d}J]^{T}\right) \tag{1.1}$$

shows that the symmetric part consists of linear strain tensor at a material point whereas the skew symmetric part contains rotations (called internal rotations as these are due to ${}^{d}\boldsymbol{J}$) defined about the axes of a triad located at each material point with its axes parallel to x-frame. Alternatively, the rotations can also be obtained using

$$\boldsymbol{\nabla} \times \boldsymbol{u} = \boldsymbol{e}_i \times \boldsymbol{e}_j \frac{\partial u_j}{\partial x_i} = \epsilon_{ijk}\boldsymbol{e}_k \frac{\partial u_j}{\partial x_i} \tag{1.2}$$

In (1.2) the internal rotations are twice (total) those of in (1.1) and are positive when counterclockwise.

Remarks

(a) The internal rotations (defined by (1.1) or (1.2)) are completely neglected in classical con-

tinuum mechanics, i.e. the classical continuum theory is based on $\boldsymbol{u}$ and $\boldsymbol{\varepsilon}$.

(b) In this theory rotations and moments are only created by equal and opposite displacements and forces separated by a distance. In other words, rotations and moments are not independent of displacements and forces.

(c) When deriving mathematical description for a desired physics (as beam theories considered here), use of balance of linear momenta will result in dynamic force balance equations. However, balance of angular momenta i.e. moment of forces cannot be used to obtain any additional equations as this balance law only results in symmetry of Cauchy stress tensor.

(d) From (a)–(c) it is clear that if the kinematic assumptions in beam theories requires use of rotations in (1.1) or in (1.2), then classical continuum mechanics and its conservation and the balance laws cannot be used for deriving the mathematical models as the rotations used in the kinematic assumptions cannot be considered within the classical continuum mechanics framework. Insistence on using classical continuum mechanics in such cases would result in inconsistent mathematical descriptions of the physics.

In the following we simply present the final equations resulting from the conservation and balance laws of classical continuum mechanics: conservation of mass (CM), balance of linear momenta (BLM), balance of angular momenta (BAM), first law of thermodynamics (FLT), and second law of thermodynamics (SLT) (entropy inequality) including linear constitutive theories in $\mathbb{R}^3$ [24] for thermoelastic solids, thermoviscoelastic solids without memory, and thermoviscoelastic solids with memory, in Lagrangian description. The following conservation and balance laws are presented for irreversible deformation physics. When the mechanical deformation is reversible, these are simplified.

$$\rho_0 = |J|\rho \ ; \quad |J| \simeq 1 \text{ for small deformation, small strain.} \quad \text{(CM)} \tag{1.3}$$

$$\rho_0 \frac{\partial^2 \boldsymbol{u}}{\partial t^2} - \rho_0 \boldsymbol{F}^b - \boldsymbol{\nabla} \cdot \boldsymbol{\sigma}^T = 0 \quad \text{(BLM)} \tag{1.4}$$

$$\boldsymbol{\sigma} = \boldsymbol{\sigma}^T \quad \text{(BAM)} \tag{1.5}$$

$$\rho_0 \frac{De}{Dt} + \boldsymbol{\nabla} \cdot \boldsymbol{q} - \text{tr}\left([\sigma]^T[\dot{\varepsilon}]^T\right) = 0 \quad \text{(FLT)} \tag{1.6}$$

$$\rho_0 \left(\frac{D\Phi}{Dt} + \eta \frac{D\theta}{Dt}\right) + \frac{q_i g_i}{\theta} - \text{tr}\left([\sigma]^T[\dot{\varepsilon}]^T\right) \leq 0 \quad \text{(SLT)} \tag{1.7}$$

in which CM, BLM, BAM, FLT and SLT refer to conservation of mass, balance of linear momenta, balance of angular momenta, first law of thermodynamics and second law of thermodynamics, respectively. $\mathbf{J}$ is Jacobian of deformation, $\boldsymbol{F}^b$ are body forces per unit mass, $\boldsymbol{q}$ is heat flux, θ is temperature, Φ is Helmholtz free energy density, η is entropy density, $\boldsymbol{g}$ is temperature gradient, and $e = e(\theta)$ is specific internal energy. The constitutive theories for reversible and irreversible mechanical deformations are naturally different. These are considered in the following.

1.2.1.1 Thermoelastic Solids

In such materials mechanical deformation is reversible. Following [24, 25] the constitutive variables and their argument tensors are given in the following. This choice is supported by the rate of work conjugate pairs in the second law of thermodynamics (entropy inequality (1.7)).

$$\boldsymbol{\sigma} = \boldsymbol{\sigma}(\boldsymbol{\varepsilon}, \theta) \tag{1.8}$$

$$\boldsymbol{q} = \boldsymbol{q}(\boldsymbol{g}, \theta) \tag{1.9}$$

Simple linear constitutive theories for $\boldsymbol{\sigma}$ and $\boldsymbol{q}$ for thermoelastic solids [24, 25] are

$$\boldsymbol{\sigma} = 2\mu(\boldsymbol{\varepsilon}) + \lambda(\text{tr}(\boldsymbol{\varepsilon}))\boldsymbol{I} \tag{1.10}$$

$$\boldsymbol{q} = -k\boldsymbol{g} \ ; \ \boldsymbol{q} = -k\boldsymbol{\nabla}\theta \tag{1.11}$$

in which k is thermal conductivity, μ and λ are Lame's constants. Expanded forms of conservation and balance laws (equations (1.3)–(1.7)) and linear constitutive theories ((1.10), (1.11)) in $\mathbb{R}^2$ are

given below:

$$\rho_0 \frac{\partial^2 u_1}{\partial t^2} - \rho_0 F_1^b - \frac{\partial}{\partial x_1}(\sigma_{11}) - \frac{\partial}{\partial x_2}(\sigma_{21}) = 0 \tag{1.12}$$

$$\rho_0 \frac{\partial^2 u_2}{\partial t^2} - \rho_0 F_2^b - \frac{\partial}{\partial x_1}(\sigma_{12}) - \frac{\partial}{\partial x_2}(\sigma_{22}) = 0 \tag{1.13}$$

$$\sigma_{21} = \sigma_{12} \tag{1.14}$$

$$\rho_0 \frac{De}{Dt} + \frac{\partial q_i}{\partial x_i} - \sigma_{ji}\dot{\varepsilon}_{ij} = 0 \ ; \ i,j = 1,2 \tag{1.15}$$

$$\rho_0 \left(\frac{D\Phi}{Dt} + \eta \frac{D\theta}{Dt} \right) + \frac{q_i g_i}{\theta} - \sigma_{ji}\dot{\varepsilon}_{ij} \leq 0 \ ; \ i,j = 1,2 \tag{1.16}$$

$$\begin{aligned} \sigma_{ij} &= 2\mu\varepsilon_{ij} + \lambda\varepsilon_{kk}\delta_{ij} \ ; \ i,j = 1,2 \\ \varepsilon_{ij} &= \frac{1}{2}(u_{i,j} + u_{j,i}) \ ; \ i,j = 1,2 \\ q_i &= -kg_i \ ; \ g_i = \frac{\partial \theta}{\partial x_i} \ ; \ i,j = 1,2 \end{aligned} \tag{1.17}$$

In which ρ_0 is the mass density in the reference configuration. u_1, u_2 are displacements in x_1, x_2 directions. F_1^b, F_2^b are body force per unit mass in x_1 and x_2 directions. σ_{ij}, ε_{ij} are Cauchy stress and linear strain tensors, q_i is heat tensor, and g_i is temperature gradient tensor.

1.2.1.2 Thermoviscoelastic Solids without Memory

In such solids some part of the mechanical work is reversible (elastic behavior) whereas some is irreversible (dissipation). The dissipation mechanism produces entropy that result in heat, hence temperature changes occur. Surana [24] and Surana et al. [26,27] have shown that for such physics ordered rate constitutive theories are possible for the constitutive variable Cauchy stress tensor. With principle of equipresence such constitutive theories show dependence of stress tensor and heat tensor on strain tensor, strain rate tensors upto orders n, temperature gradient $\boldsymbol{g}$ and temperature θ.

It has been shown in references [24, 26, 27], that in the derivation of the constitutive theory for the stress tensor $\boldsymbol{\sigma}$ its decomposition into equilibrium stress tensor ${}_e\boldsymbol{\sigma}$ and deviatoric stress tensor

${}_d\boldsymbol{\sigma}$ is needed

$$\boldsymbol{\sigma} = {}_e\boldsymbol{\sigma} + {}_d\boldsymbol{\sigma} \tag{1.18}$$

In which the constitutive theory for ${}_e\boldsymbol{\sigma}$ for incompressible solid matter can be derived [24, 26, 27]

$${}_e\boldsymbol{\sigma} = p(\theta)\boldsymbol{I} \tag{1.19}$$

$p(\theta)$ is mechanical pressure. For isothermal process with small deformation, small strain $p(\theta)$ is simply mean normal stress i.e. $p(\theta) = \sigma_{kk}$. The argument tensor of ${}_d\boldsymbol{\sigma}$ as well as $\boldsymbol{q}$ (based on principle of equipresence) are given by

$$\begin{aligned} {}_d\boldsymbol{\sigma} &= {}_d\boldsymbol{\sigma}(\boldsymbol{\varepsilon}, \boldsymbol{\varepsilon}_{[i]}\,;\, i = 1, 2, \ldots, n, \boldsymbol{g}, \theta) \\ \boldsymbol{q} &= \boldsymbol{q}(\boldsymbol{\varepsilon}, \boldsymbol{\varepsilon}_{[i]}\,;\, i = 1, 2, \ldots, n, \boldsymbol{g}, \theta) \end{aligned} \tag{1.20}$$

If we assume that ${}_d\boldsymbol{\sigma}$ only depends upon $\boldsymbol{\varepsilon}$, $\dot{\boldsymbol{\varepsilon}}$ (i.e. $\varepsilon_{[0]}, \varepsilon_{[1]}$) and θ and $\boldsymbol{q}$ on $\boldsymbol{g}$ and θ (based on the conjugate pairs in the SLT), then for $n = 1$ we have ordered rate constitutive theory for ${}_d\boldsymbol{\sigma}$ of order one.

$$\begin{aligned} {}_d\boldsymbol{\sigma} &= {}_d\boldsymbol{\sigma}(\boldsymbol{\varepsilon}, \dot{\boldsymbol{\varepsilon}}, \theta) \\ \boldsymbol{q} &= \boldsymbol{q}(\boldsymbol{g}, \theta) \end{aligned} \tag{1.21}$$

Simple linear constitutive theories for ${}_d\boldsymbol{\sigma}$ and $\boldsymbol{q}$ for thermoviscoelastic solids without memory [24, 26, 27] are

$${}_d\boldsymbol{\sigma} = 2\mu\boldsymbol{\varepsilon} + \lambda \mathrm{tr}(\boldsymbol{\varepsilon}) + 2\underset{\sim}{\mu}\dot{\boldsymbol{\varepsilon}} + \underset{\sim}{\lambda}\mathrm{tr}(\dot{\boldsymbol{\varepsilon}})\boldsymbol{I} \tag{1.22}$$

$${}_e\boldsymbol{\sigma} = p(\theta)\boldsymbol{I} \quad \text{or} \quad {}_e\boldsymbol{\sigma} = \mathrm{tr}(\boldsymbol{\sigma})\boldsymbol{I} \tag{1.23}$$

$$\boldsymbol{q} = -k\boldsymbol{g} \;:\; \boldsymbol{q} = -k\boldsymbol{\nabla}\theta \tag{1.24}$$

in which $\underset{\sim}{\mu}$ and $\underset{\sim}{\lambda}$ are additional material coefficients due to presence of dissipation when $n = 1$.

Expanded forms of conservation and balance laws (equations (1.3)–(1.7)) and linear constitutive equations (1.22) – (1.24) in $\mathbb{R}^2$ are given in the following.

$$\rho_0 \frac{\partial^2 u_1}{\partial t^2} - \rho_0 F_1^b - \frac{\partial}{\partial x_1}({}_e\sigma_{11}) - \frac{\partial}{\partial x_1}({}_d\sigma_{11}) - \frac{\partial}{\partial x_2}({}_d\sigma_{21}) = 0 \tag{1.25}$$

$$\rho_0 \frac{\partial^2 u_2}{\partial t^2} - \rho_0 F_2^b - \frac{\partial}{\partial x_1}({}_d\sigma_{12}) - \frac{\partial}{\partial x_2}({}_e\sigma_{22}) - \frac{\partial}{\partial x_2}({}_d\sigma_{22}) = 0 \tag{1.26}$$

$${}_d\sigma_{21} = {}_d\sigma_{12} \tag{1.27}$$

$$\rho_0 \frac{De}{Dt} + \frac{\partial q_i}{\partial x_i} - {}_d\sigma_{ji}\dot{\varepsilon}_{ij} = 0 \ ; \ i,j = 1,2 \tag{1.28}$$

$$\rho_0 \left(\frac{D\Phi}{Dt} + \eta \frac{D\theta}{Dt} \right) + \frac{q_i g_i}{\theta} - {}_d\sigma_{ji}\dot{\varepsilon}_{ij} \leq 0 \ ; \ i,j = 1,2 \tag{1.29}$$

$$\begin{aligned}
&{}_d\sigma_{ij} = 2\mu\varepsilon_{ij} + \lambda\varepsilon_{kk}\delta_{ij} + 2\underset{\sim}{\mu}\dot{\varepsilon}_{ij} + \underset{\sim}{\lambda}\dot{\varepsilon}_{kk}\delta_{ij} \ ; \ i,j = 1,2 \\
&\varepsilon_{ij} = \frac{1}{2}(u_{i,j} + u_{j,i}) \ ; \ \dot{\varepsilon}_{ij} = \frac{1}{2}\left(\frac{\partial u_{i,j}}{\partial t} + \frac{\partial u_{j,i}}{\partial t} \right) \ ; \ i,j = 1,2 \\
&q_i = -k g_i \ : \ g_i = \frac{\partial \theta}{\partial x_i} \ ; \ i,j = 1,2 \\
&\text{also } {}_e\sigma_{ij} = p(\theta)\delta_{ij} \ ; \ i,j = 1,2 \quad \text{or } {}_e\sigma_{ij} = \text{tr}([\sigma])\delta_{ij}
\end{aligned} \tag{1.30}$$

In which ρ_0 is the mass density in the reference configuration. u_1, u_2 are displacements in x_1, x_2 directions. F_1^b, F_2^b are body force per unit mass in x_1 and x_2 directions. ${}_d\sigma_{ij}$, ε_{ij}, $\dot{\varepsilon}_{ij}$ are deviatoric part of the Cauchy stress tensor, linear strain tensor, and linear strain rate tensor, respectively, q_i is heat tensor, and g_i is temperature gradient tensor.

1.2.1.3 Thermoviscoelastic Solids with Memory

Such solids have mechanisms of elasticity, dissipation and memory. Dissipation mechanism is similar to the thermoviscoelastic solids without memory. Memory mechanism is due to long chain molecules of the polymer [28]. It is well known that the constitutive theories for stresses for such solids must be differential equations in stresses in time, only then the memory mechanism,

rheology and relaxation phenomena are possible. Surana [24] and Surana et al. [29] have shown that for such solids ordered rate constitutive theories of orders (n, m) are possible, where n is the order of the highest strain rates and m is the order of the highest order of the stress rate. The dependent variables and their argument tensors [24, 29] can be defined as (using principle of equipresence)

$$\boldsymbol{\sigma}^{[m]} = \boldsymbol{\sigma}^{[m]}(\boldsymbol{\varepsilon}, \boldsymbol{\varepsilon}_{[i]}\,;\, i = 1, 2, \ldots, n,\ \boldsymbol{\sigma}, \boldsymbol{\sigma}^{[j]}\,;\, j = 1, 2, \ldots, m-1, \boldsymbol{g}, \theta) \tag{1.31}$$

$$\boldsymbol{q} = \boldsymbol{q}(\boldsymbol{\varepsilon}, \boldsymbol{\varepsilon}_{[i]}\,;\, i = 1, 2, \ldots, n,\ \boldsymbol{\sigma}^{[j]}\,;\, j = 1, 2, \ldots, m-1, \boldsymbol{g}, \theta) \tag{1.32}$$

Derivation of the constitutive theory for the stress tensor requires its decomposition into equilibrium stress tensor ${}_e\boldsymbol{\sigma}$ and the deviatoric stress tensor ${}_d\boldsymbol{\sigma}$.

$$\boldsymbol{\sigma} = {}_e\boldsymbol{\sigma} + {}_d\boldsymbol{\sigma} \tag{1.33}$$

For incompressible matter [24] we have

$${}_e\boldsymbol{\sigma} = p(\theta)\boldsymbol{I} \tag{1.34}$$

Using (1.33), (1.31) is modified

$${}_d\boldsymbol{\sigma}^{[m]} = {}_d\boldsymbol{\sigma}^{[m]}(\boldsymbol{\varepsilon}, \boldsymbol{\varepsilon}_{[i]}\,;\, i = 1, 2, \ldots, n,\ {}_d\boldsymbol{\sigma}, {}_d\boldsymbol{\sigma}^{[j]}\,;\, j = 1, 2, \ldots, m-1, \boldsymbol{g}, \theta) \tag{1.35}$$

If we assume $m = 1$ and $n = 1$ and $\boldsymbol{\varepsilon}_{[1]} = \dot{\boldsymbol{\varepsilon}}$ and further assume that ${}_d\boldsymbol{\sigma}^{[1]}$ does not depend upon $\boldsymbol{g}$ and that the argument tensors of $\boldsymbol{q}$ are only $\boldsymbol{g}$ and θ, then we have

$${}_d\boldsymbol{\sigma}^{[1]} = {}_d\boldsymbol{\sigma}^{[1]}(\boldsymbol{\varepsilon}, \dot{\boldsymbol{\varepsilon}},\ {}_d\boldsymbol{\sigma}, \theta) \tag{1.36}$$

$$\boldsymbol{q} = \boldsymbol{q}(\boldsymbol{g}, \theta) \tag{1.37}$$

Following references [24, 29], linear constitutive theories for ${}_d\boldsymbol{\sigma}$ and $\boldsymbol{q}$ can be derived.

$$ {}_d\boldsymbol{\sigma} + \lambda({}_d\boldsymbol{\sigma}^{[1]}) = 2\mu\boldsymbol{\varepsilon} + \lambda(\mathrm{tr}(\boldsymbol{\varepsilon}))\boldsymbol{I} + 2\underset{\sim}{\mu}\dot{\boldsymbol{\varepsilon}} + \underset{\sim}{\lambda}\mathrm{tr}(\dot{\boldsymbol{\varepsilon}})\boldsymbol{I} \tag{1.38} $$

$$ {}_e\boldsymbol{\sigma} = p(\theta)\boldsymbol{I} \tag{1.39} $$

$$ \boldsymbol{q} = -k\boldsymbol{g} \ : \ \boldsymbol{q} = -k\boldsymbol{\nabla}\theta \tag{1.40} $$

in which $\underset{\sim}{\mu}$ and $\underset{\sim}{\lambda}$ are material constants. Expanded forms of conservation and balance laws and linear constitutive theories of equations in $\mathbb{R}^2$ are given below:

$$ \rho_0 \frac{\partial^2 u_1}{\partial t^2} - \rho_0 F_1^b - \frac{\partial}{\partial x_1}({}_e\sigma_{11}) - \frac{\partial}{\partial x_1}({}_d\sigma_{11}) - \frac{\partial}{\partial x_2}({}_d\sigma_{21}) = 0 \tag{1.41} $$

$$ \rho_0 \frac{\partial^2 u_2}{\partial t^2} - \rho_0 F_2^b - \frac{\partial}{\partial x_1}({}_d\sigma_{12}) - \frac{\partial}{\partial x_2}({}_e\sigma_{22}) - \frac{\partial}{\partial x_2}({}_d\sigma_{22}) = 0 \tag{1.42} $$

$$ {}_d\sigma_{21} = {}_d\sigma_{12} \tag{1.43} $$

$$ \rho_0 \frac{De}{Dt} + \frac{\partial q_i}{\partial x_i} - {}_d\sigma_{ji}\dot{\varepsilon}_{ij} = 0 \ ; \ i,j = 1,2 \tag{1.44} $$

$$ \rho_0 \left(\frac{D\Phi}{Dt} + \eta \frac{D\theta}{Dt} \right) + \frac{q_i g_i}{\theta} - {}_d\sigma_{ji}\dot{\varepsilon}_{ij} \leq 0 \ ; \ i,j = 1,2 \tag{1.45} $$

$$ {}_e\sigma_{11} = {}_e\sigma_{22} = {}_d\sigma_{11} + {}_d\sigma_{22} $$

$$ \begin{Bmatrix} {}_d\sigma_{11} \\ {}_d\sigma_{22} \\ {}_d\sigma_{12} \end{Bmatrix} + \lambda \begin{Bmatrix} \dfrac{\partial({}_d\sigma_{11})}{\partial t} \\ \dfrac{\partial({}_d\sigma_{22})}{\partial t} \\ \dfrac{\partial({}_d\sigma_{12})}{\partial t} \end{Bmatrix} = [D] \begin{Bmatrix} \varepsilon_{11} \\ \varepsilon_{22} \\ \varepsilon_{12} \end{Bmatrix} + [\underset{\sim}{D}] \begin{Bmatrix} \dot{\varepsilon}_{11} \\ \dot{\varepsilon}_{22} \\ \dot{\varepsilon}_{12} \end{Bmatrix} \tag{1.46} $$

$$ \varepsilon_{ij} = \frac{1}{2}(u_{i,j} + u_{j,i}) \ ; \ \dot{\varepsilon}_{ij} = \frac{1}{2}\left(\frac{\partial u_{i,j}}{\partial t} + \frac{\partial u_{j,i}}{\partial t} \right) \ ; \ i,j = 1,2 $$

$$
\begin{aligned}
[D] = [D(\mu,\lambda)] = [D(E,\nu)] &= \begin{bmatrix} 2\mu+\lambda & \lambda & 0 \\ \lambda & 2\mu+\lambda & 0 \\ 0 & 0 & 2\mu \end{bmatrix} \\
[\underset{\sim}{D}] = [\underset{\sim}{D}(\underset{\sim}{\mu},\underset{\sim}{\lambda})] &= \begin{bmatrix} 2\underset{\sim}{\mu}+\underset{\sim}{\lambda} & \underset{\sim}{\lambda} & 0 \\ \underset{\sim}{\lambda} & 2\underset{\sim}{\mu}+\underset{\sim}{\lambda} & 0 \\ 0 & 0 & 2\underset{\sim}{\mu} \end{bmatrix} \\
q_i = -kg_i \; ; \; g_i &= \frac{\partial\theta}{\partial x_i} \; ; \; i,j = 1,2
\end{aligned}
\tag{1.47}
$$

In which ρ_0 is the mass density in the reference configuration. u_1, u_2 are displacements in x_1, x_2 directions. F_1^b, F_2^b are body force per unit mass in x_1 and x_2 directions. ${}_d\sigma_{ij}$, ε_{ij}, $\dot{\varepsilon}_{ij}$ are deviatoric part of the Cauchy stress, linear strain tensors, and linear strain rate tensor, respectively, q_i is heat vector, and g_i is temperature gradient.

1.2.2 Non-classical continuum mechanics

Non-classical continuum mechanics permits consideration of physics in the mathematical description of the deforming matter that is not possible to consider within the framework of classical continuum mechanics. We discuss some details that are of interest in context to the present work on beam theories.

If $\boldsymbol{u}$ and ${}^d\boldsymbol{J}$ are measures of complete physics of deformation at a material point, then a thermodynamic framework to address this physics must consider $\boldsymbol{u}$ and ${}^d\boldsymbol{J}$ in their entirety in the derivation of the conservation and the balance laws. Decomposition (1.1) points that the classical continuum mechanics conservation and balance laws that already are based on $\boldsymbol{\varepsilon}$ must be modified to incorporate ${}^d_a\boldsymbol{J}$ or $\boldsymbol{\nabla}\times\boldsymbol{u}$ that contains internal rotations if complete ${}^d\boldsymbol{J}$ is to be considered in the conservation and the balance laws. In a deforming solid matter in general ${}^d\boldsymbol{J}$ varies between a material point and its neighbors i.e. the internal rotations vary between neighboring material points. When these are resisted by the deforming matter, conjugate moments are created. The rotations and the conjugate moments result in additional energy storage. This physics is ignored in classical

continuum mechanics. The continuum mechanics theories that incorporate internal rotations due to ${}^{\mathcal{D}}_{\alpha}\boldsymbol{J}$ or $\boldsymbol{\nabla} \times \boldsymbol{u}$ are *non-classical continuum theories*, more specifically *non-classical continuum theories incorporating internal rotations*.

We note that internal rotations exist in all deforming solid matter due to ${}^{\mathcal{D}}_{\alpha}\boldsymbol{J}$ or $\boldsymbol{\nabla} \times \boldsymbol{u}$. In addition to these we can also consider a non-classical continuum theory in which additional unknown rotations are assumed to exist about the axes of the same triad about which the internal rotations exist. These theories are called non-classical continuum theories with internal rotations and Cosserat rotations. Thus, now we can possibly have a non-classical continuum theory in which either internal or both internal and Cosserat rotations are considered. Internal rotations are defined by $\boldsymbol{\nabla} \times \boldsymbol{u}$, hence no additional unknown degrees of freedom at a material point are needed but Cosserat rotations are additional three degrees of freedom at a material point. Consideration of Cosserat rotations in addition to internal rotations in the non-classical continuum theory presents possibility of enhancing the physics in the mathematical model by possibility of considering more complex physics than due to internal rotations alone. Surana et al. [30–40] have presented details of non-classical continuum theories including constitutive theories for solid and fluent continua based on internal rotations. The resulting conservation and balance laws from these theories may have some resemblance to couple stress theories. The motivation and the consideration of physics by Surana et al. [30–40] is completely different than the couple stress theories. More recently Surana et al. [41–45] have also presented non-classical continuum theories and associated constitutive theories that consider internal rotations as well as Cosserat rotations. Many other published works [22, 46–84] on couple stress theories, Cosserat theories and related concepts are also relevant in context of the works in reference [30–45]. Discussion of these works can be found in references [30–45] and are not repeated here, but the publications are listed in the list of references in this paper for the interested readers.

Remarks

(1) Significant strength of the non-classical theories based on internal and/or Cosserat rotations

is that they provide more complete and enhanced thermodynamic framework compared to classical continuum theories.

(2) In these theories internal and Cosserat rotations are additional degrees of freedom at a material point. The internal rotations are not unknown degrees of freedom at a material point as they are defined by $\boldsymbol{\nabla} \times \boldsymbol{u}$ but Cosserat rotations are three additional degrees of freedom.

(3) These theories require rederivation of conservation and balance laws [30–34]. This results in modification of existing balance laws and require an additional balance law due to the new physics (compared to classical continuum mechanics) associated with the rotations.

(4) In these theories Cauchy stress tensor is not symmetric and there is existence of Cauchy moment tensor [30–34]. Balance of angular momenta results in additional three equations (in $\mathbb{R}^3$) that describe a relationship between the antisymmetric components of Cauchy stress tensor and the gradients of Cauchy moment tensor.

(5) Due to consideration of rotation and their rates and conjugate moment tensor, additional balance law *"balance of moment of moments"* is required in non-classical continuum mechanics theories. Yang et al. [85] and Surana et al. [86, 87] have shown that this balance law is essential and it results in symmetry of Cauchy moment tensor.

(6) First and the second laws of thermodynamics are modified to incorporate new physics related to additional rate of work due to rotation and rotation rates present in the non-classical continuum mechanics.

(7) Entropy inequality establishes constitutive variables, rate of work conjugate pairs, hence provides some insight into the argument tensors of the constitutive variables as well as provides conditions for deriving the constitutive theories.

1.3 Non-classical continuum mechanics with internal rotations due to $\overset{d}{\boldsymbol{J}}$

The conservation and the balance laws: conservation of mass, balance of linear momenta, balance of angular momenta, balance of moment of moments [85–87], first and second laws of thermodynamics and the constitutive theories are summarized in the following [30–40] in Lagrangian description.

$$\rho_{_0} = |J|\rho \; ; \; |J| \simeq 1 \text{ for small deformation, small strain.} \quad \text{(CM)} \tag{1.48}$$

$$\rho_{_0} \frac{\partial^2 \boldsymbol{u}}{\partial t^2} - \rho_{_0} \boldsymbol{F}^b - \boldsymbol{\nabla \cdot \sigma}^T = 0 \quad \text{(BLM)} \tag{1.49}$$

$$\boldsymbol{\sigma} = {}_s\boldsymbol{\sigma} + {}_a\boldsymbol{\sigma} \tag{1.50}$$

$$m_{mk,m} = \epsilon_{ijk}\sigma_{ij} = \epsilon_{ijk}({}_a\sigma_{ij}) \quad \text{(BAM)} \tag{1.51}$$

$$\epsilon_{ijk} m_{ij} = 0 \quad \text{(BMM)} \tag{1.52}$$

$$\rho_{_0} \frac{De}{Dt} + \boldsymbol{\nabla \cdot q} - \text{tr}\left([{}_s\sigma]^T[\dot{\varepsilon}]^T\right) - \text{tr}\left([m]^T[{}^{\dot{\Theta}}_{s}J]^T\right) = 0 \quad \text{(FLT)} \tag{1.53}$$

$$\rho_{_0}\left(\frac{D\Phi}{Dt} + \eta\frac{D\theta}{Dt}\right) + \frac{q_i g_i}{\theta} - \text{tr}\left([{}_s\sigma]^T[\dot{\varepsilon}]^T\right) - \text{tr}\left([m]^T[{}^{\dot{\Theta}}_{s}J]^T\right)) \leq 0 \quad \text{(SLT)} \tag{1.54}$$

The internal rotations due to displacement gradient tensor are given by

$$\boldsymbol{\nabla} \times \boldsymbol{u} = \boldsymbol{e}_1({}_i\Theta_{x_1}) + \boldsymbol{e}_2({}_i\Theta_{x_2}) + \boldsymbol{e}_3({}_i\Theta_{x_3}) \tag{1.55}$$

Alternatively, internal rotations ${}_i\Theta_{x_1}$, ${}_i\Theta_{x_2}$, ${}_i\Theta_{x_3}$ can be obtained using $[\,{}^{d}_{}J]$, displacement gradient tensor

$$\left[\frac{\partial\{u\}}{\partial\{x\}}\right] = [\,{}^{d}_{}J] = [\,{}^{d}_{s}J] + [\,{}^{d}_{d}J] = [\varepsilon] + [\,{}^{i}_{d}r] \tag{1.56}$$

with definitions of ${}_i\Theta_{x_1}$, ${}_i\Theta_{x_2}$ and ${}_i\Theta_{x_3}$ in (1.56), we have

$$\begin{aligned} &\overset{i}{d}r_{12} = {}_i\Theta_{x_3} \quad ; \quad \overset{i}{d}r_{13} = -{}_i\Theta_{x_2} \quad ; \quad \overset{i}{d}r_{23} = {}_i\Theta_{x_1} \\ \text{and} \quad &\overset{i}{d}r_{21} = -\overset{i}{d}r_{12} \quad ; \quad \overset{i}{d}r_{31} = -\overset{i}{d}r_{13} \quad ; \quad \overset{i}{d}r_{32} = -\overset{i}{d}r_{23} \end{aligned} \tag{1.57}$$

all others are zero. The rotations ${}_i\Theta_{x_1}$, ${}_i\Theta_{x_2}$ and ${}_i\Theta_{x_3}$ are about the axes (parallel to fixed x-frame) of the triad located at a material point.

If $\{{}_i\Theta\}^T = [{}_i\Theta_{x_1}, {}_i\Theta_{x_2}, {}_i\Theta_{x_3}]$, then the gradients of $\{{}_i\Theta\}$ are given by

$$[{}^{i\Theta}J] = \left[\frac{\partial\{{}_i\Theta\}}{\partial\{x\}}\right] \; ; \; [{}^{i\Theta}_{s}J] + [{}^{i\Theta}_{a}J] \tag{1.58}$$

$$[{}^{i\Theta}_{s}J] = \frac{1}{2}\left([{}^{i\Theta}J] + [{}^{i\Theta}J]^T\right) \; , \; [{}^{i\Theta}_{a}J] = \frac{1}{2}\left([{}^{i\Theta}J] - [{}^{i\Theta}J]^T\right) \tag{1.59}$$

From the conjugate pairs in the entropy inequality, we can write the following for thermoelastic solids

$$\begin{aligned} {}_s\boldsymbol{\sigma} &= {}_s\boldsymbol{\sigma}(\boldsymbol{\varepsilon}, \theta) \\ \boldsymbol{m} &= \boldsymbol{m}({}^{i\Theta}_{s}\boldsymbol{J}, \theta) \\ \boldsymbol{q} &= \boldsymbol{q}(\boldsymbol{g}, \theta) \end{aligned} \tag{1.60}$$

General constitutive theories based on (1.60) using integrity can be derived [24]. Simple linear constitutive theories for $\boldsymbol{\sigma}$, $\boldsymbol{m}$ and $\boldsymbol{q}$ are given by

$$\begin{aligned} {}_s\boldsymbol{\sigma} &= 2\mu\boldsymbol{\varepsilon} + \lambda(\text{tr}(\boldsymbol{\varepsilon}))\boldsymbol{I} \\ {}_s\boldsymbol{m} &= 2\underset{\sim}{\mu}\,{}^{i\Theta}_{s}\boldsymbol{J} \; ; \; \text{tr}({}^{i\Theta}_{s}\boldsymbol{J}) = 0 \\ \boldsymbol{q} &= -k\boldsymbol{g} \; ; \; \boldsymbol{g} = \boldsymbol{\nabla}\theta \end{aligned} \tag{1.61}$$

in which $\underset{\sim}{\mu}$ is a material coefficient.

For the deformation in x_1x_2 plane only ${}_i\Theta_{x_3} = \left(\dfrac{\partial u_2}{\partial x_1} - \dfrac{\partial u_1}{\partial x_2}\right)$ is non zero, i.e. ${}_i\Theta_{x_1}$ and ${}_i\Theta_{x_2}$ are

zero. Thus, all components of $[{}^{i}_{s}\Theta J]$ are zero except

$$ {}^{i}_{s}\Theta J_{13} = \frac{1}{2}\frac{\partial({}_{i}\Theta_{x_3})}{\partial x_1} \tag{1.62} $$

For x_1x_2 space the simple linear constitutive theories in equation (1.61) can be written as

$$ {}_{s}\sigma_{ij} = 2\mu\varepsilon_{ij} + \lambda\varepsilon_{kk}\delta_{ij} \; ; \; i,j = 1,2 \tag{1.63} $$

and

$$ m_{13} = 2\underset{\sim}{\mu}({}^{i}_{s}\Theta J_{13}) = 2\underset{\sim}{\mu}\left(\frac{1}{2}\frac{\partial({}_{i}\Theta_{x_3})}{\partial x_1}\right) = \underset{\sim}{\mu}\frac{\partial({}_{i}\Theta_{x_3})}{\partial x_1} \tag{1.64} $$

Remarks

(1) For thermoelastic beams, we consider linear elastic behavior with small strain and small deformation without any thermal effects, hence heat flux $\boldsymbol{q}$ and temperature θ need not be considered.

(2) We note that Cauchy stress tensor $\boldsymbol{\sigma}$ in (1.49) and (1.51) is not symmetric.

(3) The Cauchy moment tensor $\boldsymbol{m}$ is symmetric due to balance of moment of moments balance law [85–87], equation (1.52).

$$ \boldsymbol{m} = {}_{s}\boldsymbol{m} \text{ and } {}_{a}\boldsymbol{m} = 0 $$

This is an additional balance law required in non-classical continuum mechanics [85–87].

(4) From energy equation and from the entropy inequality we note that $[{}_{s}\sigma]$, $[\dot{\varepsilon}]$ and $[m]$, $[\,{}^{\Theta}_{s}\dot{J}]$ are rate of work conjugate pairs, hence (1.60).

1.3.1 Non-classical continuum mechanics with internal and Cosserat rotations

The conservation and the balance laws: conservation of mass, balance of linear momenta, balance of angular momenta, balance of moment of moments, first and second laws of thermodynamics and the constitutive theories are summarized in the following [42] in Lagrangian description.

$$\rho_0 = |J|\rho \; ; \; |J| \simeq 1 \text{ for small deformation, small strain.} \quad \text{(CM)} \tag{1.65}$$

$$\rho_0 \frac{\partial^2 \boldsymbol{u}}{\partial t^2} - \rho_0 \boldsymbol{F}^b - \boldsymbol{\nabla \cdot} \boldsymbol{\sigma}^T = 0 \quad \text{(BLM)} \tag{1.66}$$

$$\boldsymbol{\sigma} = {}_s\boldsymbol{\sigma} + {}_a\boldsymbol{\sigma} \tag{1.67}$$

$$m_{mk,m} = \epsilon_{ijk}\sigma_{ij} = \epsilon_{ijk}({}_a\sigma_{ij}) \quad \text{(BAM)} \tag{1.68}$$

$$\epsilon_{ijk} m_{ij} = 0 \quad \text{(BMM)} \tag{1.69}$$

$$\rho_0 \frac{De}{Dt} + \boldsymbol{\nabla \cdot} \boldsymbol{q} - \text{tr}\left([{}_s\sigma]^T [\dot{\varepsilon}]^T\right) - \text{tr}\left([{}_a\sigma]^T [{}^t_a\dot{r}]^T\right) - \text{tr}\left([m]^T [{}^{t\Theta}_{s}\dot{J}]^T\right) = 0 \quad \text{(FLT)} \tag{1.70}$$

$$\rho_0 \left(\frac{D\Phi}{Dt} + \eta \frac{D\theta}{Dt}\right) + \frac{\boldsymbol{q} \cdot \boldsymbol{g}}{\theta} - \text{tr}\left([{}_s\sigma]^T [\dot{\varepsilon}]^T\right) - \text{tr}\left([{}_a\sigma]^T [{}^t_a\dot{r}]^T\right) - \text{tr}\left([m]^T [{}^{t\Theta}_{s}\dot{J}]^T\right) \leq 0 \quad \text{(SLT)} \tag{1.71}$$

$${}_i\dot{\boldsymbol{\Theta}} \cdot (\boldsymbol{\epsilon} : \boldsymbol{\sigma}) = 0 \qquad \text{(compatibility)} \tag{1.72}$$

Internal rotations $\{{}_i\Theta\}^T = [{}_i\Theta_{x_1}, {}_i\Theta_{x_2}, {}_i\Theta_{x_3}]$ are given by

$$\boldsymbol{\nabla} \times \boldsymbol{u} = \boldsymbol{e}_1({}_i\Theta_{x_1}) + \boldsymbol{e}_2({}_i\Theta_{x_2}) + \boldsymbol{e}_3({}_i\Theta_{x_3}) \tag{1.73}$$

or alternatively the internal rotations can be obtained from antisymmetric part of the displacement gradient tensor $[{}^d_J]$.

$$[{}^d_J] = [{}^d_s J] + [{}^d_a J] = [\varepsilon] + [{}^i_a r] \tag{1.74}$$

Let ${}_e\boldsymbol{\Theta}$ be external (unknown) or Cosserat rotations, then the total rotations ${}_t\boldsymbol{\Theta}$ are given by

$$ {}_t\boldsymbol{\Theta} = {}_i\boldsymbol{\Theta} + {}_e\boldsymbol{\Theta} \tag{1.75} $$

$$ [{}^t_a r] = [{}^i_a r] + [{}^e_a r] \tag{1.76} $$

Gradients of ${}_t\boldsymbol{\Theta}$, $[{}^t\Theta J]$ and its symmetric and antisymmetric components are given by

$$ [{}^t\Theta J] = \left[\frac{\partial\{{}_t\Theta\}}{\partial\{x\}}\right] \; ; \; [{}^t_s\Theta J] + [{}^t_a\Theta J] \tag{1.77} $$

$$ [{}^t_s\Theta J] = \frac{1}{2}\left([{}^t\Theta J] + [{}^t\Theta J]^T\right) \; , \; [{}^t_a\Theta J] = \frac{1}{2}\left([{}^t\Theta J] - [{}^t\Theta J]^T\right) \tag{1.78} $$

From the conjugate pairs in the entropy inequality we calculate the following for thermoelastic solid

$$ \begin{aligned} {}_s\boldsymbol{\sigma} &= {}_s\boldsymbol{\sigma}(\boldsymbol{\varepsilon}, \theta) \\ \boldsymbol{m} &= \boldsymbol{m}({}^t_s\boldsymbol{\Theta J}, \theta) \\ {}_a\boldsymbol{\sigma} &= {}_a\boldsymbol{\sigma}({}^t_a\boldsymbol{r}, \theta) \\ \boldsymbol{q} &= \boldsymbol{q}(\boldsymbol{g}, \theta) \end{aligned} \tag{1.79} $$

General constitutive theories based on integrity can be derived using (1.79) and representation theorem [42]. Simplified linear constitutive theories are given by

$$ \begin{aligned} {}_s\boldsymbol{\sigma} &= 2\mu\boldsymbol{\varepsilon} + \lambda(\mathrm{tr}(\boldsymbol{\varepsilon}))\boldsymbol{I} \\ {}_s\boldsymbol{m} &= 2\underset{\sim}{\mu}({}^t_s\boldsymbol{\Theta J}) \\ {}_a\boldsymbol{\sigma} &= \kappa({}^t_a\boldsymbol{r}) \\ \boldsymbol{q} &= -k\boldsymbol{g} \; ; \; \boldsymbol{g} = \boldsymbol{\nabla}\theta \end{aligned} \tag{1.80} $$

Where κ is additional material coefficient.

For the deformation in x_1x_2 plane all components of $[{}^{t}_{s}\Theta J]$ are zero except

$$ {}^{t}_{s}\Theta J_{13} = \frac{1}{2}\frac{\partial({}_t\Theta_{x_3})}{\partial x_1} \tag{1.81} $$

For x_1x_2 space the simple linear constitutive theories in equation (1.80) can be written as

$$ {}_s\sigma_{ij} = 2\mu\varepsilon_{ij} + \lambda\varepsilon_{kk}\delta_{ij} \; ; \; i,j = 1,2 \tag{1.82} $$

$$ m_{13} = 2\underset{\sim}{\mu}({}^{t}_{s}\Theta J_{13}) = 2\underset{\sim}{\mu}\left(\frac{1}{2}\frac{\partial({}_t\Theta_{x_3})}{\partial x_1}\right) = \underset{\sim}{\mu}\frac{\partial({}_t\Theta_{x_3})}{\partial x_1} \tag{1.83} $$

$$ {}_a\sigma_{12} = \kappa({}_t\Theta_{x_3}) \tag{1.84} $$

Remarks

(1) For thermoelastic beams, we consider linear elastic behavior with small strain and small deformation without any thermal effects, hence $\boldsymbol{q}$ and θ need not be considered if entropy production due to dissipation is small.

(2) In this case also we note that Cauchy stress tensor $\boldsymbol{\sigma}$ is not symmetric, hence (1.67) in which ${}_s\boldsymbol{\sigma}$ and ${}_a\boldsymbol{\sigma}$ are symmetric and antisymmetric tensor.

(3) The Cauchy moment tensor $\boldsymbol{m}$ is symmetric,

$$ \boldsymbol{m} = {}_s\boldsymbol{m} \text{ and } {}_a\boldsymbol{m} = 0 $$

due to balance of moment of moments balance law [85–87]. This is an additional balance law required in non-classical continuum theories.

(4) From energy equation or entropy inequality ${}_s\boldsymbol{\sigma}$, $\dot{\boldsymbol{\varepsilon}}$; $\boldsymbol{m}$, ${}^{t}_{s}\dot{\boldsymbol{J}}$ and ${}_a\boldsymbol{\sigma}$, ${}^{t}_{a}\dot{\boldsymbol{r}}$ are rate of work

conjugate pairs, hence (1.79).

1.4 Scope of Work

In this dissertation the first part of the research is devoted to establishing thermodynamic consistency of the currently used mathematical models for bending of beams that are derived using principle of virtual work or the energy methods. In accomplishing we follow the steps outlined below.

(1) We consider bending of beams in $\mathbb{R}^2$, i.e. in x_1x_2 plane.

(2) We assume small deformation, small strain and reversible mechanical deformation (i.e. linear elastic solid matter), hence isothermal deformation process for thermoelastic beams.

(3) The Euler-Bernoulli beam theory (EBBT) and Timoshenko beam theory (TBT) mathematical models used currently contain all features of majority of the beam mathematical models used currently; hence, we only consider these two mathematical models of beam bending in x_1x_2 space as representative mathematical model for determining thermodynamic consistency of all currently used beam mathematical model.

(4) For a continuous isotropic and homogeneous medium in 2D the deformation physics (in x_1x_2 plane in this case) must be described using the conservation and balance laws and the consistent constitutive theories of continuum mechanics to ensure thermodynamic consistency of the resulting mathematical models. Thus, for determining thermodynamic consistency of the mathematical models for EBBT and TBT we must begin with conservation and the balance laws of continuum mechanics and then incorporate the assumed kinematic relations of EBBT and TBT in these to arrive at the final mathematical models. The mathematical models so derived are obviously thermodynamically consistent as well as will honor the assumed kinematic relations of EBBT and TBT. The mathematical models so derived for EBBT and TBT are compared with the currently used mathematical models for EBBT and TBT.

(a) If the mathematical models of EBBT and TBT derived in this dissertation (using the approach described above) are exactly same as those used currently, then the currently used mathematical models for EBBT and TBT are thermodynamically consistent; hence, further enhancement in these mathematical models such as incorporating dissipation and memory mechanisms can be done using principle of thermodynamics or continuum mechanics.

(b) If we find that the currently used mathematical models for EBBT and TBT are not the same as the mathematical models derived here, then the currently used mathematical models for EBBT and TBT are thermodynamically inconsistent. In this case any further enhancement (such as incorporating dissipation and memory mechanisms) in the currently used mathematical models for EBBT and TBT is not possible using conservation and the balance laws of continuum mechanics.

(c) If we find that (b) holds, then obviously there is a need for thermodynamically consistent mathematical model describing beam bending physics based on conservation and balance laws of continuum mechanics that can describe the slender as well as thick or deep beam deformation physics without violating thermodynamic consistency.

(5) The outline of the work presented in this dissertation is given in the following

(a) Equations resulting from the conservation and the balance laws and linear constitutive theories are presented in section 1.2 for

(i) Classical continuum mechanics [24].

(ii) Non-classical continuum mechanics using internal rotation [30, 31, 34].

(iii) Non-classical continuum mechanics using internal and Cosserat rotations [42–44].

(b) Section 1.2 contains equations resulting from the CCM conservation and balance laws, the basic definitions of rotations and linear constitutive relations for non-classical continuum mechanics based on internal rotations and internal and Cosserat rotations.

(c) The currently used mathematical models for EBBT and TBT are presented and described briefly.

(d) Conservation and the balance laws of classical and non-classical continuum mechanics (CCM, NCCM) are used in conjunction with kinematic assumptions of the EBBT and TBT to derive the resulting mathematical models for EBBT and TBT based on CCM as well as NCCM conservation and balance laws. These mathematical models honor the conservation and the balance laws as well as kinematic assumptions.

(e) The mathematical models derived in (d) are compared with the currently used mathematical models of EBBT and TBT.

(f) Derivation of the new kinematic assumption-free thermodynamically consistent beam mathematical model capable of describing slender as well as thick or deep beam deformation physics is presented next.

(g) The new formulation is extended to bending of thermoviscoelastic beams without memory (dissipation) and thermoviscoelastic beams with memory (dissipation and rheology).

(h) Model problem studies comparing results from currently used EBBT, TBT and the new formulation presented for slender as well as non-slender beam deformations is presented for static problem.

(i) Model problem studies are presented for bending of thermoviscoelastic beams without memory (dissipation).

(j) Summary and conclusions are given in the last chapter.

Chapter 2

Thermodynamic Consistency of Currently Used Beam Mathematical Models and New Formulation

2.1 Currently used Mathematical Models for EBBT and TBT and their Thermodynamic Consistency

For simplicity consider bending of a beam of length L in x_1x_2 plane. o-x_1 is the beam axis and x_2 direction is transverse deflection direction. Without loss of generality we assume that the cross-section of the beam is $h \times b$, b being the dimension normal to x_1x_2 plane and h is the depth of the beam (in x_2-direction). Details are shown in Figure 2.1.

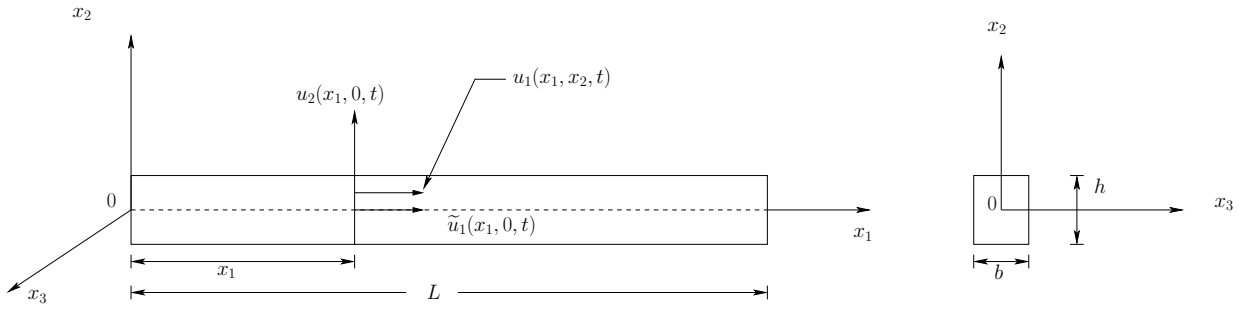

Figure 2.1: Schematic of a beam in x_1x_2 plane.

This configuration and notation will be used for all beam mathematical models considered in this dissertation.

2.1.1 Euler-Bernoulli beam mathematical model based on energy functional or principle of virtual work

In EBBT that considers pure axial deformation in x_1 direction as well as bending in x_1x_2 plane, the following kinematic assumptions are used

$$\begin{aligned} u_1(x_1,x_2,t) &= \widetilde{u}_1(x_1,0,t) - x_2\frac{\partial u_2}{\partial x_1} \\ u_2 &= u_2(x_1,0,t) \end{aligned} \tag{2.1}$$

Linear strain measure and linear constitutive theory gives the following based on (2.1)

$$\begin{aligned} &\varepsilon_{11} = \frac{\partial u_1}{\partial x_1} = \frac{\partial \widetilde{u}_1}{\partial x_1} - x_2\frac{\partial^2 u_2}{\partial {x_1}^2} \quad ; \quad \varepsilon_{12} = \varepsilon_{21} = \frac{1}{2}\left(\frac{\partial u_2}{\partial x_1} + \frac{\partial u_1}{\partial x_2}\right) = 0 \\ &\sigma_{11} = E\varepsilon_{11} \text{ and } \sigma_{12} = \sigma_{21} = 2G\varepsilon_{12} = 0 \quad ; \quad \varepsilon_{22} = 0\ ,\ \sigma_{22} = 0 \end{aligned} \tag{2.2}$$

Based on (2.2), the strain energy is only due to σ_{11} and ε_{11}. σ_{12} and ε_{12} are both zero and hence make no contribution to strain energy. The mathematical model for EBBT based on (2.1) and (2.2) can be derived by considering energy functional (I) consisting of kinetic energy, strain energy and the potential energy of loads over time, length L and the area of cross-section A i.e. integral over

the volume of the beam and time. The following Euler's equations derived from $\delta I = 0$ (first variation of I) for arbitrary length L and time t constitute the mathematical model for EBBT.

$$\rho_0 A\frac{\partial^2\widetilde{u}_1}{\partial t^2} - \frac{\partial}{\partial x_1}\left(EA\frac{\partial\widetilde{u}_1}{\partial x_1}\right) - \rho_0 AF_1^b = 0 \tag{2.3}$$

$$\rho_0 A\frac{\partial^2 u_2}{\partial t^2} + \frac{\partial^2}{\partial {x_1}^2}\left(EI\frac{\partial^2 u_2}{\partial {x_1}^2}\right) - \rho_0 I\frac{\partial^4 u_2}{\partial t^2\partial x_1^2} - \rho_0 AF_2^b = 0 \tag{2.4}$$

$$\mathscr{Q}_{12} = 0\ ;\ N_{11} = \int_A \sigma_{11}dA = EA\frac{\partial\widetilde{u}_1}{\partial x_1}\ ;\ \underset{\sim}{m}_{13} = -EI\frac{\partial^2 u_2}{\partial {x_1}^2} \tag{2.5}$$

The second term in (2.3) and (2.4) is due to $\sigma_{11}\varepsilon_{11}$ in the energy functional I. Since $\sigma_{12} = \sigma_{21} = 0$, its integral over the cross-section A i.e. the shear force $\mathscr{Q}_{12}$ is zero. N_{11} is axial force. Moment $\underset{\sim}{m}_{13}$ about x_3 axis is due to kinematic assumption (2.1) i.e.

$$\underset{\sim}{m}_{13} = \int_A x_2\sigma_{11}dA \tag{2.6}$$

ρ_0 is density in the reference configuration, E is modulus of elasticity and I in (2.4) and (2.5) is bending moment of inertia. F_1^b and F_2^b are body forces per unit mass in x_1 and x_2 directions.

We note that the Euler's equations (2.3) and (2.4) are coefficients of the $\delta\widetilde{u}_1$ and δu_2. Equations (2.3) and (2.4) are the mathematical model in $\widetilde{u}_1$ and u_2 with $\mathscr{Q}_{12} = 0$. Substitutions from (2.5) can be made in (2.3) and (2.4), thereby obtaining the following mathematical model.

$$\rho_0 A\frac{\partial^2\widetilde{u}_1}{\partial t^2} - \frac{\partial}{\partial x_1}(N_{11}) - \rho_0 AF_1^b = 0 \tag{2.7}$$

$$\rho_0 A\frac{\partial^2 u_2}{\partial t^2} - \frac{\partial^2}{\partial {x_1}^2}(\underset{\sim}{m}_{13}) - \rho_0 AF_2^b = 0 \tag{2.8}$$

with $\mathscr{Q}_{12} = 0$.

This mathematical model consists of equations (2.7), (2.8) and the equations for N_{11} and $\underset{\sim}{m}_{13}$ defined in (2.5), in the dependent variables $\widetilde{u}_1$, u_2, N_{11} and $\underset{\sim}{m}_{13}$, also with $\mathscr{Q}_{12} = 0$.

2.1.2 Timoshenko beam mathematical model based on energy functional or principle of virtual work

Here also we consider pure axial deformation in x_1 direction as well as bending in x_1x_2 plane. The following kinematic assumptions are used.

$$\begin{aligned} u_1(x_1, x_2, t) &= \widetilde{u}_1(x_1, 0, t) - x_2\phi(x_1, 0, t) \\ u_2 &= u_2(x_1, 0, t) \end{aligned} \tag{2.9}$$

in which ϕ is the rotation of the cross-section about the x_3 axis. Rotation ϕ is unknown and is like Cosserat rotation in NCCM. Strain measures based on (2.9) and stresses based on linear constitutive theory are given by

$$\begin{aligned} &\varepsilon_{11} = \frac{\partial \widetilde{u}_1}{\partial x_1} - x_2\frac{\partial \phi}{\partial x_1} \quad ; \quad \varepsilon_{12} = \varepsilon_{21} = \frac{1}{2}\left(\frac{\partial u_1}{\partial x_2} + \frac{\partial u_2}{\partial x_1}\right) = \frac{1}{2}\left(\frac{\partial u_2}{\partial x_1} - \phi\right) \\ &\sigma_{11} = E\varepsilon_{11} \quad ; \quad \sigma_{12} = \sigma_{21} = 2G\varepsilon_{12} = G\left(\frac{\partial u_2}{\partial x_1} - \phi\right) \quad ; \quad \sigma_{22} = 0 \end{aligned} \tag{2.10}$$

Based on (2.10), the strain energy is due to $\sigma_{11}\varepsilon_{11}$ and $\sigma_{12}\varepsilon_{12}$. The mathematical model for TBT based on (2.9) and (2.10) can be derived by considering energy functional (I) consisting of kinetic energy, strain energy and potential energy of loads over time, length and area of cross-section i.e. integral over volume of the beam and time. Using $\delta I = 0$ for arbitrary length L and time t and integrating over beam cross-section A of the beam, we obtain the following mathematical model of the TBT by extracting Euler's equations from $\delta I = 0$.

$$\rho_0 A\frac{\partial^2 \widetilde{u}_1}{\partial t^2} - \frac{\partial}{\partial x_1}\left(EA\frac{\partial \widetilde{u}_1}{\partial x_1}\right) - \rho_0 AF_1^b = 0 \tag{2.11}$$

$$\rho_0 A\frac{\partial^2 u_2}{\partial t^2} - \frac{\partial}{\partial x_1}({}^sQ_{12}) - \rho_0 AF_2^b = 0 \tag{2.12}$$

$$\rho_0 I\frac{\partial^2 \phi}{\partial t^2} - \frac{\partial}{\partial x_1}\left(EI\frac{\partial \phi}{\partial x_1}\right) - {}^sQ_{12} = 0 \tag{2.13}$$

From the kinematic assumptions we have

$$N_{11} = \int_A \sigma_{11}\, dA = EA\frac{\partial \widetilde{u}_1}{\partial x_1} \quad ; \quad \underset{\sim}{m}_{13} = -EI\frac{\partial \phi}{\partial x_1} \quad ; \quad {}^{s}Q_{12} = \int_A \sigma_{12}\, dA = GA\left(\frac{\partial u_2}{\partial x_1} - \phi\right) \tag{2.14}$$

We note that the Euler's equations (2.11)–(2.13) are indeed coefficients of $\delta\widetilde{u}_1$, δu_2 and $\delta\phi$ in the first variation of the energy functional set to zero.

Alternatively, we can obtain the following system of equations in terms of the resultants N_{11}, ${}^{s}Q_{12}$ and $\underset{\sim}{m}_{13}$.

$$\rho_0 A\frac{\partial^2 \widetilde{u}_1}{\partial t^2} - \frac{\partial}{\partial x_1}(N_{11}) - \rho_0 A F_1^b = 0 \tag{2.15}$$

$$\rho_0 A\frac{\partial^2 u_2}{\partial t^2} - \frac{\partial}{\partial x_1}({}^{s}Q_{12}) - \rho_0 A F_2^b = 0 \tag{2.16}$$

$$\rho_0 I\frac{\partial^2 \phi}{\partial t^2} + \frac{\partial}{\partial x_1}(\underset{\sim}{m}_{13}) - {}^{s}Q_{12} = 0 \tag{2.17}$$

In this case (2.15)–(2.17) and the equations for N_{11}, $\underset{\sim}{m}_{13}$ and ${}^{s}Q_{12}$ in (2.14) constitute a system of six partial differential equations in $\widetilde{u}_1$, u_2, ϕ, N_{11}, $\underset{\sim}{m}_{13}$ and ${}^{s}Q_{12}$.

On the other hand, if we substitute ${}^{s}Q_{12}$ from (2.14) into (2.12) and (2.13), then the resulting system of equations (2.11) and new (2.12), (2.13) are a system of three PDEs in $\widetilde{u}_1$, u_2 and ϕ. All three models have closure.

2.1.3 Thermodynamic consistency of the currently used beam mathematical model

In this section we attempt derivations of Euler-Bernoulli beam mathematical model and Timoshenko beam mathematical model using conservation and balance laws and constitutive theory of classical mechanics as well as non-classical mechanics based on internal rotations due to antisymmetric part of the displacement gradient tensor as well as internal rotations and Cosserat rotations in conjunction with the kinematic assumptions used in EBBT and TBT.

2.1.3.1 Euler-Bernoulli beam mathematical model derivation using classical continuum mechanics

We begin by considering the conservation and the balance laws and the constitutive theory in subsection 1.2.1 of section 1.2. These laws hold for the deformation of continuous matter in $\mathbb{R}^2$ (x_1x_2 plane in this case) that is the thermodynamically consistent mathematical model; hence, this model is valid for bending of beam in x_1x_2 plane. Euler-Bernoulli beam mathematical model requires that we satisfy kinematic assumptions (2.1). Thus, we need to incorporate the kinematic assumptions (2.1) in the mathematical model of subsection 1.2.1 in section 1.2. Based on (2.1), we have the strain measures and the stress relations given in (2.2).

We substitute from equation (2.2) in the balance of linear momenta in equations (1.12) and (1.13), integrate over the cross-section $A = h \times b$ and also over length $[0, L]$ and time $[0, t]$. We first integrate over $A = h \times b$, i.e. for $x_2 \in [-h/2, h/2]$ and b (perpendicular to x_1x_2 plane). The resulting integrals over $[0, L]$ and $[0, t]$ are valid for arbitrary L and t, hence the integrands must be zero, which gives us the following equations.

$$\rho_0 A\frac{\partial^2\widetilde{u}_1}{\partial t^2} - \rho_0 AF_1^b - \frac{\partial}{\partial x_1}\left(EA\frac{\partial\widetilde{u}_1}{\partial x_1}\right) = 0 \tag{2.18}$$

$$\rho_0 A\frac{\partial^2 u_2}{\partial t^2} - \rho_0 AF_2^b = 0 \tag{2.19}$$

$$N_{11} = \int_A \sigma_{11}dA = EA\frac{\partial\widetilde{u}_1}{\partial x_1} \tag{2.20}$$

$$\mathcal{M}_{13} = -EI\frac{\partial^2 u_2}{\partial x_1^2} \tag{2.21}$$

$$^{s}Q_{12} = 0 \quad (\text{as } \sigma_{12} = \sigma_{21} = 0) \tag{2.22}$$

The mathematical model consists of (2.18) and (2.19) in $\widetilde{u}_1$ and u_2 or equations (2.18)–(2.21) in $\widetilde{u}_1$, u_2 and N_{11} if $EA(\frac{\partial\widetilde{u}_1}{\partial x_1})$ is substituted in (2.18) from (2.20).

Remarks

(1) This mathematical model is obviously not the same as the currently used mathematical model given in subsection 2.1.1. Thus, we can conclude that the mathematical model of subsection 2.1.1 (currently used) is thermodynamically inconsistent based on classical continuum mechanics.

(2) This mathematical model ((2.18) and (2.19)) is erroneous. Balance of linear momenta only has inertial and body forces. The $\frac{\partial}{\partial x_1}(\mathscr{Q}_{12})$ or $\frac{\partial}{\partial x_1}(EA_s\sigma_{12})$ term is essential in this equation but is absent due to $\sigma_{12} = \sigma_{21} = 0$, a consequence of kinematic assumption.

(3) We observe that we began with perfectly valid balance laws of classical continuum mechanics, a valid mathematical model for continuous deformation in $\mathbb{R}^2$, but these are altered and damaged due to kinematic assumptions (2.1).

2.1.3.2 Euler-Bernoulli beam mathematical model derivation using non-classical continuum mechanics based on internal rotations

From section 1.2 subsection 1.3 we note that the internal rotation ${}_i\Theta_{x_3}$ is the only nonzero rotation for deformation in $\mathbb{R}^2$ and is given by

$$ {}_i\Theta_{x_3} = \left(\frac{\partial u_2}{\partial x_1} - \frac{\partial u_1}{\partial x_2} \right) \tag{2.23} $$

using kinematic relations (2.1) in (2.23) we obtain

$$ {}_i\Theta_{x_3} = 2\frac{\partial u_2}{\partial x_1} \tag{2.24} $$

Using (2.24) the assumed kinematic relations (2.1) can be written as

$$ \begin{aligned} u_1(x_1, x_2, t) &= \widetilde{u}_1(x_1, 0, t) - x_2 \left(\frac{1}{2}({}_i\Theta_{x_3}) \right) \\ u_2 &= u_2(x_1, 0, t) \end{aligned} \tag{2.25} $$

Appearance of the internal rotation ${}_i\Theta_{x_3}$ in the kinematic relation (2.25) suggests that perhaps use of balance laws of non-classical continuum mechanics incorporating internal rotations may be beneficial in deriving the mathematical model for Euler-Bernoulli beam. We use (2.1) or (2.25) in the further derivations. From section 1.2 subsection 1.3 we have

$$\boldsymbol{\sigma} = {}_s\boldsymbol{\sigma} + {}_a\boldsymbol{\sigma} \quad ; \quad \sigma_{11} = {}_s\sigma_{11} \ , \ {}_s\sigma_{12} = {}_s\sigma_{21} \ , \ {}_a\sigma_{12} = -{}_a\sigma_{21} \tag{2.26}$$

and

$$\begin{aligned} &\varepsilon_{11} = \frac{\partial u_1}{\partial x_1} = \frac{\partial \widetilde{u}_1}{\partial x_1} - x_2 \frac{\partial^2 u_2}{\partial {x_1}^2} \ , \ \varepsilon_{12} = \varepsilon_{21} = \frac{1}{2}\left(\frac{\partial u_2}{\partial x_1} + \frac{\partial u_1}{\partial x_2}\right) = 0 \\ &\varepsilon_{22} = 0 \ , \ \sigma_{22} = {}_s\sigma_{22} = 0 \ , \ {}_a\sigma_{12} \neq 0 \end{aligned} \tag{2.27}$$

using equations (2.26) and (2.27) in the balance of linear momenta equation (1.49) and performing integration over the cross-section A of the beam $[-h/2, h/2\,;\, b]$, length $[0, L]$ and time $[0, t]$ and realizing that the resulting integral over $[0, L]$ and $[0, t]$ (after integrating over area A) holds for arbitrary L and t, hence setting integrand to zero gives the following.

$$\rho_0 A \frac{\partial^2 \widetilde{u}_1}{\partial t^2} - \rho_0 A F_1^b - \frac{\partial}{\partial x_1}\left(EA \frac{\partial \widetilde{u}_1}{\partial x_1}\right) = 0 \tag{2.28}$$

$$\rho_0 A \frac{\partial^2 u_2}{\partial t^2} - \rho_0 A F_2^b - \frac{\partial ({}^aQ_{12})}{\partial x_1} = 0 \tag{2.29}$$

in which

$${}^aQ_{12} = \int_A {}_a\sigma_{12}\, dA \tag{2.30}$$

and

$$N_{11} = \int_A \sigma_{11}\, dA = EA \frac{\partial \widetilde{u}_1}{\partial x_1} \tag{2.31}$$

The mathematical model (2.28)–(2.30) is in dependent variables $\widetilde{u}_1$, u_2, ${}^aQ_{12}$ and ${}_a\sigma_{12}$, hence we need additional equation for this model to have closure.

Balance of angular momenta (section 1.2 subsection 1.3)

$$\frac{\partial m_{13}}{\partial x_1} = 2({}_a\sigma_{12}) \quad \text{or} \quad \frac{\partial(\frac{m_{13}}{2})}{\partial x_1} = {}_a\sigma_{12} \tag{2.32}$$

Integrating second equation in (2.32) over area A gives

$$\frac{\partial \underset{\sim}{m}_{13}}{\partial x_1} = {}^aQ_{12} \quad ; \quad \underset{\sim}{m}_{13} = \int_A \frac{m_{31}}{2} dA \tag{2.33}$$

The constitutive theory for σ_{11} has already been used, but we still need constitutive theory for m_{13}. From section 1.2 subsection 1.3 we note that m_{13} is conjugate with $\frac{\partial^2 u_2}{\partial x_1^2}$. A linear constitutive theory for m_{13} can be written as

$$m_{13} = C\frac{\partial^2 u_2}{\partial {x_1}^2} \tag{2.34}$$

in which C is material coefficient. We divide (2.34) by two and integrate over area A.

$$\int_A \left(\frac{m_{13}}{2}\right) dA = \left(\int_A \frac{C}{2} dA\right) \frac{\partial^2 u_2}{\partial {x_1}^2} \tag{2.35}$$

or

$$\underset{\sim}{m}_{13} = \underset{\sim}{c}\frac{\partial^2 u_2}{\partial {x_1}^2} \tag{2.36}$$

The coefficient $\underset{\sim}{c}$ contains material property as well as cross-sectional property and is yet to be determined. Based on the kinematic assumption, we must have

$$\underset{\sim}{m}_{13} = \int_A x_2 \sigma_{11} dA = -EI\frac{\partial^2 u_2}{\partial {x_1}^2} \tag{2.37}$$

We note that expression for $\underset{\sim}{m}_{13}$ in (2.36) is from constitutive theory consideration using conjugate pair in the entropy inequality, whereas $\underset{\sim}{m}_{13}$ in (2.37) is due to kinematic assumption. For uniqueness of $\underset{\sim}{m}_{13}$, $\underset{\sim}{c} = -EI$ must hold. Thus, now the constitutive theory for $\underset{\sim}{m}_{13}$ becomes

$$\underset{\sim}{m}_{13} = -EI\frac{\partial^2 u_2}{\partial {x_1}^2} \tag{2.38}$$

which is same as due to kinematic considerations. We summarize the complete mathematical model in the following (equations (2.28), (2.29), (2.33), and (2.38))

$$\rho_0 A\frac{\partial^2\widetilde{u}_1}{\partial t^2} - \rho_0 AF_1^b - \frac{\partial}{\partial x_1}\left(EA\frac{\partial\widetilde{u}_1}{\partial x_1}\right) = 0 \tag{2.39}$$

$$\rho_0 A\frac{\partial^2 u_2}{\partial t^2} - \rho_0 AF_2^b - \frac{\partial({}^{a}\underset{\sim}{Q}_{12})}{\partial x_1} = 0 \tag{2.40}$$

$$\frac{\partial(\underset{\sim}{m}_{13})}{\partial x_1} = {}^{a}\underset{\sim}{Q}_{12} \tag{2.41}$$

$$\underset{\sim}{m}_{13} = -EI\frac{\partial^2 u_2}{\partial x_1^2} \tag{2.42}$$

this mathematical model consists of four equations in four dependent variables $\widetilde{u}_1$, u_2, ${}^{a}\underset{\sim}{Q}_{12}$ and $\underset{\sim}{m}_{13}$, hence has closure. Additionally, we note that

$$N_{11} = \int_A \sigma_{11}dA = EA\frac{\partial\widetilde{u}_1}{\partial x_1} \tag{2.43}$$

$${}^{a}\underset{\sim}{Q}_{12} = \int_A {}_{a}\sigma_{12}\, dA \tag{2.44}$$

Remarks

(1) Obviously, the mathematical model used currently consisting of (2.3) and (2.4) is not the same as derived here using NCCM consisting of equations (2.39)–(2.40) or (2.45) and (2.46). The appearance of the mixed derivative terms is a consequence of energy approach and it cannot be explained or supported by the NCCM balance laws.

(2) We note that last term in (2.39) and (2.40) are due to gradients of stresses as they normally appear in balance of linear momenta.

(3) ${}_{s}\sigma_{12}$ and ${}^{s}\underset{\sim}{Q}_{12}$ are zero in this case also but ${}^{a}\underset{\sim}{Q}_{12}$ due to ${}_{a}\sigma_{12}$ is not zero.

(4) Existence of ${}_a\sigma_{12}$ or ${}^q\mathcal{Q}_{12}$ is due to gradient of the moment $\underset{\sim}{m}_{13}$ (balance of angular momenta); thus, no constitutive theory is needed for ${}_a\sigma_{12}$ (or ${}^q\mathcal{Q}_{12}$). This conclusion is supported by entropy inequality [30, 31].

(5) Moment tensor $\boldsymbol{m}$ is symmetric due to balance of moment of moments balance law i.e. $\underset{\sim}{m}_{13} = \underset{\sim}{m}_{31}$.

(6) $\underset{\sim}{m}_{13}$ in (2.42) is due to constitutive theory that is also in agreement with $\underset{\sim}{m}_{13}$ due to kinematic assumptions (equation (2.37)).

(7) Physics in this mathematical model is totally different than the currently used model (2.3) and (2.4) in which there is no concept of ${}^q\mathcal{Q}_{12}$ (due to ${}_a\sigma_{12}$) and secondly the existence of $\underset{\sim}{m}_{13}$ in (2.5) is purely due to kinematic assumption and not due to the constitutive theory.

(8) We remark that if we substitute $\underset{\sim}{m}_{13}$ from (2.42) in (2.41) and then ${}^q\mathcal{Q}_{12}$ from (2.41) into (2.40), then the mathematical model (2.39) to (2.42) reduces to

$$\rho_0 A\frac{\partial^2\widetilde{u}_1}{\partial t^2} - \rho_0 AF_1^b - \frac{\partial}{\partial x_1}\left(EA\frac{\partial\widetilde{u}_1}{\partial x_1}\right) = 0 \tag{2.45}$$

$$\rho_0 A\frac{\partial^2 u_2}{\partial t^2} - \rho_0 AF_2^b + \frac{\partial^2}{\partial {x_1}^2}\left(EI\frac{\partial^2 u_2}{\partial {x_1}^2}\right) = 0 \tag{2.46}$$

with

$${}^s\mathcal{Q}_{12} = 0 \tag{2.47}$$

Equations (2.45)–(2.46) are exactly same as (2.3) and (2.4) except for the third term in (2.4) (mixed second derivatives of u_2) and ${}^s\mathcal{Q}_{12} = 0$ in both models.

Thus, the solutions of model BVPs (in which the time derivative terms are absent) by using (2.3) and (2.4) without the time derivative terms will be exactly same as those from (2.39)–(2.42) or (2.45) and (2.46) (without time derivative terms) with the one exception, that in case of (2.39)–(2.42) or (2.45) and (2.46) shear force ${}^q\mathcal{Q}_{12} \neq 0$ but ${}^s\mathcal{Q}_{12} = 0$. Whereas in case of the mathematical model consisting of (2.3) and (2.4), ${}^s\mathcal{Q}_{12} = 0$ and ${}^q\mathcal{Q}_{12}$ does not exist.

The conclusion that the models (2.3) and (2.4) and (2.39)–(2.42) are same for BVPs based on comparison of (2.45) and (2.46) with (2.3) and (2.4) without the time terms in both i.e. for BVPs is obviously incorrect as discussed above.

(9) Finally, we conclude that the mathematical model (2.39)–(2.42) based on NCCM balance laws with internal rotations is thermodynamically consistent with the assumed kinematic description; however, the mathematical model (2.3) and (2.4) used currently is different than (2.39)–(2.42) or (2.45) and (2.46); hence, it is not supported by NCCM with internal rotations and hence is thermodynamically inconsistent.

(10) Since the kinematic assumptions (2.1) in EBBT does not contain unknown rotations (Cosserat rotations) about x_3 axis, there is no motivation for undertaking the derivation of the EBBT mathematical model based on NCCM using Cosserat rotations or internal and Cosserat rotations.

2.1.3.3 Timoshenko beam mathematical model derivation using classical continuum mechanics

As in case of EBBT in section 2.1.3.1, here also we begin with the conservation and the balance laws and the constitutive theory in subsection 1.2.1 of section 1.2. Timoshenko beam theory requires that we satisfy kinematic assumptions (2.9) in addition to the conservation and the balance laws of CCM. Based on (2.9), we have strain and stress measures in (2.10). We substitute from equation (2.10) into the balance of linear momenta equations (1.12) and (1.13). We integrate over the cross-section area A, length $[0, L]$ and time $[0, t]$. First, we perform integration over area A (i.e. $[-h/2, h/2\,;\, b]$). The resulting expression with integrals over $[0, L]$ and $[0, t]$ is valid for arbitrary L and t, hence we can set the integrand to zero which gives

$$\rho_0 A \frac{\partial^2 \widetilde{u}_1}{\partial t^2} - \rho_0 A F_1^b - \frac{\partial}{\partial x_1}\left(EA \frac{\partial \widetilde{u}_1}{\partial x_1}\right) = 0 \tag{2.48}$$

$$\rho_0 A \frac{\partial^2 u_2}{\partial t^2} - \rho_0 A F_2^b - \frac{\partial}{\partial x_1}({}^{s}Q_{12}) = 0 \tag{2.49}$$

in which

$$^{s}Q_{12} = \int_A \sigma_{12} dA = GA\left(\frac{\partial u_2}{\partial x_1} - \phi\right) \tag{2.50}$$

and

$$m_{13} = -EI\frac{\partial \phi}{\partial x_1} \tag{2.51}$$

Additionally

$$N_{11} = \int_A \sigma_{11} dA = EA\frac{\partial \widetilde{u}_1}{\partial x_1} \tag{2.52}$$

Equations (2.48)–(2.50) are the Timoshenko beam mathematical model based on balance laws of CCM with kinematic assumptions (2.9). This mathematical model consists of three equations ((2.48)–(2.50)) in four dependent variables $\widetilde{u}_1$, u_2, $^{s}Q_{12}$ and ϕ, hence does not have closure, and thus is invalid. We note that (2.50)–(2.52) are due to kinematic assumptions.

Remarks

(1) A valid mathematical model for Timoshenko beam cannot be derived using balance laws of CCM in conjunction with the kinematic assumptions (2.9) used in TBT.

(2) Based on ((1)), the currently used Timoshenko beam model is not thermodynamically consistent.

(3) We note that since ϕ in the kinematic assumption (2.9) is unknown rotation (additional rotational degree of freedom at a material point), $\dot{\phi}$ is rotation rate and $\ddot{\phi}$ is angular acceleration. None of these terms obviously have any place in balance of linear momenta. The balance of angular momenta in classical continuum mechanics only incorporates moments due to forces and results in symmetry of Cauchy stress tensor. Thus, m_{13} cannot be incorporated in the balance of angular momenta either.

(4) We have seen that the conservation and the balance laws of classical continuum mechanics are not adequate to derive mathematical description of Timoshenko beam based on kinematic

assumption (2.9) due to the fact that the kinematic assumption contains Cosserat rotation ϕ and in the further derivation of mathematical model we encounter both internal and Cosserat rotations, both of which cannot be supported by CCM.

2.1.3.4 Timoshenko beam mathematical model derivation using NCCM based on internal and Cosserat rotations

Using the kinematic assumptions (2.9) the antisymmetric part of the displacement gradient tensor or $\boldsymbol{\nabla} \times \boldsymbol{u}$ yields

$$\boldsymbol{\nabla} \times \boldsymbol{u} = (0)\boldsymbol{e}_1 + (0)\boldsymbol{e}_2 + \left(\frac{\partial u_2}{\partial x_1} + \phi\right)\boldsymbol{e}_3 \tag{2.53}$$

Thus, in this case the rotation about the x_3 axis is $(\partial u_2/\partial x_1 + \phi)$ which is known internal rotation $\partial u_2/\partial x_1$ and unknown Cosserat rotation ϕ, both of which are not supported by the CCM. This suggests that perhaps we should undertake the derivation of the Timoshenko beam mathematical model using balance laws of NCCM that considers internal as well as Cosserat rotations. The conservation and the balance laws and the linear constitutive theories for NCCM incorporating internal and Cosserat rotations are given in section 1.2 subsection 1.3.1. We present details of the derivation in the following.

Based on the kinematic assumptions we have

$$\varepsilon_{11} = \frac{\partial \widetilde{u}_1}{\partial x_1} - x_2\frac{\partial \phi}{\partial x_1} \quad ; \quad \varepsilon_{12} = \frac{1}{2}\left(\frac{\partial u_1}{\partial x_2} + \frac{\partial u_2}{\partial x_1}\right) = \frac{1}{2}\left(\frac{\partial u_2}{\partial x_1} - \phi\right) \tag{2.54}$$

$$\begin{aligned}
&\sigma_{11} = {}_s\sigma_{11} = E\varepsilon_{11}\ ,\ \sigma_{12} = {}_s\sigma_{12} + {}_a\sigma_{12}\ ,\ \sigma_{21} = {}_s\sigma_{21} + {}_a\sigma_{21}\\
&{}_s\sigma_{12} = {}_s\sigma_{21} \quad \text{and} \quad {}_a\sigma_{12} = -{}_a\sigma_{21}\\
&{}_s\sigma_{12} = {}_s\sigma_{21} = 2G\varepsilon_{12} = G\left(\frac{\partial u_2}{\partial x_1} - \phi\right)\\
&\sigma_{22} = 0
\end{aligned} \tag{2.55}$$

We substitute (2.54) and (2.55) in the balance of linear momenta equation (1.66) and integrate these over the cross-section A, length $[0, L]$ and time $[0, t]$. If we first integrate over the cross-section A (i.e. $[-h/2, h/2\,;\, b]$), then the resulting expressions (integrals over $[0, L]$ and time $[0, t]$) are valid for arbitrary L and t, hence the integrands can be set to zero which gives the following two equations.

$$\rho_0 A\frac{\partial^2\widetilde{u}_1}{\partial t^2} - \rho_0 AF_1^b - \frac{\partial}{\partial x_1}\left(EA\frac{\partial\widetilde{u}_1}{\partial x_1}\right) = 0 \tag{2.56}$$

$$\rho_0 A\frac{\partial^2 u_2}{\partial t^2} - \rho_0 AF_2^b - \frac{\partial}{\partial x_1}({}^{s}Q_{12}) - \frac{\partial}{\partial x_1}({}^{a}Q_{12}) = 0 \tag{2.57}$$

in which

$${}^{s}Q_{12} = \int_A {}_{s}\sigma_{12}\, dA = GA\left(\frac{\partial u_2}{\partial x_1} - \phi\right) \tag{2.58}$$

$${}^{a}Q_{12} = \int_A {}_{a}\sigma_{12}\, dA \tag{2.59}$$

balance of angular momenta gives

$$\frac{\partial(m_{13})}{\partial x_1} = 2({}_{a}\sigma_{12}) \tag{2.60}$$

Let ${}_{t}\Theta_{x_3}$ be the total rotation about x_3 axis. Then if

$${}_{t}\Theta_{x_3} = {}_{i}\Theta_{x_3} + {}_{e}\Theta_{x_3} = \frac{\partial u_2}{\partial x_1} + \phi \tag{2.61}$$

${}_{i}\Theta_{x_3}$ and ${}_{e}\Theta_{x_3}(=\phi)$ being internal rotation (known) and external rotation (or Cosserat rotation ϕ). Then, the constitutive theory for m_{13} (section 1.2 subsection 1.3.1) requires symmetric part of the gradient of ${}_{t}\Theta_{x_3}$ i.e.

$$\frac{1}{2}\frac{\partial}{\partial x_1}({}_{t}\Theta_{x_3}) = \frac{1}{2}\left(\frac{\partial^2 u_2}{\partial x_1^2} + \frac{\partial\phi}{\partial x_1}\right) \tag{2.62}$$

A linear constitutive theory for m_{13} can be written as

$$m_{13} = C\left(\frac{\partial({}_{t}\Theta_{x_3})}{\partial x_1}\right) = C\frac{1}{2}\left(\frac{\partial^2 u_2}{\partial x_1^2} + \frac{\partial\phi}{\partial x_1}\right) \tag{2.63}$$

In which C is a material coefficient.

Dividing (2.63) by two and integrating over the cross-section A

$$\int_A \frac{m_{13}}{2} = \underset{\sim}{m}_{13} = \left(\frac{\partial^2 u_2}{\partial x_1^2} + \frac{\partial \phi}{\partial x_1}\right) \int_A \frac{C}{4} dA \tag{2.64}$$

or

$$\underset{\sim}{m}_{13} = \underset{\sim}{c} \left(\frac{\partial^2 u_2}{\partial x_1^2} + \frac{\partial \phi}{\partial x_1}\right) \tag{2.65}$$

Also dividing (2.60), balance of angular momenta by two and integrating over the area A gives

$$\frac{\partial(\underset{\sim}{m}_{13})}{\partial x_1} = {}^{a}\underset{\sim}{Q}_{12} \tag{2.66}$$

Coefficient $\underset{\sim}{c}$ contains material coefficients and the properties of the cross-section. Based on the kinematic assumption (2.9), the integral of $x_2\sigma_{11}$ over the beam cross-section yields the moment about the ox_3 axis, that is

$$\underset{\sim}{m}_{13} = \int_A x_2(\sigma_{11}) = \int_A x_2 \left(E\frac{\partial u_1}{\partial x_1}\right) dA = \int_A -x_2^2 E \frac{\partial \phi}{\partial x_1} dA \tag{2.67}$$

Hence,

$$\underset{\sim}{m}_{13} = -EI\frac{\partial \phi}{\partial x_1} \tag{2.68}$$

If we choose

$$\underset{\sim}{c} = -EI \tag{2.69}$$

then, (2.65) can be written as

$$\underset{\sim}{m}_{13} = -EI\left(\frac{\partial^2 u_2}{\partial x_1^2} + \frac{\partial \phi}{\partial x_1}\right) \tag{2.70}$$

We recall from section 1.2 subsection 1.3.1, equation (1.79)

$${}_{a}\sigma_{12} = {}_{a}\sigma_{12}({}_{t}\Theta_{x_3}) \tag{2.71}$$

$$ {}_a\sigma_{12} = {}_a\sigma_{12}\left(\frac{\partial u_2}{\partial x_1} + \phi\right) \tag{2.72} $$

or

$$ {}_a\sigma_{12} = \kappa\left(\frac{\partial u_2}{\partial x_1} + \phi\right) = G\left(\frac{\partial u_2}{\partial x_1} + \phi\right) \quad ; \quad \text{choose } \kappa = G \tag{2.73} $$

integrating over area A

$$ \int_A {}_a\sigma_{12} dA = {}^aQ_{12} = \int_A G\left(\frac{\partial u_2}{\partial x_1} + \phi\right) dA = GA\left(\frac{\partial u_2}{\partial x_1} + \phi\right) \tag{2.74} $$

Also

$$ {}^sQ_{12} = \int_A {}_s\sigma_{12} = \int_A 2G\varepsilon_{12} dA = \int_A 2G\left(\frac{1}{2}\left(\frac{\partial u_2}{\partial x_1} - \phi\right)\right) dA \tag{2.75} $$

$$ \therefore {}^sQ_{12} = GA\left(\frac{\partial u_2}{\partial x_1} - \phi\right) \tag{2.76} $$

Summary of the mathematical model:

$$ \rho_0 A\frac{\partial^2 \widetilde{u}_1}{\partial t^2} - \rho_0 A F_1^b - \frac{\partial}{\partial x_1}\left(EA\frac{\partial \widetilde{u}_1}{\partial x_1}\right) = 0 \tag{2.77} $$

$$ \rho_0 A\frac{\partial^2 u_2}{\partial t^2} - \rho_0 A F_2^b - \frac{\partial({}^sQ_{12})}{\partial x_1} - \frac{\partial({}^aQ_{12})}{\partial x_1} = 0 \tag{2.78} $$

$$ \frac{\partial(\underset{\sim}{m}_{13})}{\partial x_1} - {}^aQ_{12} = 0 \tag{2.79} $$

$$ {}^sQ_{12} = GA\left(\frac{\partial u_2}{\partial x_1} - \phi\right) \tag{2.80} $$

$$ {}^aQ_{12} = GA\left(\frac{\partial u_2}{\partial x_1} + \phi\right) \tag{2.81} $$

$$ \underset{\sim}{m}_{13} = -EI\frac{\partial \phi}{\partial x_1} \; ; \quad \text{due to kinematic assumption} \tag{2.82} $$

or

$$ \underset{\sim}{m}_{13} = -EI\left(\frac{\partial^2 u_2}{\partial x_1^2} + \frac{\partial \phi}{\partial x_1}\right) \; ; \quad \text{due to constitutive theory} \tag{2.83} $$

Equations (2.77)–(2.82) or (2.83) are six partial differential equations in $\widetilde{u}_1$, u_2, ${}^{s}\underset{\sim}{Q}_{12}$, ${}^{a}\underset{\sim}{Q}_{12}$, $\underset{\sim}{m}_{13}$ and ϕ, hence the mathematical model has closure, but is this model thermodynamically consistent and how does it compare with the mathematical model derived using energy functional? We make some remarks in the following.

Remarks

(1) Moment $\underset{\sim}{m}_{13}$ based on kinematic assumption (2.82) is not the same as its derivation in (2.83) based on the constitutive theory. Choosing (2.83) violates kinematic assumption, whereas if we choose (2.82), then this results in violation of constitutive consideration based on entropy inequality.

(2) Based on (1), this beam mathematical model derived here cannot be supported by the principles of non-classical continuum mechanics if the kinematic assumption (2.9) is to be enforced.

(3) Thus, this beam mathematical model derived using NCCM with internal and Cosserat rotations is thermodynamically inconsistent and obviously is not the same as the currently used Timoshenko beam model presented in subsection 2.1.2 derived using energy functional.

(4) We clearly see that currently used Timoshenko beam mathematical model cannot be derived using non-classical continuum mechanics with internal and Cosserat rotations either.

(5) Hence, Timoshenko beam mathematical model is thermodynamically inconsistent based on CCM as well as NCCM using internal and Cosserat rotations.

2.2 General Remarks

(1) We have shown that currently used mathematical models for the Euler-Bernoulli beam theory and Timoshenko beam theory cannot be derived using conservation and the balance laws of

classical as well as non-classical continuum mechanics based on internal or internal and Cosserat rotations.

(2) Mathematical model for EBBT requires use of internal rotation(s) and TBT uses internal as well as Cosserat rotation(s). All currently used beam mathematical models either require use of internal rotation(s) and/or Cosserat rotations. Thus, use of EBBT and TBT as typical representative beam mathematical models for investigating thermodynamic consistency of all currently used beam mathematical models is justified. Hence, the remarks and the inferences presented for EBBT and TBT hold in general for all currently used beam mathematical models.

(3) A serious consequence of the thermodynamic inconsistency of the currently used beam mathematical models is that dissipation and memory mechanism can only be incorporated in these theories using phenomenological approach in $\mathbb{R}^1$. Due to absence of energy equation and entropy inequality thermodynamically consistent treatment of dissipation and memory mechanisms is not possible in the current beam mathematical models.

2.3 Kinematic Assumption Free Methodology for Bending of Beams

In the currently used beam theories the kinematic assumptions contain internal rotation(s) due to displacement gradients and/or Cosserat rotations (that are additional unknown degree(s) of freedom) at a material point. We have shown using EBBT and TBT that if kinematic assumptions are a requirement, then the currently used mathematical models for the beam theories cannot be derived using the conservation and the balance laws of classical continuum mechanics or non-classical continuum mechanics incorporating internal rotations or the internal rotations and the Cosserat rotations. Shortcomings of the energy functional approach or principle of virtual work in deriving beam mathematical models that require mechanism of dissipation and memory have already been

discussed and is the main motivation for this work.

As we know the balance laws of CCM and NCCM always yield thermodynamically consistent mathematical models and are always the first step in all of the derivations presented in this paper for establishing thermodynamic consistency of the currently used beam mathematical models. It is only after incorporating the kinematic assumptions in the balance laws that the resulting mathematical model loses thermodynamic consistency. We make some remarks.

(1) It is perhaps meritorious to consider an approach in which the kinematic assumptions in their present form are not considered. Instead, we begin with the mathematical model in $\mathbb{R}^2$ consisting of conservation and the balance laws and incorporate desired kinematics of deformation at some later state in a much more general manner so that slender as well as non-slender beam physics is transparently incorporated in a single mathematical description.

(2) For continuous media, classical and non-classical continuum mechanics are two possible approaches of deriving mathematical description of deforming continua. Classical continuum mechanics has been the foundation for describing the deformation physics of continuous media. Non-classical continuum mechanics incorporates additional physics in the mathematical models over and beyond classical continuum mechanics. This may be beneficial in some cases. None the less for isotropic, homogeneous linear elastic continuous matter, classical continuum mechanics must at least provide some reasonable description of the deformation physics regardless of $\mathbb{R}^1$, $\mathbb{R}^2$ and $\mathbb{R}^3$.Thus, we should be able to describe beam bending behavior using classical as well as non-classical continuum mechanics if we eliminate the kinematic assumptions at the onset of the derivation of the mathematical model. In the following we consider use of classical continuum mechanics conservation and the balance laws in describing beam bending behavior.

(3) The finite element method is perhaps the most general and versatile technique of obtaining solution of the mathematical models describing beam deformation. Such solutions are numerical but piecewise analytical and with higher order global differentiability local ap-

proximations; these solutions can truly approach theoretical solutions [8–10]. Thus, if the finite element technique is eventually to be used to solve beam equations, then keeping this in mind we can begin with conservation and balance laws of classical continuum mechanics in $\mathbb{R}^2$ and $\mathbb{R}^3$, followed by the design of a geometric description of the beam finite element that is identical to the manner in which beams are geometrically described currently i.e. centerline and the beam cross-sections normal at the centerline.

(4) We map the geometry of the beam element in (3) say in $\mathbb{R}^2$ into a natural coordinate space $\xi\eta$ in which ξ is along the axis of the beam and η is normal to the ξ axis and the origin of the coordinate system $\xi\eta$ is at the center of the beam element.

(5) We design p-version hierarchical local approximation in ξ and η using p-levels of p_ξ and p_η with appropriate choice of the orders of the space to ensure derived global differentiability of the local approximations. In this local approximation, displacements u_1 and u_2 are approximated by higher degree polynomials in ξ and η as well as of higher orders. Choices of p-levels p_ξ and p_η and the orders of the approximation space define deformation behavior of the beam axis as well as the deformation behavior of the beam cross-section. Thus, by choosing appropriate p_ξ and p_η desired kinematic description of the deformation of the beam axis as well as its cross-section can be achieved.

(6) Thus, now we have (1) conservation and balance laws (2) geometric description and local approximation for the beam finite element. The algebraic equation for the beam element are derived using Galerkin method with weak form (GM/WF) or residual functional i.e. least squares method [8–10]. For linear elastic reversible deformation, GM/WF yields unconditionally stable computational process [8, 9]. In all other cases LSM can be shown to yield unconditionally stable computational processes [8, 9].

(7) In this approach, desired kinematic requirements are realized through local approximations. The beam mathematical model can be described using classical as well as non-classical continuum mechanics. In this dissertation we only consider CCM.

2.3.1 Conservation and balance laws (CCM)

For small deformation, small strain, isothermal physics the balance of linear momenta and the linear constitutive theories for symmetric Cauchy stress tensor are given in section 1.2, subsection 1.2.1. For the new formulation presented in the following sections we consider stationary case i.e. BVPs only for the sake of simplicity in the numerical studies. Substituting strains into stresses and stresses into balance of linear momenta yield the following PDEs in u_1 and u_2 for stationary case (BVPs).

$$-\frac{\partial}{\partial x_1}\left(D_{11}\frac{\partial u_1}{\partial x_1}+D_{12}\frac{\partial u_2}{\partial x_2}\right)-\frac{\partial}{\partial x_2}\left(D_{33}\left(\frac{\partial u_1}{\partial x_2}+\frac{\partial u_2}{\partial x_1}\right)\right)-\rho_0 F_1^b=0 \tag{2.84}$$

$$\begin{aligned}-\frac{\partial}{\partial x_1}\left(D_{33}\left(\frac{\partial u_1}{\partial x_2}+\frac{\partial u_2}{\partial x_1}\right)\right)-\frac{\partial}{\partial x_2}\left(D_{21}\frac{\partial u_1}{\partial x_1}+D_{22}\frac{\partial u_2}{\partial x_2}\right)-\rho_0 F_2^b=0\\ \forall x_1, x_2 \in \Omega\end{aligned} \tag{2.85}$$

with boundary conditions

$$u_1=\hat{u}_1\ ,\ u_2=\hat{u}_2 \quad \text{on } \Gamma_1 \tag{2.86}$$

and

$$\left.\begin{aligned}\left(D_{11}\frac{\partial u_1}{\partial x_1}+D_{12}\frac{\partial u_2}{\partial x_2}\right)n_x+D_{33}\left(\frac{\partial u_1}{\partial x_2}+\frac{\partial u_2}{\partial x_1}\right)n_y=q_{n_x}\\ D_{33}\left(\frac{\partial u_1}{\partial x_2}+\frac{\partial u_2}{\partial x_1}\right)n_x+\left(D_{21}\frac{\partial u_1}{\partial x_1}+D_{22}\frac{\partial u_2}{\partial x_2}\right)n_y=q_{n_y}\end{aligned}\right\} \text{ on } \Gamma_2 \tag{2.87}$$

Ω is the open domain of the BVP and $\bar{\Omega}=\Omega\cup\Gamma$, $\Gamma=\Gamma_1\cup\Gamma_2$. n_x, n_y are direction cosines of a unit exterior normal to the boundary Γ_2. q_{n_x} and q_{n_y} are known data. The coefficients $D_{11}=D_{22}$, $D_{21}=D_{12}$ and D_{33} are functions of modulus of elasticity E and Poisson's ratio ν [8]. Equations (2.84) and (2.85) are the complete mathematical model for bending of beam in displacements u_1 and u_2 and traction boundary conditions on boundaries Γ_2 and displacement boundary conditions on Γ_1.

2.3.2 Finite element formulation

We use mathematical model (2.84) and (2.85) with boundary conditions (2.86) and (2.87) to construct a finite element formulation in which the geometry of the finite element is same as conventional beam element, but the currently used kinematic assumptions similar to EBT and TBT are not used. First, we note that the differential operator $\boldsymbol{A}$ in (2.84) and (2.85) (also (2.89)) is linear and its Adjoint $\boldsymbol{A}^*$ is same as the operator $\boldsymbol{A}$, hence Galerkin method with weak form is ideally suited for constructing a variationally consistent (VC) integral form [8]. We could also consider integral form based on residual functional for constructing finite element formulation (least squares finite element method). The integral form in this method is also VC. In the following we consider Galerkin method with weak form. If we consider $\bar{\Omega}^T$ as discretization of $\bar{\Omega}$, then

$$\bar{\Omega}^T = \underset{e}{\cup} \bar{\Omega}^e \tag{2.88}$$

in which $\bar{\Omega}^e$ is a typical element of the discretization. Let us represent (2.84) and (2.85) as

$$-\boldsymbol{A}\boldsymbol{\phi} - \boldsymbol{f} = 0 \tag{2.89}$$

in which $\boldsymbol{A}$ is the differential operator $\boldsymbol{\phi}$ consists of u_1 and u_2 and $\boldsymbol{f}$ is a vector of $\rho_0 F_1^b$ and $\rho_0 F_2^b$. Let $\boldsymbol{\phi}_h$ be approximation of $\boldsymbol{\phi}$ over $\bar{\Omega}^T$, then using fundamental lemma of calculus of variation [8] we can write

$$(-\boldsymbol{A}\boldsymbol{\phi}_h - \boldsymbol{f}, \boldsymbol{v})_{\bar{\Omega}^T} = 0 \tag{2.90}$$

Let

$$\boldsymbol{\phi}_h = \underset{e}{\cup} \boldsymbol{\phi}_h^e \tag{2.91}$$

be the approximation of ϕ over $\bar{\Omega}^T$ in which $\boldsymbol{\phi}_h^e$ is the local approximation of $\boldsymbol{\phi}$ over an element e with spatial domain $\bar{\Omega}^e$ and $\boldsymbol{v}$ is the test function. In Galerkin method and in Galerkin method with weak form we choose $\boldsymbol{v} = \delta\boldsymbol{\phi}_h$.

Using (2.91), we can write (2.90) as

$$\sum_e (-\boldsymbol{A}\boldsymbol{\phi}_h^e - \boldsymbol{f}, \boldsymbol{v})_{\bar{\Omega}^e} = 0 \quad ; \quad \boldsymbol{v} = \delta\boldsymbol{\phi}_h^e \tag{2.92}$$

We consider $(-\boldsymbol{A}\boldsymbol{\phi}_h^e - \boldsymbol{f}, \boldsymbol{v})_{\bar{\Omega}^e}$ for an element e and transfer half of the differentiation from $\boldsymbol{\phi}_h^e$ to $\boldsymbol{v}$ using integration by parts [8] to obtain

$$(-\boldsymbol{A}\boldsymbol{\phi}_h^e - \boldsymbol{f}, \boldsymbol{v})_{\bar{\Omega}^e} = B^e(\boldsymbol{\phi}_h^e, \boldsymbol{v}) - l^e(\boldsymbol{v}) - \underset{\sim}{l}^e(\boldsymbol{v}) \tag{2.93}$$

in which $l^e(\boldsymbol{v})$ is due to $\boldsymbol{f}$ and $\underset{\sim}{l}^e(\boldsymbol{v})$ is due to integration by parts, hence contains secondary variables similar to those defined by (2.87).

We substitute $\boldsymbol{\phi}_h^e$ and $\boldsymbol{v} = \delta\boldsymbol{\phi}_h^e$ in (2.93) once local approximation $\boldsymbol{\phi}_h^e$ is defined by

$$\{\phi_h^e\} = [N]\{\delta^e\} = [N] \begin{Bmatrix} \{\delta_{u_1}^e\} \\ \{\delta_{u_2}^e\} \end{Bmatrix} \tag{2.94}$$

in which $[N]$ are local approximation functions and $\{\delta_{u_1}^e\}$ and $\{\delta_{u_2}^e\}$ are nodal degrees of freedom for the local approximations $(u_1)_h^e$ and $(u_2)_h^e$ of u_1 and u_2 in $\{\phi_h^e\}$ over $\bar{\Omega}^e$. The resulting equations for an element e can be written as

$$(-\boldsymbol{A}\boldsymbol{\phi}_h^e - \boldsymbol{f}, \boldsymbol{v})_{\bar{\Omega}^e} = [K^e]\{\delta^e\} - \{f^e\} - \{P^e\} \tag{2.95}$$

in which

$$[K^e] = \int_{\bar{\Omega}^e} [B]^T [D][B] d\Omega \tag{2.96}$$

$$\{f^e\} = \int_{\bar{\Omega}^e} [N]^T \{f\} d\Omega \tag{2.97}$$

$$\{P^e\} \ : \ \text{a vector of unknown secondary varible} \tag{2.98}$$

The matrix $[B]$ is defined by

$$\{\varepsilon\} = [B]\{\delta^e\} \tag{2.99}$$

Thus, to calculate $[K^e]$ and $\{f^e\}$ we need to establish local approximation $\{\phi_h^e\}$ in (2.94). We note that $[K^e] = [K^e]^T$, a consequence of $\boldsymbol{A}^* = \boldsymbol{A}$ and the integration by parts.

2.3.2.1 Beam element geometry and local approximation

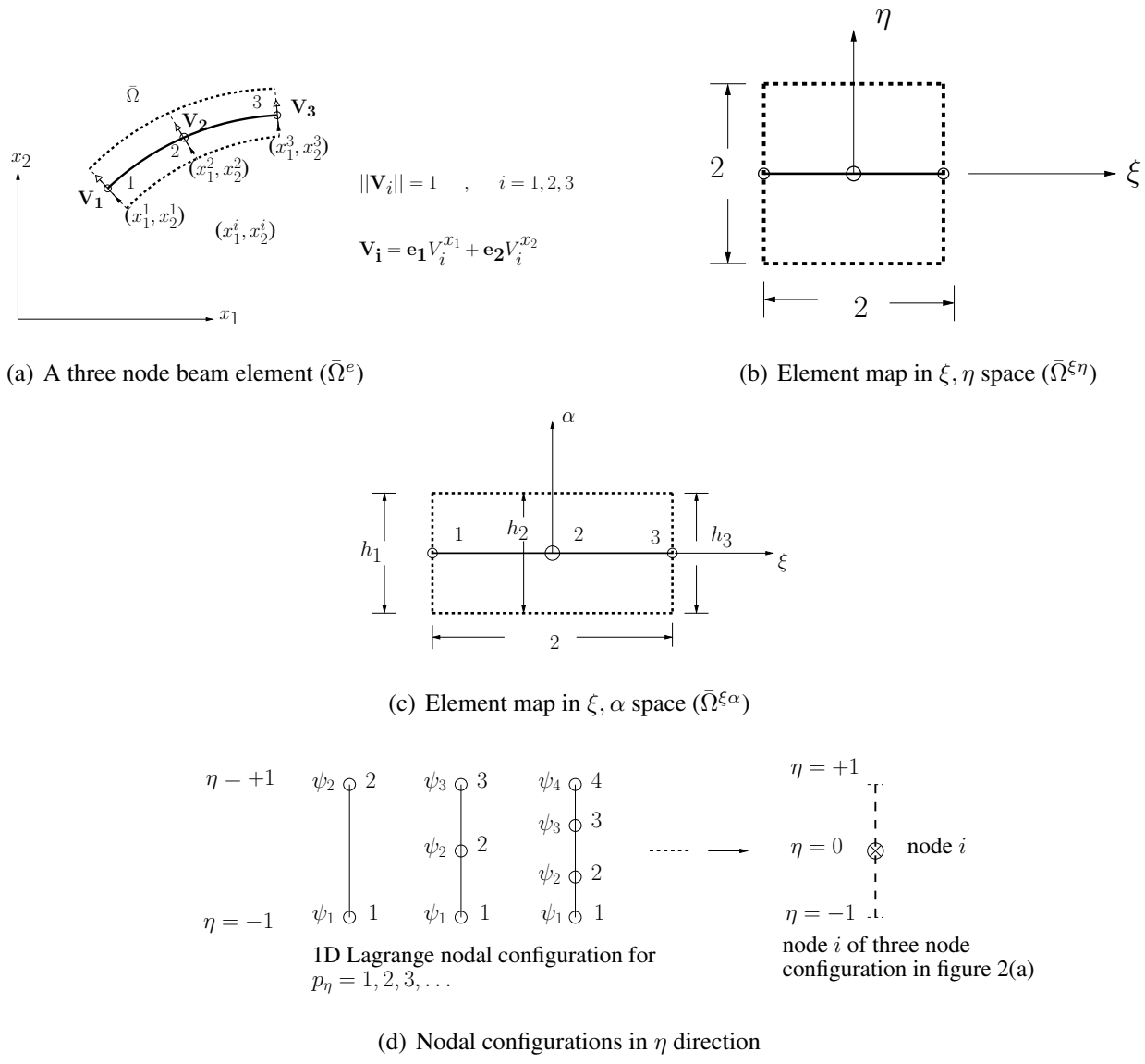

(a) A three node beam element ($\bar{\Omega}^e$)

(b) Element map in ξ, η space ($\bar{\Omega}^{\xi\eta}$)

(c) Element map in ξ, α space ($\bar{\Omega}^{\xi\alpha}$)

(d) Nodal configurations in η direction

Figure 2.2: Beam element geometry, mappings and nodal configurations

Consider a 2D beam element in x_1x_2 space shown in Figure 2.2(a). The element geometry consists of three nodes located at the centerline with unit vectors $\boldsymbol{V}_i$, $i = 1, 2, 3$ normal to the middle surface at each node. The beam height and width (normal to x_1x_2 plane) can vary along the length of the beam. Let h_i, b_i ; $i = 1, 2, 3$ be their values at the nodes. The element geometry $\bar{\Omega}^e$ in the physical space x_1, x_2 is mapped into natural coordinate space ξ, η in a two unit square ($\bar{\Omega}^{\xi\eta}$) using

$$\begin{Bmatrix} x_1(\xi,\eta) \\ x_2(\xi,\eta) \end{Bmatrix} = \sum_{i=1}^{3} \widetilde{N}_i(\xi) \begin{Bmatrix} (x_1)^i \\ (x_2)^i \end{Bmatrix} + \sum_{i=1}^{3} \widetilde{N}_i(\xi) \frac{\eta}{2} h_i \begin{Bmatrix} V_i^{x_1} \\ V_i^{x_2} \end{Bmatrix} \tag{2.100}$$

in which

$$\boldsymbol{V}_i = \boldsymbol{e}_1 V_i^{x_1} + \boldsymbol{e}_2 V_i^{x_2} \quad \text{and} \quad ||\boldsymbol{V}_i|| = 1 \ ; \ i = 1, 2, 3 \tag{2.101}$$

$\widetilde{N}(\xi)$ are standard Lagrange quadratic interpolation functions (for p-level of two).

Consider local approximations $(u_1)_h^e(\xi,\eta)$ and $(u_2)_h^e(\xi,\eta)$ of u_1 and u_2 over $\bar{\Omega}^{\xi\eta}$ for an element e (Figure 2.2(b)). We construct this by taking tensor product of appropriate 1D functions in ξ and η direction, keeping in mind that since all dofs at the nodes are not the same, the tensor product procedure necessitates that we take tensor product of the functions and nodal variable operators separately. After the tensor product the resulting 2D nodal variable operators when act on the dependent variable produces the corresponding degrees of freedom that correspond to the functions generated by taking tensor product of 1D approximations in ξ and η for the beam element in x_1x_2 space.

For simplicity consider $C^{00}(\bar{\Omega}^e)$ local approximation for u_1 and u_2. To illustrate the details of the derivation, let us consider ψ to be the dependent variable for which we wish to establish local approximation functions $[N(\xi,\eta)]$ such that

$$\psi_h^e(\xi,\eta) = [N(\xi,\eta)]\{\delta_\psi^e\} \tag{2.102}$$

the C^0 p-version local approximation for ψ in the ξ direction for the three node configuration at

the centerline ($\eta = 0$) can be written as [8].

$$\psi(\xi) = \left(\frac{1-\xi}{2}\right)\psi_1 + \left(\frac{1+\xi}{2}\right)\psi_3 + \sum_{i=1}^{p_\xi}\left(\frac{\xi^i - a}{i!}\right)\left.\frac{\partial^i \psi}{\partial \xi^i}\right|_{\xi=0}$$
$$a = \begin{cases} 1\ ; & \text{if } i \text{ is even} \\ \xi\ ; & \text{if } i \text{ is odd} \end{cases} \tag{2.103}$$

In the η direction the beam element node locations are at $\eta = 0$ (Figure 2.2(a)), hence the Lagrange local approximations in the η direction for $p_\eta = 1, 2, 3, \ldots$, etc. corresponding to nodal configurations containing nodes $2, 3, 4, \ldots$, etc. respectively need to be reduced down to a single node located at $\eta = 0$.

Figure 2.2(d) shows the $2, 3, 4, \ldots$, etc. nodal configurations in η direction for $p = 1, 2, 3, \ldots$ and a desired single node configuration in which the node is located at $\eta = 0$.

Figure 2.2(c) shows a map of $\bar{\Omega}^{\xi\eta}$ into $\bar{\Omega}^{\xi\alpha}$ in which at each of the three nodes we have

$$\eta = \frac{\alpha}{h_i/2}\ ;\ i = 1, 2, 3 \tag{2.104}$$

we consider a typical node i ($i = 1, 2, 3$; Figure 2.2(a)). For $p_\eta = 1$, the Lagrange interpolation for the two node configuration of Figure 2.2(d) in η direction can be written as

$$\psi(\eta) = \left(\frac{\psi_2 + \psi_1}{2}\right) + \eta\left(\frac{\psi_2 - \psi_1}{2}\right) \tag{2.105}$$

Substituting from (2.104) in (2.105)

$$\psi(\alpha) = \left(\frac{\psi_2 + \psi_1}{2}\right) + \frac{\alpha}{h_i/2}\left(\frac{\psi_2 - \psi_1}{2}\right) \tag{2.106}$$

$$\frac{\partial \psi}{\partial \alpha} = \frac{1}{h_i/2}\left(\frac{\psi_2 - \psi_1}{2}\right) = \left.\frac{\partial \psi}{\partial \alpha}\right|_{\alpha=0} \tag{2.107}$$

Hence,

$$\left(\frac{\psi_2 - \psi_1}{2}\right) = \frac{h_i}{2}\left.\frac{\partial \psi}{\partial \alpha}\right|_{\alpha=0} \tag{2.108}$$

and

$$\left(\frac{\psi_2 + \psi_1}{2}\right) = \psi \quad \text{for the node } i \text{ at } \eta = 0 \text{ or } \alpha = 0 \tag{2.109}$$

using (2.108) and (2.109) in (2.105)

$$\psi(\eta) = \psi + \left(\frac{\eta h_i}{2}\right)\left.\frac{\partial \psi}{\partial \alpha}\right|_{\alpha=0} \tag{2.110}$$

Likewise for $p_\eta = 2$, for the three node configuration in Figure 2.2(d), we can write (Lagrange interpolation)

$$\psi(\eta) = \psi_2 + \frac{\eta}{2}\left(\frac{\psi_3 - \psi_1}{2}\right) + \frac{\eta^2}{2}\left(\frac{\psi_1 - 2\psi_2 - \psi_3}{2}\right) \tag{2.111}$$

Following the same procedure as for $p_\eta = 1$ except that in this case differentiating $\psi(\alpha)$ twice with respect to α and evaluating the derivatives at $\alpha = 0$, we can obtain the following for node i.

$$\psi(\eta) = \psi + \left(\frac{\eta h_i}{2}\right)\left.\frac{\partial \psi}{\partial \alpha}\right|_{\alpha=0} + \left(\frac{\eta h_i}{2}\right)^2 \frac{1}{2!}\left.\frac{\partial^2 \psi}{\partial \alpha^2}\right|_{\alpha=0} \tag{2.112}$$

Following the same procedure, we can derive the following for a node i located at $\eta = 0$ for p-level of p_η.

$$\psi(\eta) = \psi + \left(\frac{\eta h_i}{2}\right)\left.\frac{\partial \psi}{\partial \alpha}\right|_{\alpha=0} + \left(\frac{\eta h_i}{2}\right)^2 \frac{1}{2!}\left.\frac{\partial^2 \psi}{\partial \alpha^2}\right|_{\alpha=0} + \cdots + \left(\frac{\eta h_i}{2}\right)^{p_\eta} \frac{1}{p_\eta!}\left.\frac{\partial^{\,p_\eta} \psi}{\partial \alpha^{p_\eta}}\right|_{\alpha=0} \tag{2.113}$$

we note that $\psi(\eta)$ in (2.113) is hierarchical i.e. lower p-level approximation is a complete subset of the higher p-level approximation.

In one-dimensional approximations (2.103) and (2.113) we separate the nodal variable operators and the approximation functions.

In ξ direction: for nodes 1, 2 *and* 3

Nodal variable operators: $1\ ;\ \dfrac{\partial^2}{\partial\xi^2}\ ,\ \ldots\ ,\ \dfrac{\partial^{p_\xi}}{\partial\xi^{p_\xi}}\ ;1$

Approximation functions: $\dfrac{1-\xi}{2}\ ;\ \dfrac{\xi^i-a}{i!}\ ;\ i=2,3,\ldots,p_\xi\ ;\ \dfrac{1+\xi}{2}$

In η direction: for node i at $\eta=0$ or $\alpha=0$

Nodal variable operators: $1\ ,\ \left.\dfrac{\partial}{\partial\alpha}\right|_{\alpha=0}\ ,\ \left.\dfrac{\partial^2}{\partial\alpha^2}\right|_{\alpha=0}\ ,\ \ldots\ ,\ \left.\dfrac{\partial^{\,p_\eta}}{\partial\alpha^{p_\eta}}\right|_{\alpha=0}$

Approximation functions: $1\ ,\ \dfrac{\eta h_i}{2}\ ,\ \left(\dfrac{\eta h_i}{2}\right)^2\dfrac{1}{2!}\ ,\ \ldots\ ,\ \left(\dfrac{\eta h_i}{2}\right)^{p_\eta}\dfrac{1}{p_\eta!}$

By taking tensor products of the 1D nodal variable operators in ξ and η and letting them act on ψ we obtain the degrees of freedom for $\psi_h^e(\xi,\eta)$ and the corresponding approximation functions are obtained by taking the tensor product of the 1D approximation functions in ξ and η, and we can write

$$\psi_h^e(\xi,\eta)=[N(\xi,\eta)]\{\delta_\psi^e\} \tag{2.114}$$

in which $\{\delta_\psi^e\}$ are the degrees of freedom. Using (2.114) for u_1 and u_2 we can write the following p-version hierarchical local approximation for u_1 and u_2 for an element e (assuming p_ξ and p_η to be same for u_1 and u_2).

$$\{\phi_h^e\}=\begin{Bmatrix}(u_1)_h^e\\(u_2)_h^e\end{Bmatrix}=\begin{bmatrix}[N(\xi,\eta)] & [0]\\ [0] & [N(\xi,\eta)]\end{bmatrix}\begin{Bmatrix}\{\delta_{u_1}^e\}\\\{\delta_{u_2}^e\}\end{Bmatrix} \tag{2.115}$$

In which $\{\delta_{u_1}^e\}$ and $\{\delta_{u_2}^e\}$ are the degrees of freedom for u_1 and u_2.

Computations of the coefficients of $[K^e]$ and $\{f^e\}$ in (2.96) and (2.97) are performed using gauss quadrature and the element map in $\bar{\Omega}^{\xi\eta}$. The details are a routine exercise (see [8]), hence not included here.

Remarks

(1) In this formulation p-levels in ξ and η direction control deformation behavior of the beam

axis as well as its cross-section.

(2) Increasing p_ξ yields higher degree approximations of u_1 and u_2 along the beam axis. While increase in p_η permits higher degree approximations of u_1 and u_2 in the directions of the depth of the beam.

(3) With $C^{00}(\bar{\Omega}^e)$ local approximation described here, the integral over $\bar{\Omega}^T$ are in Lebesgue sense. However, we could still study the convergence of the L_2-norm of the residual as a function of mesh refinement (h) and p-level increases ($p_\xi = p_\eta = p$), thus convergence of the solutions of class $C^{00}(\bar{\Omega}^e)$ to $C^{11}(\bar{\Omega}^e)$ in the weak sense. This provides a measure of the error in the computed solution.

(4) Local approximations of the higher order global differentiability can be easily derived and used as well [8].

(5) The new formulation presented here was originally derived in references [88–93] but using principle of virtual work and it holds only for reversible mechanical deformation.

Chapter 3

A New 2D Thermoviscoelastic beam formulation with damping

The New formulation developed in chapter 2 section 2.3 for the bending of Thermoelastic beams in which mechanical deformation is reversible is extended for bending of Thermoviscoelastic beams with damping (dissipation). We begin with the conservation and balance laws in $\mathbb{R}^2$ for Thermoviscoelastic solid matter with damping, presented in chapter 1, subsection 1.2.1.2. In this chapter finite element formulation based on this mathematical model in $\mathbb{R}^2$ is presented for bending of Thermoviscoelastic beams with damping.

The space-time differential operator in this case where the balance of linear momenta are expressed in terms of displacement is non-self adjoint (excluding energy equation), hence if we consider a space-time coupled finite element formulation, then only the space-time finite element formulation based on residual functional (space-time least squares finite element method) is space-time variationally consistent [9]. A space-time decoupled formulation based on Galerkin method with weak form in space [9] is constructed using balance of linear momenta expressed in displacements in the present work. As well known in this approach the space-time partial differential equations, Balance of Linear Momenta (BLM) are converted into a system of coupled Ordinary differential equations (ODEs) in time. Solutions of these equations are obtained using

(1) Direct time integration methods such as Wilson's θ method and Newmark method [9].

(2) Finite element method in time based on residual functional in time (Least Squares Method in time).

(3) The ODEs in time are transformed to modal basis using undamped natural modes of vibration. By introducing modal damping the ODEs in time become decoupled. These can be time integrated or we can use their theoretical solution [9]. Transient dynamic response is constructed using mode superposition technique.

Details of these formulations will be presented in this chapter. The energy equation can be treated decoupled from the balance of linear momenta if the material properties are not functions of temperature. A space-time least squares formulation can be constructed for the energy equation. For each time step the balance of linear momenta are solved first followed by the energy equation. This process is continued till the desired time is reached.

3.1 Mathematical Model

The mathematical model for bending of beam with dissipation mechanism in $2D$ consists of conservation and balance laws of classical continuum mechanics: conservation of mass, balance of linear momenta, balance of angular momenta, energy equation, entropy inequality and the constitutive theories for the stress tensor and the heat vector. Unlike thermoelastic beam, the thermoviscoelastic beams (without memory) have mechanism of dissipation which results in rate of generation of entropy, thus heat, hence in this physics the energy equation becomes intrinsic part of the mathematical model. The role of entropy inequality is primarily in the derivation of the constitutive theories and not in terms of additional equation in the mathematical model. In addition to isotropic homogeneous matter with small deformation and small strain we further assume that the material properties remain constant during the evolution, hence are not function of temperature (θ). The last assumption permits us to decouple energy equation from the balance of linear momenta.

We consider small strain, small deformation and isotropic homogeneous matter. The conservation and the balance laws of classical continuum mechanics: conservation of mass (CM), balance of linear momenta (BLM), balance of angular momenta (BAM), first law of thermodynamics (FLT), and the second law of thermodynamics (SLT) in Lagrangian description can be written as (in $\mathbb{R}^2$ for incompressible matter) follows for $\forall(x,t) \in \Omega_x = \Omega_x \times \Omega_t$

$$\rho_0 = |J|\rho \ ; \ |J| = 1 \quad \text{(CM)} \tag{3.1}$$

$$\rho_0 \frac{\partial^2 u_i}{\partial t^2} - \rho_0 F_i^b - \frac{\partial \sigma_{ji}}{\partial x_j} = 0 \ ; \ i,j = 1,2 \quad \text{(BLM)} \tag{3.2}$$

$$\sigma_{ij} = \sigma_{ji} \quad \text{(BAM)} \tag{3.3}$$

$$\rho_0 \frac{De}{Dt} + \frac{\partial q_i}{\partial x_i} - \sigma_{ij}\dot{\varepsilon}_{ji} = 0 \ ; \ i,j = 1,2 \quad \text{(FLT)} \tag{3.4}$$

$$\rho_0 \left(\frac{D\Phi}{Dt} + \eta \frac{D\theta}{Dt} \right) + \frac{q_i g_i}{\theta} - \sigma_{ij}\dot{\varepsilon}_{ji} \leq 0 \ ; \ i,j = 1,2 \quad \text{(SLT)} \tag{3.5}$$

in which u_i are displacements, F_i^b are body forces per unit mass, σ_{ij} are the Cauchy stress tensor, e is the specific internal energy, q_i are heat flux, $\dot{\varepsilon}_{ij}$ are strain rates, Φ is Helmholtz free energy density, η is entropy density, θ is absolute temperature. We note that $\sigma_{ij}\dot{\varepsilon}_{ji}$ is rate of work per unit volume. From entropy inequality $\boldsymbol{\sigma}$ and $\dot{\boldsymbol{\varepsilon}}$ are rate of work conjugate and $\boldsymbol{q}$ and $\boldsymbol{g}$ are conjugate pair. Choice of Φ, η, $\boldsymbol{\sigma}$, and $\boldsymbol{q}$ as constitutive variables is rather straight forward. $\boldsymbol{\varepsilon}$ is argument tensor of $\boldsymbol{\sigma}$, $\boldsymbol{g}$ is argument tensor of $\boldsymbol{q}$. Additionally $\dot{\boldsymbol{\varepsilon}}$ or $\boldsymbol{\varepsilon}_{[1]}$ needs to be argument tensor of $\boldsymbol{\sigma}$ due to dissipation. Further generalization of the choice of $\boldsymbol{\varepsilon}_{[1]}$ leads to $\boldsymbol{\varepsilon}_{[i]} \ ; \ i = 1,2,\ldots,n$ as argument tensors of $\boldsymbol{\sigma}$. Based on principle of equipresence we can write the following

$$\begin{aligned}
\Phi &= \Phi(\boldsymbol{\varepsilon}, \boldsymbol{\varepsilon}_{[i]} \ ; \ i = 1,2,\ldots,n, \boldsymbol{g}, \theta) \\
\eta &= \eta(\boldsymbol{\varepsilon}, \boldsymbol{\varepsilon}_{[i]} \ ; \ i = 1,2,\ldots,n, \boldsymbol{g}, \theta) \\
\boldsymbol{\sigma} &= \boldsymbol{\sigma}(\boldsymbol{\varepsilon}, \boldsymbol{\varepsilon}_{[i]} \ ; \ i = 1,2,\ldots,n, \boldsymbol{g}, \theta) \\
\boldsymbol{q} &= \boldsymbol{q}(\boldsymbol{\varepsilon}, \boldsymbol{\varepsilon}_{[i]} \ ; \ i = 1,2,\ldots,n, \boldsymbol{g}, \theta)
\end{aligned} \tag{3.6}$$

Substituting $\dot{\Phi}$ (obtained by using chain rule of differentiation) in the entropy inequality and group-

ing the terms and ensuring that entropy inequality is satisfied for arbitrary but admissible rates of various quantities, we obtain the following [24].

$$\begin{aligned}
&\Phi = \Phi(\boldsymbol{\varepsilon}, \theta) \\
&\eta = -\frac{\partial \Phi}{\partial \theta} \\
&\boldsymbol{\sigma} = \boldsymbol{\sigma}(\boldsymbol{\varepsilon}, \boldsymbol{\varepsilon}_{[i]} \ ; \ i = 1, 2, \ldots, n, \theta) \\
&\boldsymbol{q} = \boldsymbol{q}(\boldsymbol{g}, \theta)
\end{aligned} \tag{3.7}$$

and entropy inequality reduces to

$$\left(\rho_0 \frac{\partial \Phi}{\partial \varepsilon_{kl}} - \sigma_{lk} \right) \dot{\varepsilon}_{kl} + \frac{q_i g_i}{\theta} \leq 0 \tag{3.8}$$

We have assumed that $\boldsymbol{\sigma}$ and $\boldsymbol{q}$ have no dependence on $\boldsymbol{g}$ and $\boldsymbol{\varepsilon}, \boldsymbol{\varepsilon}_{[i]} \ ; \ i = 1, 2, \ldots, n$, respectively.

For incompressible solid continua decomposition of Cauchy stress tensor into equilibrium and deviatoric stress is not needed. The constitutive theory for $\boldsymbol{\sigma}$ suffices and $\Phi = \Phi(\theta)$, hence the first of the three terms in (3.8) is zero, thus (3.8) reduces to

$$\frac{q_i g_i}{\theta} - \sigma_{ij} \dot{\varepsilon}_{ji} \leq 0 \tag{3.9}$$

Thus, (3.9) is satisfied if $\frac{q_i g_i}{\theta} \leq 0$ and rate of work is non-negative i.e. $\sigma_{ij} \dot{\varepsilon}_{ji} \geq 0$. The final argument

$$\begin{aligned}
&\Phi = \Phi(\theta) \\
&\eta = -\frac{\partial \Phi}{\partial \theta} \\
&\boldsymbol{\sigma} = \boldsymbol{\sigma}(\boldsymbol{\varepsilon}, \boldsymbol{\varepsilon}_{[i]} \ ; \ i = 1, 2, \ldots, n) \\
&\boldsymbol{q} = \boldsymbol{q}(\boldsymbol{g}, \theta)
\end{aligned} \tag{3.10}$$

Using representation theorem, ordered rate constitutive theory of order n (in strain rates) can be derived for $\boldsymbol{\sigma}$ [24]. Likewise we can derive constitutive theory for $\boldsymbol{q}$ in $\boldsymbol{g}$ and θ. These constitutive

theories are obviously nonlinear in the components of the argument tensors. In the work presented here we only consider linear constitutive theories for $\boldsymbol{\sigma}$ and $\boldsymbol{q}$ in which product terms, initial stress field and temperature terms are neglected. These constitutive theories for $\boldsymbol{\sigma}$ and $\boldsymbol{q}$ are given by [24].

$$\boldsymbol{\sigma} = a_1\boldsymbol{\varepsilon} + a_2\big(\mathrm{tr}(\boldsymbol{\varepsilon})\big)\boldsymbol{I} + \sum_{i=1}^{n} b_i^1\boldsymbol{\varepsilon}_{[i]} + \sum_{i=1}^{n} b_i^2\big(\mathrm{tr}(\boldsymbol{\varepsilon}_{[i]})\big)\boldsymbol{I} \tag{3.11}$$

If we express $\boldsymbol{\sigma}$, $\boldsymbol{\varepsilon}$, and $\boldsymbol{\varepsilon}_{[i]}$; $i = 1, 2, \ldots, n$ in Voigt's notation using $\{\sigma\}^T = [\sigma_{11} \quad \sigma_{22} \quad \sigma_{12}]$ and defining $\{\varepsilon\}^T = [\varepsilon_{11} \quad \varepsilon_{22} \quad \varepsilon_{12}]$, $\{\dot{\varepsilon}_{[i]}\}^T = [(\dot{\varepsilon}_{[i]})_{11} \quad (\dot{\varepsilon}_{[i]})_{22} \quad (\dot{\varepsilon}_{[i]})_{12}]$.

$$\{\sigma\} = [\underline{a}]\{\varepsilon\} + \sum_{i=1}^{n} [\underline{b}_i]\{\varepsilon_{[i]}\} \tag{3.12}$$

in which

$$[\underline{a}] = \begin{bmatrix} a_1 + a_2 & a_2 & 0 \\ a_2 & a_1 + a_2 & 0 \\ 0 & 0 & a_2 \end{bmatrix} \tag{3.13}$$

for isotropic linear elastic solid matter $a_1 = 2\mu$ and $a_2 = \lambda$, Lame's constants (assumed constant in the present work). $[\underline{b}_i]$ are obtained from $[\underline{a}]$ by replacing a_1 with b_i^1 and a_2 with b_i^2. $\{\varepsilon\}$ contributes to reversible elasticity where as $\{\dot{\varepsilon}_{[i]}\}$ contribute to ordered rate dissipation mechanism and

$$q_i = -kg_i \tag{3.14}$$

For simple physics we can consider the following for e.

$$e = C_v\theta \tag{3.15}$$

in which C_v is specific heat (assumed constant) and k is thermal conductivity (also assumed constant).

The final mathematical model is given in the following for $\forall(x,t) \in \Omega_{xt} = \Omega_x \times \Omega_t$.

$$\left.\begin{aligned} A_1(u_1,u_2) = \quad & \rho_0 \frac{\partial^2 u_1}{\partial t^2} - \rho_0 F_1^b - \frac{\partial \sigma_{11}}{\partial x_1} - \frac{\partial \sigma_{21}}{\partial x_2} = 0 \\ A_2(u_1,u_2) = \quad & \rho_0 \frac{\partial^2 u_2}{\partial t^2} - \rho_0 F_2^b - \frac{\partial \sigma_{12}}{\partial x_1} - \frac{\partial \sigma_{22}}{\partial x_2} = 0 \end{aligned}\right\} \quad \text{(BLM)} \tag{3.16}$$

$$\sigma_{21} = \sigma_{12} \quad \text{(BAM)} \tag{3.17}$$

$$\{\sigma\} = [\underset{\sim}{a}]\{\varepsilon\} + \sum_{i=1}^{n} [b_i]\{\varepsilon_{[i]}\} \tag{3.18}$$

$$\{\varepsilon\} = \begin{Bmatrix} \dfrac{\partial u_1}{\partial x_1} \\ \dfrac{\partial u_2}{\partial x_2} \\ \dfrac{1}{2}\left(\dfrac{\partial u_1}{\partial x_2} + \dfrac{\partial u_2}{\partial x_1}\right) \end{Bmatrix} \tag{3.19}$$

$$\rho_0 C_v \frac{\partial \theta}{\partial t} - k\left(\frac{\partial^2 \theta}{\partial {x_1}^2} + \frac{\partial^2 \theta}{\partial {x_2}^2}\right) - \sigma_{ij}\dot{\varepsilon}_{ji} = 0 \ ; \ i,j = 1,2 \quad \text{(FLT)} \tag{3.20}$$

$\{q_i\}$ and e from (3.14) and (3.15) have been substituted in the energy equation in (3.20). If the material coefficients are constant (not a function of θ) then equations (3.16), (3.18), and (3.19) can be considered decoupled from the energy equation. In this approach, we can solve for u_1, u_2 and then $\boldsymbol{\varepsilon}$, $\boldsymbol{\varepsilon}_{[i]}$, and $\boldsymbol{\sigma}$ from (3.18) and (3.19) for an increment of time and then use these in the energy equation to solve for temperature θ. That is, for each increment of time we solve (3.16), (3.18), and (3.19) followed by solution of (3.20). If we substitute (3.19) in (3.18), and substitute (3.18) in the BLM (3.16), then we obtain a system of two equations in displacement u_1 and u_2. These are ideally suited for using space-time decoupled finite element method in time in which the integral form in space is constructed by using Galerkin method with weak form (GM/WF). In case of the energy equation (3.20) a space-time finite element method based on residual functional (space-time least squares process, STLSP) is ideally suited as in (3.20) the $A^* \neq A$ in which the space-time operator A is given by

$$A = \rho_0 C_v \frac{\partial}{\partial t} - k\left(\frac{\partial^2}{\partial {x_1}^2} + \frac{\partial^2}{\partial {x_2}^2}\right) \tag{3.21}$$

obviously

$$A^* = -\rho_0 C_v \frac{\partial}{\partial t} - k\left(\frac{\partial^2}{\partial {x_1}^2} + \frac{\partial^2}{\partial {x_2}^2}\right) \neq A \tag{3.22}$$

we present both finite element formulation in the following.

3.2 Finite element formations of the BLM equations and the energy equation

3.2.1 Finite element formulation of the BLM equations using space-time decoupled GM/WF

This formulation is facilitated if we consider equations (3.16), (3.18), and (3.19) as they are. Let $\bar{\Omega}_x^T$ be discretization of spatial domain $\bar{\Omega}_x$ such that

$$\bar{\Omega}_x^T = \underset{e}{\cup} \bar{\Omega}_x^e \tag{3.23}$$

in which $\bar{\Omega}_x^e$ is a typical 2D beam element (figure 3.1(a)). Figure 3.1(b) shows map of $\bar{\Omega}_x^e$ in natural coordinate space $\xi\eta$ in a two unit square. Following details in reference [9] we construct integral form of equation (3.16) over $\bar{\Omega}^e$ using Fundamental Lemma of the calculus of variations [9]. Let $(u_1)_h^e$, $(u_2)_h^e$ be approximation of u_1, u_2 over $\bar{\Omega}_x^e$, then using equal order equal degree approximations of u_1 and u_2 we have

$$\begin{aligned} (u_1(\xi,\eta,t))_h^e &= \sum_{i=1}^{n^{u_1}} N_i^{u_1}(\xi,\eta)\delta_i^{u_1}(t) \\ (u_2(\xi,\eta,t))_h^e &= \sum_{i=1}^{n^{u_2}} N_i^{u_2}(\xi,\eta)\delta_i^{u_2}(t) \end{aligned} \tag{3.24}$$

in which $N_i^{u_1}(\xi,\eta)$ and $N_i^{u_2}(\xi,\eta)$ are approximation functions (only functions of spatial coordinates ξ,η) for $(u_1)_h^e$ and $(u_2)_h^e$ and $\delta_i^{u_1}(t)$ and $\delta_i^{u_2}(t)$ are nodal degrees of freedom (functions of time

only) for u_1 and u_2. Let w_1 and w_2 be test function such that $w_1 = \delta(u_1)_h^e$ and $w_2 = \delta(u_2)_h^e$, then obviously

$$\begin{aligned} w_1 &= N_j^{u_1}(\xi,\eta)\ ;\ j = 1,2,\ldots,n^{u_1} \\ w_2 &= N_j^{u_2}(\xi,\eta)\ ;\ j = 1,2,\ldots,n^{u_2} \end{aligned} \tag{3.25}$$

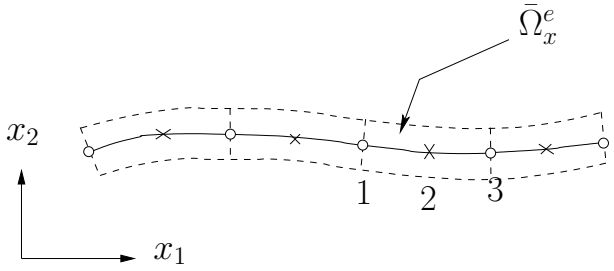

(a) Discretization $\bar{\Omega}_x^T$ of $\bar{\Omega}_x$

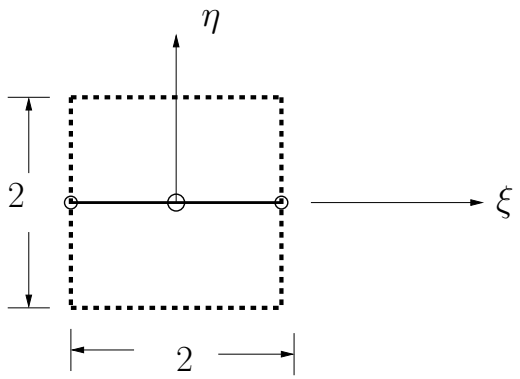

(b) Map of $\bar{\Omega}_x^e$ in natural coordinate space $\xi\eta$

Figure 3.1: Discretization of spatial domain $\bar{\Omega}$ into $\bar{\Omega}^T$ and map of an element $\bar{\Omega}_x^e$ in natural coordinate space

Consider scalar products

$$(A_1((u_1)_h^e,(u_2)_h^e),w_1)_{\bar{\Omega}_x^e} \quad \text{and} \quad (A_2((u_1)_h^e,(u_2)_h^e),w_2)_{\bar{\Omega}_x^e} \tag{3.26}$$

$$(A_1((u_1)_h^e,(u_2)_h^e),w_1)_{\bar{\Omega}_x^e}=\left(\rho_0\frac{\partial^2(u_1)_h^e}{\partial t^2},w_1\right)_{\bar{\Omega}_x^e}-\left(\rho_0 F_1^b,w_1\right)_{\bar{\Omega}_x^e}-\left(\left(\frac{\partial(\sigma_{11})_h^e}{\partial x_1}+\frac{\partial(\sigma_{21})_h^e}{\partial x_2}\right),w_1\right)_{\bar{\Omega}_x^e} \tag{3.27}$$

$$(A_2((u_1)_h^e,(u_2)_h^e),w_2)_{\bar{\Omega}_x^e}=\left(\rho_0\frac{\partial^2(u_2)_h^e}{\partial t^2},w_2\right)-\left(\rho_0 F_2^b,w_2\right)_{\bar{\Omega}_x^e}-\left(\left(\frac{\partial(\sigma_{12})_h^e}{\partial x_1}+\frac{\partial(\sigma_{22})_h^e}{\partial x_2}\right),w_2\right)_{\bar{\Omega}_x^e} \tag{3.28}$$

Integrate by parts once in the third term in equation (3.27) and (3.28)

$$(A_1((u_1)_h^e,(u_2)_h^e),w_1)_{\bar{\Omega}_x^e}=\left(\rho_0\frac{\partial^2(u_1)_h^e}{\partial t^2},w_1\right)_{\bar{\Omega}_x^e}-\left(\rho_0 F_1^b,w_1\right)_{\bar{\Omega}_x^e}+\int\limits_{\bar{\Omega}_x^e}\left(\frac{\partial w_1}{\partial x_1}(\sigma_{11})_h^e+\frac{\partial w_1}{\partial x_2}(\sigma_{21})_h^e\right)d\Omega-\oint\limits_{\Gamma^e}\Big((\sigma_{11})_h^e n_{x1}+(\sigma_{21})_h^e n_{x2}\Big)w_1 d\Gamma \tag{3.29}$$

and

$$(A_2((u_1)_h^e,(u_2)_h^e),w_2)_{\bar{\Omega}_x^e}=\left(\rho_0\frac{\partial^2(u_2)_h^e}{\partial t^2},w_2\right)-\left(\rho_0 F_2^b,w_2\right)_{\bar{\Omega}_x^e}+\int\limits_{\bar{\Omega}_x^e}\left(\frac{\partial w_2}{\partial x_1}(\sigma_{12})_h^e+\frac{\partial w_2}{\partial x_2}(\sigma_{22})_h^e\right)d\Omega-\oint\limits_{\Gamma^e}\Big((\sigma_{12})_h^e n_{x1}+(\sigma_{22})_h^e n_{x2}\Big)w_2 d\Gamma \tag{3.30}$$

Let t_x and t_y be the secondary variables defined by

$$t_x=(\sigma_{11})_h^e n_{x1}+(\sigma_{21})_h^e n_{x2}\quad,\quad t_y=(\sigma_{12})_h^e n_{x1}+(\sigma_{22})_h^e n_{x2} \tag{3.31}$$

Substituting $(u_1)_h^e$ and $(u_2)_h^e$ from (3.24) into equation (3.18) we obtain

$$\{(\sigma)_h^e\}=[\underline{a}]\{(\varepsilon)_h^e\}+\sum_{i=1}^{n}[\underline{b}_i]\{(\varepsilon_{[i]})_h^e\} \tag{3.32}$$

Substituting (3.31), (3.32), (3.25), and (3.24) in (3.29) and (3.30) and noting

$$\frac{\partial^2(u_1)_h^e}{\partial t^2} = \sum_{i=1}^{n^{u_1}} N_i^{u_1}(\xi,\eta)\ddot{\delta}_{u_1}^e(t) \ , \ \frac{\partial^2(u_2)_h^e}{\partial t^2} = \sum_{i=1}^{n^{u_2}} N_i^{u_2}(\xi,\eta)\ddot{\delta}_{u_2}^e(t) \tag{3.33}$$

we obtain the following

$$\begin{Bmatrix} (A_1((u_1)_h^e,(u_2)_h^e),w_1)_{\bar{\Omega}_x^e} \\ (A_2((u_1)_h^e,(u_2)_h^e),w_2)_{\bar{\Omega}_x^e} \end{Bmatrix} = [M^e]\{\delta_{[2]}^e\} + \sum_{i=1}^{n}[C_{[i]}^e]\{\delta_{[i]}^e\} + [K^e]\{\delta^e\} - \{F^e\} - \{P^e\} \tag{3.34}$$

where

$$\begin{aligned} [M^e] &= \begin{bmatrix} [M_{11}^e] & [M_{12}^e] \\ [M_{21}^e] & [M_{22}^e] \end{bmatrix} \ ; \ [C_{[i]}^e] = \begin{bmatrix} [(C_{[i]}^e)_{11}^e] & [(C_{[i]}^e)_{12}^e] \\ [(C_{[i]}^e)_{21}^e] & [(C_{[i]}^e)_{22}^e] \end{bmatrix} \\ [K^e] &= \begin{bmatrix} [K_{11}^e] & [K_{12}^e] \\ [K_{21}^e] & [K_{22}^e] \end{bmatrix} \ ; \ \{\delta^e\} = \begin{Bmatrix} \{\delta_{u_1}^e\} \\ \{\delta_{u_2}^e\} \end{Bmatrix} \end{aligned} \tag{3.35}$$

$$\{\delta_{[i]}^e\} = \left\{\frac{d^i}{dt^i}\{\delta^e\}\right\} = \begin{Bmatrix} \frac{d^i}{dt^i}\{\delta_{u_1}^e\} \\ \frac{d^i}{dt^i}\{\delta_{u_2}^e\} \end{Bmatrix} \ ; i = 1,2,\ldots,n \tag{3.36}$$

in which

$$\begin{aligned} (M_{11}^e)_{ij} &= \int_{\bar{\Omega}_x^e} N_i^{u_1} N_j^{u_1} d\Omega \ ; \ i,j = 1,2,\ldots,n^{u_1} \\ (M_{12}^e)_{ij} &= [M_{21}^e] = [0] \\ (M_{22}^e)_{ij} &= \int_{\bar{\Omega}_x^e} N_i^{u_2} N_j^{u_2} d\Omega \ ; \ i,j = 1,2,\ldots,n^{u_2} \end{aligned} \tag{3.37}$$

$$
\begin{aligned}
(K^e_{11})_{ij} &= \int_{\bar{\Omega}^e_x} \frac{\partial N^{u_1}_i}{\partial x_1} \underline{a}_{11} \frac{\partial N^{u_1}_j}{\partial x_1} + \frac{\partial N^{u_1}_i}{\partial x_2} \underline{a}_{33} \frac{\partial N^{u_1}_j}{\partial x_2} d\Omega \; ; \; i,j = 1,2,\ldots,n^{u_1} \\
(K^e_{12})_{ij} &= \int_{\bar{\Omega}^e_x} \frac{\partial N^{u_1}_i}{\partial x_1} \underline{a}_{12} \frac{\partial N^{u_2}_j}{\partial x_2} + \frac{\partial N^{u_1}_i}{\partial x_2} \underline{a}_{33} \frac{\partial N^{u_2}_j}{\partial x_1} d\Omega \; ; \; \begin{matrix} i = 1,2,\ldots,n^{u_1} \\ j = 1,2,\ldots,n^{u_2} \end{matrix} \\
(K^e_{21})_{ij} &= \int_{\bar{\Omega}^e_x} \frac{\partial N^{u_2}_i}{\partial x_1} \underline{a}_{33} \frac{\partial N^{u_1}_j}{\partial x_2} + \frac{\partial N^{u_2}_i}{\partial x_2} \underline{a}_{21} \frac{\partial N^{u_1}_j}{\partial x_1} d\Omega \; ; \; \begin{matrix} i = 1,2,\ldots,n^{u_2} \\ j = 1,2,\ldots,n^{u_1} \end{matrix} \\
(K^e_{22})_{ij} &= \int_{\bar{\Omega}^e_x} \frac{\partial N^{u_2}_i}{\partial x_1} \underline{a}_{33} \frac{\partial N^{u_2}_j}{\partial x_1} + \frac{\partial N^{u_2}_i}{\partial x_2} \underline{a}_{22} \frac{\partial N^{u_2}_j}{\partial x_2} d\Omega \; ; \; i,j = 1,2,\ldots,n^{u_2}
\end{aligned}
\tag{3.38}
$$

Coefficients of $[(C^e_{[i]})^e_{11}]$, $[(C^e_{[i]})^e_{12}]$, $[(C^e_{[i]})^e_{21}]$, and $[(C^e_{[i]})^e_{22}]$ $; i = 1,2,\ldots,n$ can be obtained using equation (3.38) and replacing $\underline{a}_{11}$, $\underline{a}_{12}$, $\underline{a}_{21}$, $\underline{a}_{22}$, and $\underline{a}_{33}$ with $(\underline{b}_i)_{11}$, $(\underline{b}_i)_{12}$, $(\underline{b}_i)_{21}$, $(\underline{b}_i)_{22}$, and $(\underline{b}_i)_{33}$ $; i = 1,2,\ldots,n$.

In (3.35) $[M^e]$ is element mass matrix, $[C^e_{[i]}]$ $; i = 1,2,\ldots,n$ are element damping matrices corresponding to strain rates $[\dot{\varepsilon}_{[i]}]$ $; i = 1,2,\ldots,n$ and $[K^e]$ is the element stiffness matrix. $[M^e]$, $[C^e_{[i]}]$ $; i = 1,2,\ldots,n$ and $[K^e]$ are all symmetric. Equations (3.34) when assembled for $\bar{\Omega}^T_x$ yield a system of ODEs in time, given below.

$$
[M]\{\delta_{[2]}\} + \sum_{i=1}^{n} [C_{[i]}]\{\delta_{[i]}\} + [K]\{\delta\} - \{F\} - \{P\} = 0 \tag{3.39}
$$

Where, $[M]$ is the global mass matrix, $[C_{[i]}]$ $;$ $i = 1,2,\ldots,n$ are global damping matrices, and $[K]$ is the global stiffness matrix. These are solved by implicit or explicit time integration method or finite element in time or by transformation to modal basis with the assumption of Rayleigh damping. Details are discussed in section 3.2.2. The local approximations for $(u_1)^e_h$ and $(u_2)^e_h$ remain the same for the beam element as derived in chapter 2.

3.2.2 Solution methods for system of ODEs in time resulting from decoupling of space-time using GM/WF in space

The different methods to solve the system of ODEs in time were discussed in the beginning of chapter 3 and are discussed in detail by Surana et al. [9], and summarized here. This system of ODEs in time can be solved to obtain time response using LSFEM in time, or using explicit or implicit time integration scheme, or using normal mode synthesis.

3.2.2.1 Normal Mode Synthesis

In normal mode synthesis, the undamped normal modes are determined by solving the eigenvalue problem.

$$[K]\{\phi\} - \lambda[M]\{\phi\} = 0 \; ; \; \lambda = \omega_i^2 \tag{3.40}$$

Where, ω is the natural frequency, and $\{\phi\}$ is the corresponding eigenvector.

Let ω_i be the i^{th} natural frequency, $\{\phi\}_i$ be the corresponding eigenvector, and $[\Lambda]$ be a diagonal matrix whose diagonal entries are $\omega_i^2 \; i = 1, 2, \ldots, m$. Also consider $[\Phi]$ to be an $n \times m$ matrix of eigenvectors whose columns are eigenvectors $\{\phi\}_i \; i = 1, 2, \ldots, m, \; m \leq n$. Then, the system of ODEs in time in equation (3.39) can be transformed into the modal basis by the following change of basis.

$$\begin{aligned} \{\delta\} &= [\Phi]\{x\} \\ \{\dot{\delta}\} &= [\Phi]\{\dot{x}\} \\ \{\ddot{\delta}\} &= [\Phi]\{\ddot{x}\} \end{aligned} \tag{3.41}$$

In which $\{x\}$ are modal participation factors. Substituting equation (3.41) into equation (3.39) and premultiplying by $[\Phi]^T$, and using the following

$$[\Phi]^T[M][\Phi] = [I] \quad \text{and} \quad [\Phi]^T[K][\Phi] = [\Lambda] \tag{3.42}$$

we get the system of ODEs in time in the modal basis as

$$\{x_{[2]}\} + \sum_{j=1}^{n} [\Phi]^T [C_j][\Phi]\{x_{[j]}\} + [\Lambda]\{x\} = [\Phi]^T\{F\} + [\Phi]^T\{P\} \tag{3.43}$$

Where, $\Lambda_i = \omega_i^2 \ ; \ i = 1, 2, \ldots, m$.

If we consider $j = 1$ (ordered rate theory for $\boldsymbol{\sigma}$ of order one) then (3.43) reduces to.

$$\{x_{[2]}\} + [\Phi]^T [C_1][\Phi]\{x_{[1]}\} + [\Lambda]\{x\} = [\Phi]^T\{F\} + [\Phi]^T\{P\} \tag{3.44}$$

The damping matrix is not a diagonal matrix. By assuming Rayleigh damping, where the damping matrix $[C_1]$ is a linear function of the mass matrix $[M]$ and the stiffness matrix $[K]$, we can write

$$[C_1] = \alpha[M] + \beta[K] \tag{3.45}$$

we get

$$[\Phi]^T [C_1][\Phi] = \alpha[I] + \beta[\Lambda] \tag{3.46}$$

For any mode i, comparing equation (3.46) to the 1D spring mass damper system, we have

$$\alpha + \beta\omega_i^2 = 2\zeta_i\omega_i \tag{3.47}$$

Where ζ_i is the dimensionless modal damping parameter or the damping ratio corresponding to the frequency ω_i. Coefficients α and β are determined using ζ_i vs ω_i data for a material. This requires only two representative ω_i and ζ_i values that describe the entire range, once we know α and β we can obtain ζ_i for any frequency ω_i using

$$\zeta_i = \frac{\alpha + \beta\omega_i^2}{2\omega_i} \tag{3.48}$$

This approach is obviously phenomenological. Thus, equations (3.39) now become ODEs in time

with modal damping.

$$\begin{aligned} &\{x_{[2]}\} + 2[\zeta\omega]\{x_{[1]}\} + [\Lambda]\{x\} = \{\underset{\sim}{F}\} + \{\underset{\sim}{P}\} \\ \text{or} \quad &\ddot{x}_i + 2\zeta_i\omega_i\dot{x}_i + \omega_i^2 x_i = \underset{\sim}{F}_i + \underset{\sim}{P}_i \; ; \; i = 1, 2, \ldots, m \end{aligned} \tag{3.49}$$

We now have a system of decoupled ODEs in time, so each ODE can be time integrated independent of the other. These are second order linear ODEs and have theoretical solutions for simple nonhomogeneous cases. Thus, a theoretical solution for $\{x\}$ at any time t, $\{x\}_t$ can be obtained, instead of using methods of approximation in time. By transforming $\{x\}$ back to $\{\delta\}$, using the relation $\{\delta\} = [\Phi]\{x\}$, we get time response $\{\delta\}_t$ at any time t.

3.2.2.2 Wilson's θ method with linear acceleration

In Wilson's θ method with linear acceleration, the acceleration $\{\ddot{\delta}\}$ is assumed to be a linear function of time in the interval $[t, t + \theta\Delta t]$, where $\theta > 1$. For this method to be unconditionally stable, $\theta \geq 1.37$, but $\theta = 1.4$ is generally used. In equation (3.39) consider $j = 1$ only, i.e. the ordered rate constitutive theory for the stress tensor of order one, then we have

$$[M]\{\delta_{[2]}\} + [C_1]\{\delta_{[1]}\} + [K]\{\delta\} - \{F\} - \{P\} = 0 \tag{3.50}$$

The method to time integrate equation (3.50) using Wilson's θ method with linear acceleration is briefly outlined below [9].

(i) When the initial conditions at time t_0 is given, say $\{\delta\}_{t_0}$ and $\{\dot{\delta}\}_{t_0}$, then the initial acceleration $\{\ddot{\delta}\}_{t_0}$ is obtained by solving for $\{\ddot{\delta}\}_{t_0}$ in equation (3.50) at time t_0.

$$\{\delta_{[2]}\}_{t_0} = [M]^{-1}\left(\{F\}_{t_0} + \{P\}_{t_0} - [C_1]\{\delta_{[1]}\}_{t_0} - [K]\{\delta\}_{t_0}\right) \tag{3.51}$$

(ii) Calculate $\{\delta\}_{t+\theta\Delta t}$ by solving the equation below [9].

$$\left[\frac{6}{(\theta\Delta t)^2}[M]+\frac{3}{\theta\Delta t}[C_1]+[K]\right]\{\delta\}_{t+\theta\Delta t} = \{f\}_{t+\theta\Delta t}+\left[\frac{6}{(\theta\Delta t)^2}[M]+\frac{3}{\theta\Delta t}[C_1]\right]\{\delta\}_t + \left[\frac{6}{\theta\Delta t}[M]+2[C_1]\right]\{\dot{\delta}\}_t+\left[2[M]+\frac{\theta\Delta t}{2}[C_1]\right]\{\ddot{\delta}\}_t \quad (3.52)$$

(iii) Evaluate $\{\dot{\delta}\}_{t+\theta\Delta t}$ using the equation below.

$$\{\dot{\delta}\}_{t+\theta\Delta t}=\frac{3}{\theta\Delta t}(\{\delta\}_{t+\theta\Delta t}-\{\delta\}_t)-2\{\dot{\delta}\}_t-\frac{\theta\Delta t}{2}\{\ddot{\delta}\}_t \quad (3.53)$$

(iv) Evaluate $\{\ddot{\delta}\}_{t+\theta\Delta t}$ using the equation below.

$$\{\ddot{\delta}\}_{t+\theta\Delta t}=\frac{6}{(\theta\Delta t)^2}(\{\delta\}_{t+\theta\Delta t}-\{\delta\}_t)-\frac{6}{\theta\Delta t}\{\dot{\delta}\}_t-2\{\ddot{\delta}\}_t \quad (3.54)$$

(v) Then, the solution ($\{\delta\}$, $\{\dot{\delta}\}$, and $\{\ddot{\delta}\}$) at the next time step $t+\Delta t$ is evaluated by the following equation.

$$\begin{aligned}
\{\delta\}_{t+\Delta t} &= \{\delta\}_t+\Delta t\{\dot{\delta}\}_t+\frac{(\Delta t)^2}{2}\{\ddot{\delta}\}_t+\frac{(\Delta t)^2}{6\theta}(\{\ddot{\delta}\}_{t+\theta\Delta t}-\{\ddot{\delta}\}_t)\\
\{\dot{\delta}\}_{t+\Delta t} &= \{\dot{\delta}\}_t+\Delta t\{\ddot{\delta}\}_t+\frac{\Delta t}{2\theta}(\{\ddot{\delta}\}_{t+\theta\Delta t}-\{\ddot{\delta}\}_t)\\
\{\ddot{\delta}\}_{t+\Delta t} &= \{\ddot{\delta}\}_t+\frac{1}{\theta}(\{\ddot{\delta}\}_{t+\theta\Delta t}-\{\ddot{\delta}\}_t)
\end{aligned} \quad (3.55)$$

Steps (ii) to (v) are repeated until the desired final time is reached.

Wilson's θ method if applied to the ODEs in time before transformation to modal basis will require damping coefficients. $\theta \geq 1.37$ is a requirement for Wilson's θ method to be unconditionally stable. But a small enough Δt must still be chosen for accuracy of the solution [9].

3.2.2.3 Remarks

(1) Damping mechanism in the present work is due to SLT.

(2) $\underset{\sim}{\mu}$ and $\underset{\sim}{\lambda}$ are to be determined experimentally to calibrate the model.

(3) Normal mode synthesis uses modal damping, i.e. assumes the damping matrix $[C_1]$ to be linear function of mass matrix $[M]$ and stiffness matrix $[K]$ (Rayleigh damping) which results in decoupling of the system of ODEs in time in the modal basis. Each mode has it's own damping coefficient ζ_i associated with that mode's natural frequency ω_i. This is a phenomenological model of damping.

(4) Since the system of ODEs in time are decoupled in normal mode synthesis, each ODE can be solved independent of the other. Since each equation is a second order linear ODE in time, they can be solved analytically to get the theoretical solution. Thus, there is no need to use methods of approximation in time and therefore the solution can be evaluated at any time and one need not be concerned about the accuracy of the solution as a function of the size of Δt.

3.2.3 Space-time finite element method based on residual functional for the energy equation

Consider energy equation (3.20)

$$\begin{aligned} &\rho_0 C_v \frac{\partial \theta}{\partial t} - k\left(\frac{\partial^2 \theta}{\partial {x_1}^2} + \frac{\partial^2 \theta}{\partial {x_2}^2}\right) = f(\boldsymbol{\sigma}, \dot{\boldsymbol{\varepsilon}}) \\ &\text{in which } f(\boldsymbol{\sigma}, \dot{\boldsymbol{\varepsilon}}) = \sigma_{ij}\dot{\varepsilon}_{ji} \end{aligned} \tag{3.56}$$

$f(\boldsymbol{\sigma}, \dot{\boldsymbol{\varepsilon}})$ is a known function. We follow the details of this method of constructing space-time integral form from reference [9]. Let Δt be an increment of time from initial time t_0, same as time increment used for integrating ODEs resulting from BLM, we discretize the space-time strip

$\bar{\Omega}_{xt} = \bar{\Omega}_x \times \bar{\Omega}_t = \bar{\Omega}_x \times [t_0, t_0 + \Delta t]$ into nine node p-version space-time finite elements. Let $\bar{\Omega}_{xt}^T = \underset{e}{\cup} \bar{\Omega}_{xt}^e$ be discretization of $\bar{\Omega}_{xt}$ in which $\bar{\Omega}_{xt}^e$ is a space-time element. Let $(\theta(x_1, x_2, t))_h^e$ be approximation of θ over $\bar{\Omega}_{xt}^e$. $\bar{\Omega}_{xt}^e$ is mapped into a two unit square [9]. Let $(\theta(\xi, \eta))_h^e$ be approximation of θ over $\bar{\Omega}_{xt}^e$ such that

$$\theta_h = \underset{e}{\cup} \theta_h^e \tag{3.57}$$

θ_h is approximation of θ over discretization $\bar{\Omega}_{xt}^T$. The space-time differential operator A in (3.56) is non-self adjoint. Let

$$E = \rho_0 C_v \frac{\partial \theta_h}{\partial t} - k \left(\frac{\partial^2 \theta_h}{\partial {x_1}^2} + \frac{\partial^2 \theta_h}{\partial {x_2}^2} \right) - f(\boldsymbol{\sigma}, \dot{\boldsymbol{\varepsilon}}) \quad \forall x, t \in \Omega_{xt}^T \tag{3.58}$$

be the residual equation. The residual functional I for $\bar{\Omega}_{xt}^T$ is given by

$$I = (E, E)_{\bar{\Omega}_{xt}^T} = \sum_e (E^e, E^e) = \sum_e I^e \tag{3.59}$$

in which

$$E^e = \rho_0 C_v \frac{\partial \theta_h^e}{\partial t} - k \left(\frac{\partial^2 \theta_h^e}{\partial {x_1}^2} + \frac{\partial^2 \theta_h^e}{\partial {x_2}^2} \right) - f(\boldsymbol{\sigma}^e, \dot{\boldsymbol{\varepsilon}}^e) \quad \forall x, t \in \Omega_{xt} \tag{3.60}$$

$$\delta I = 2(E, \delta E)_{\bar{\Omega}_{xt}^T} = \sum_e 2(E^e, \delta E^e)_{\bar{\Omega}_{xt}^e} = \sum_e \delta I^e = \sum_e \{g^e\} = \{g\} = 0 \tag{3.61}$$

$$\delta^2 I = 2(\delta E, \delta E)_{\bar{\Omega}_{xt}^T} = \sum_e 2(\delta E^e, \delta E^e)_{\bar{\Omega}_{xt}^e} > 0 \tag{3.62}$$

Thus, the integral from (3.61) is space-time variationally consistent

$$\delta E^e = \rho_0 C_v \frac{\partial v}{\partial t} - k \left(\frac{\partial^2 v}{\partial {x_1}^2} + \frac{\partial^2 v}{\partial {x_2}^2} \right) \tag{3.63}$$

in which $v = \delta \theta_h^e$.

Consider

$$\delta I^e = 2(E^e, \delta E^e)_{\bar{\Omega}_{xt}^T} \tag{3.64}$$

Substitute for E^e and δE^e in equation (3.64)

$$\delta I^e = \left(\rho_0 C_v \frac{\partial \theta_h^e}{\partial t} - k \left(\frac{\partial^2 \theta_h^e}{\partial {x_1}^2} + \frac{\partial^2 \theta_h^e}{\partial {x_2}^2} \right) - f(\boldsymbol{\sigma}^e, \dot{\boldsymbol{\varepsilon}}^e), \rho_0 C_v \frac{\partial v}{\partial t} - k \left(\frac{\partial^2 v}{\partial {x_1}^2} + \frac{\partial^2 v}{\partial {x_2}^2} \right) \right)_{\bar{\Omega}_{xt}^T} \tag{3.65}$$

Let

$$\theta_h^e = \sum_{i=1}^{n^\theta} N_i^\theta(x,t)(\delta_\theta)_i^e = \sum_{i=1}^{n^\theta} N_i^\theta(\xi,\eta)(\delta_\theta)_i^e \tag{3.66}$$

Then,

$$v = \delta\theta_h^e = N_j^\theta(\xi,\eta) \quad ; j = 1, 2, \ldots, n^\theta \tag{3.67}$$

Substituting equations (3.66) and (3.67) and using matrix vector notation

$$\delta I^e = 2(E^e, \delta E^e)_{\bar{\Omega}_{xt}^T} = [K^e]\{\delta_\theta^e\} - \{f^e\} \tag{3.68}$$

$$K_{ij}^e = \left(\rho_0 C_v \frac{\partial N_j^\theta}{\partial t} - k \left(\frac{\partial^2 N_j^\theta}{\partial {x_1}^2} + \frac{\partial^2 N_j^\theta}{\partial {x_2}^2} \right), \rho_0 C_v \frac{\partial N_i^\theta}{\partial t} - k \left(\frac{\partial^2 N_i^\theta}{\partial {x_1}^2} + \frac{\partial^2 N_i^\theta}{\partial {x_2}^2} \right) \right)_{\bar{\Omega}_{xt}^T} \tag{3.69}$$
$$; i, j, = 1, 2, \ldots, n^\theta$$

and

$$f_i^e = \left(f(\boldsymbol{\sigma}^e, \dot{\boldsymbol{\varepsilon}}^e), \rho_0 C_v \frac{\partial N_i^\theta}{\partial t} - k \left(\frac{\partial^2 N_i^\theta}{\partial {x_1}^2} + \frac{\partial^2 N_i^\theta}{\partial {x_2}^2} \right) \right)_{\bar{\Omega}_{xt}^T} \quad ; i = 1, 2, \ldots, n^\theta \tag{3.70}$$

Thus,

$$\delta I = \sum_e \delta I^e = \sum_e ([K^e]\{\delta_\theta^e\} - \{f^e\}) = 0 \tag{3.71}$$

and we have

$$[K]\{\delta\} = \{f\} \tag{3.72}$$

in which

$$[K] = \sum_e [K^e] \ , \ \{\delta\} = \bigcup_e \{\delta_\theta^e\} \ ; \ \{f\} = \sum_e \{f^e\} \tag{3.73}$$

Equation (3.72) are the final form of the algebraic equations for space-time strip $\bar{\Omega}_x \times [t_0, t_0 + \Delta t]$, we impose BCs and ICs on $\{\delta\}$ in (3.72) and solve for the remaining, giving us temperature field θ for $\forall (x, t) \in \bar{\Omega}_x \times [t_0, t_0 + \Delta t]$. This procedure of first solving for u_1, u_2, $\boldsymbol{\sigma}$, and $\dot{\boldsymbol{\epsilon}}$ and then for θ is repeated for each time increment. The temperature approximation $\theta_h^e(\xi, \eta)$ for θ is same as for displacement u_1 or u_2 derived in chapter 2.

Chapter 4

A New 2D Thermoviscoelastic beam formulation with damping and memory

The New formulation developed in chapter 2 section 2.3 for the bending of Thermoelastic beams in which mechanical deformation is reversible is extended to bending of Thermoviscoelastic beams with damping (dissipation) and memory (rheology). We begin with the conservation and balance laws and linear constitutive equations in $\mathbb{R}^2$ for Thermoviscoelastic solid matter with damping and memory, derived in chapter 1, subsection 1.2.1.3. In chapter 4 finite element formulations based on this mathematical model in $\mathbb{R}^2$ is also presented.

Due to memory the constitutive theory for the deviatoric Cauchy stress tensor is a differential equation in time. Thus, in this case substitution of the deviatoric stress tensor in the balance of linear momenta to obtain balance of linear momenta purely in terms of displacements is not possible. Due to this there is no strong incentive to decouple space and time using GM/WF in space. Only the space-time integral form based on residual functional is space-time variationally consistent and is meritorious.

4.1 Mathematical Model

The mathematical model for bending of beam with dissipation and memory mechanisms in $2D$ consists of conservation and balance laws of classical continuum mechanics. Presence of dissipation results in entropy generation and finally heat. The memory mechanism is due to long chain molecules of the polymer in the composition of the viscoelastic solid continua. It is well known that the mathematical description of memory mechanism requires that the constitutive theory for the Cauchy stress tensor at least be a first order differential equation in time for the stress tensor that contains strain and strain rate as non-homogeneous part [24] (generally referred to as rate equation in time). In this work also we consider small strain, small deformation, isotropic, homogeneous incompressible matter constituting the beam.

The conservation and the balance laws in Lagrangian description are given by the following $\forall(x,t) \in \Omega_x = \Omega_x \times \Omega_t$.

$$\rho_0 = |J|\rho \quad \text{(CM)} \tag{4.1}$$

$$\rho_0 \frac{\partial^2 u_i}{\partial t^2} - \rho_0 F_i^b - \frac{\partial \sigma_{ji}}{\partial x_j} = 0 \ ; \ i,j = 1,2 \quad \text{(BLM)} \tag{4.2}$$

$$\sigma_{ij} = \sigma_{ji} \quad \text{(BAM)} \tag{4.3}$$

$$\rho_0 \frac{De}{Dt} + \frac{\partial q_i}{\partial x_i} - \sigma_{ij}\dot{\varepsilon}_{ji} = 0 \ ; \ i,j = 1,2 \quad \text{(FLT)} \tag{4.4}$$

$$\rho_0 \left(\frac{D\Phi}{Dt} + \eta \frac{D\theta}{Dt} \right) + \frac{q_i g_i}{\theta} - \sigma_{ij}\dot{\varepsilon}_{ji} \leq 0 \ ; \ i,j = 1,2 \quad \text{(SLT)} \tag{4.5}$$

the dependent variables and other quantities have the same meaning as in chapter 3.

From entropy inequality $\boldsymbol{\sigma}$ and $\dot{\boldsymbol{\varepsilon}}$ are rate of work conjugate and $\boldsymbol{q}$ and $\boldsymbol{g}$ are conjugate pair. Choice of constitutive variables is rather straight forward: Φ, η, $\boldsymbol{\sigma}$, and $\boldsymbol{q}$. Memory requires stress rates of order one and zero (stress itself) and elasticity and dissipation require strain and strain rate tensors of order one. Based on Surana [24] and Surana et al. [29] we generalize these choices and consider the following rates of order n and m for strain tensor and the Cauchy stress tensor,

respectively.

$$\begin{aligned} &\boldsymbol{\varepsilon}_{[j]} \ ; \ j = 1, 2, \ldots, n \\ &\boldsymbol{\sigma}^{[i]} \ ; \ i = 1, 2, \ldots, m \end{aligned} \tag{4.6}$$

Using the conjugate pairs, choices of strain and stress rate of orders n and m and the principle of equipresence we can write the following for the argument tensors of the constitutive variables.

$$\begin{aligned} \Phi &= \Phi(\boldsymbol{\varepsilon}, \boldsymbol{\varepsilon}_{[i]} \ ; \ i = 1, 2, \ldots, n, \boldsymbol{\sigma}^{[j]} \ ; \ j = 0, 1, \ldots, m-1, \boldsymbol{g}, \theta) \\ \eta &= \eta(\boldsymbol{\varepsilon}, \boldsymbol{\varepsilon}_{[i]} \ ; \ i = 1, 2, \ldots, n, \boldsymbol{\sigma}^{[j]} \ ; \ j = 0, 1, \ldots, m-1, \boldsymbol{g}, \theta) \\ \boldsymbol{\sigma}^{[m]} &= \boldsymbol{\sigma}^{[m]}(\boldsymbol{\varepsilon}, \boldsymbol{\varepsilon}_{[i]} \ ; \ i = 1, 2, \ldots, n, \boldsymbol{\sigma}^{[j]} \ ; \ j = 0, 1, \ldots, m-1, \boldsymbol{g}, \theta) \\ \boldsymbol{q} &= \boldsymbol{q}(\boldsymbol{\varepsilon}, \boldsymbol{\varepsilon}_{[i]} \ ; \ i = 1, 2, \ldots, n, \boldsymbol{\sigma}^{[j]} \ ; \ j = 0, 1, \ldots, m-1, \boldsymbol{g}, \theta) \end{aligned} \tag{4.7}$$

Substituting $\dot{\Phi}$ (obtained by using Φ in equation (4.7)) in the entropy inequality and grouping the terms, we can arrive at [24, 29].

$$\begin{aligned} \Phi &= \Phi(\boldsymbol{\varepsilon}, \theta) \\ \eta &= -\frac{\partial \Phi}{\partial \theta} \\ \boldsymbol{\sigma}^{[m]} &= \boldsymbol{\sigma}^{[m]}(\boldsymbol{\varepsilon}, \boldsymbol{\varepsilon}_{[i]} \ ; \ i = 1, 2, \ldots, n, \boldsymbol{\sigma}^{[j]} \ ; \ j = 0, 1, \ldots, m-1, \theta) \\ \boldsymbol{q} &= \boldsymbol{q}(\boldsymbol{g}, \theta) \end{aligned} \tag{4.8}$$

and entropy inequality reduces to

$$\left(\rho_0 \frac{\partial \Phi}{\partial \varepsilon_{kl}} - \sigma_{lk} \right) \dot{\varepsilon}_{kl} + \frac{q_i g_i}{\theta} \leq 0 \tag{4.9}$$

In this we have assumed that $\boldsymbol{q}$ and $\boldsymbol{\sigma}^{[m]}$ only have dependence on $\boldsymbol{g}$, θ and $\boldsymbol{\varepsilon}$, $\boldsymbol{\varepsilon}_{[i]} \ ; \ i = 1, 2, \ldots, n$, $\boldsymbol{\sigma}^{[j]} \ ; \ j = 0, 1, \ldots, m-1$, respectively.

For incompressible matter $\Phi = \Phi(\theta)$ suffices, hence the first of the three terms in (4.9) is zero,

and (4.9) reduces to

$$\frac{q_i g_i}{\theta} - \sigma_{ij}\dot{\varepsilon}_{ji} \leq 0 \tag{4.10}$$

Entropy inequality (4.10) is satisfied if $\frac{q_i g_i}{\theta} \leq 0$ and $\sigma_{ij}\dot{\varepsilon}_{ji} \geq 0$ (rate of work).

Using representation theorem, ordered rate constitutive theory of order m and n in stress and stress rate can be derived [24, 29]. Likewise we can derive constitutive theory for $\boldsymbol{q}$ using $\boldsymbol{q} = \boldsymbol{q}(\boldsymbol{g}, \theta)$. These constitutive theories are obviously nonlinear in the components of the argument tensors. In the work presented here we only consider linear constitutive theories for $\boldsymbol{\sigma}^{[1]}$ and $\boldsymbol{q}$ in which product terms are also neglected. Furthermore, neglecting initial stress field and temperature term, then the resulting constitutive theories are given by

$$[\sigma^{[1]}] = -c_1[\sigma] - c_2\big(\text{tr}([\sigma])\big)[I] + \sum_{i=0}^{n} a_i^1[\varepsilon_{[i]}] + \sum_{i=0}^{n} a_i^2\big(\text{tr}([\varepsilon_{[i]}])\big)[I] \tag{4.11}$$

Using Voigt's notation we can write

$$\{\sigma^{[1]}\} + [\underline{c}]\{\sigma\} = [\underline{a}_0]\{\varepsilon\} + \sum_{i=1}^{n}[\underline{a}_i]\{\varepsilon_{[i]}\} \tag{4.12}$$

components of $\{\sigma\}$ and other vectors are arranged in the same fashion as in chapter 3.
in which

$$[\underline{c}] = \begin{bmatrix} c_1 + c_2 & c_2 & 0 \\ c_2 & c_1 + c_2 & 0 \\ 0 & 0 & c_2 \end{bmatrix} \tag{4.13}$$

Components of $[\underline{a}_0]$ and $[\underline{a}_i]$ $; i = 1, 2, \ldots, n$ are obtained by replacing c_1 and c_2 with $(\underline{a}_0)_1$ and $(\underline{a}_0)_2$, and $(\underline{a}_i)_1$ and $(\underline{a}_i)_2$ $; i = 0, 1, \ldots, n$, respectively.

$$q_i = -k g_i \tag{4.14}$$

$$e = C_v \theta \tag{4.15}$$

We assume that all material coefficients are constant. Expanded form of the complete mathematical

model is given by (after substituting q_i in the energy equation)

$$\rho_0 \frac{\partial^2 u_1}{\partial t^2} - \rho_0 F_1^b - \frac{\partial \sigma_{11}}{\partial x_1} - \frac{\partial \sigma_{21}}{\partial x_2} = 0 \tag{4.16}$$

$$\rho_0 \frac{\partial^2 u_2}{\partial t^2} - \rho_0 F_2^b - \frac{\partial \sigma_{12}}{\partial x_1} - \frac{\partial \sigma_{22}}{\partial x_2} = 0 \tag{4.17}$$

$$\sigma_{21} = \sigma_{12} \tag{4.18}$$

$$\rho_0 C_v \frac{\partial \theta}{\partial t} - k \left(\frac{\partial^2 \theta}{\partial {x_1}^2} + \frac{\partial^2 \theta}{\partial {x_2}^2} \right) - \sigma_{ij} \dot{\varepsilon}_{ji} = 0 \; ; \; i, j = 1, 2 \tag{4.19}$$

$$\{\sigma^{[1]}\} + [\underset{\sim}{c}]\{\sigma\} = [\underset{\sim}{a}_0]\{\varepsilon\} + \sum_{i=1}^{n} [\underset{\sim}{a}_i]\{\varepsilon_{[i]}\} \tag{4.20}$$

in which

$$\{\varepsilon\} = \begin{Bmatrix} \dfrac{\partial u_1}{\partial x_1} \\ \dfrac{\partial u_2}{\partial x_2} \\ \dfrac{1}{2}\left(\dfrac{\partial u_1}{\partial x_2} + \dfrac{\partial u_2}{\partial x_1} \right) \end{Bmatrix} \tag{4.21}$$

In this mathematical model (4.16) – (4.20), with (4.21), Cauchy stresses cannot be eliminated from BLM (4.16) and (4.17) using (4.20). Thus, we must maintain the equations in the model as they are in (4.16) – (4.20) except that we substitute $\{\varepsilon\}$ from (4.21) in (4.20). This mathematical model consists of six equations (4.16), (4.17), (4.19), and (4.20) six dependent variables u_1, u_2, θ, σ_{11}, σ_{22}, and σ_{12}, hence the mathematical model has closure. The only variationally consistent approach for computing solution using this mathematical model is space-time coupled finite element process based on residual functional (space-time least squares method) with time marching [8].

Chapter 5

Model Problems

In this chapter we consider model problems for thermoelastic as well as thermoviscoelastic behavior and their solutions using various computational methodologies described. Solutions of the model problem are computed using finite element method in which the integral forms are based on residual functional (least squares method) or Galerkin method with weak form, both yield integral forms that are variationally consistent. The variationally consistent integral form ensures unconditionally stable computational processes. The local element approximations are considered in hpk framework that permit higher order and higher degree local approximations to ensure that the integrals over the discretization remain Riemann or in Lebesgue sense based on our choice of the order of the approximation space k.

5.1 Thermoelastic Beams

In this section we consider a model problem that consist of boundary value problems. We consider the following mathematical models for BVPs.

(a) Euler-Bernoulli beam formulation (EBBT) derived using energy functional or principle of virtual work (subsection 2.1.1).

(b) Euler-Bernoulli beam formulation derived using non-classical mechanics EBBT/NCCM (sub-

section 2.1.3.2).

(c) Timoshenko beam theory (TBT) derived using energy functional (subsection 2.1.2).

(d) New beam formulation based on classical continuum mechanics (section 2.3)

The finite element formulations used in computations are based on residual functional (least squares process) for (a)–(c) and Galerkin method with weak form for (d). In computations, the dimensionless forms of the mathematical models are used for all four formulations. The mathematical models are non-dimensionalized using the following reference quantities.
Reference length $L_0 = 1$", reference density $(\rho_0)_{ref} = 0.289018\,\text{lbm/in}^3$, reference modulus E_0 (or stress) $= 30 \times 10^6$ psi, reference velocity $v_0 = \sqrt{E_0/\rho_0}$, reference time $t_0 = L_0/v_0$.
We choose modulus of elasticity of 30×10^6 psi, Poisson's ratio ν of 0.3, density of $0.289018\,\text{lbm/in}^3$. We consider a cantilever beam of length 12" with area of cross-section $h \times b = 0.25$" $\times\, 0.25$", 5" $\times\, 1$" and 8" $\times\, 1$". The origin of the coordinate system is at the left end ($x_1 = 0$) assumed completely clamped. x_1x_2 is the plane of bending, and x_1 is the axis of the beam (Figure 5.1).

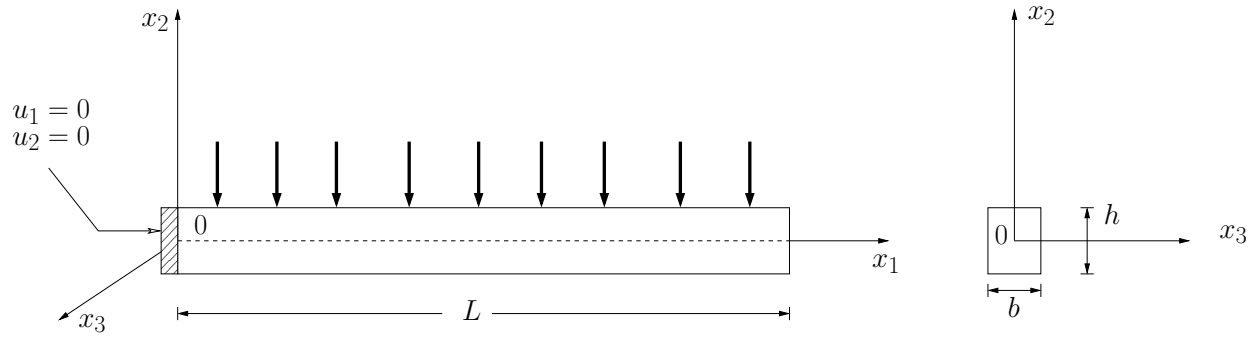

Figure 5.1: Schematic of a cantilever beam with boundary conditions in x_1x_2 plane.

The loading consists of uniformly distributed load acting along the length of the beam acting in the negative x_2 direction. The magnitude of the load (lb/inch) for each value of h and b is chosen in such a way that the Euler-Bernoulli beam theory produces a tip (at $x_1 = 12$") displacement of -0.01". This gives 0.037676 lb/inch, 1205.6327 lb/inch and 4938.2716 lb/inch as the magnitude of the uniformly distributed load for $h \times b = 0.25$" $\times\, 0.25$", 5" $\times\, 1$" and 8" $\times\, 1$", respectively.

Since the local approximations in (a)–(d) are p-version hierarchical, a single element mesh with higher p-level (at the most 4 or 5) will suffice to obtain correct solutions from the formulations (a)–(c). We have checked this to be true. This may not hold true in case of formulation (d). In the studies presented here we consider a ten element uniform discretization formulation for (a)–(d). The purpose of doing this is to illustrate the weak convergence of the lower class solutions to higher class as p-levels are increased i.e. solutions of class C^0 converging to class C^1 and those of class C^1 to C^2 but both in the weak sense. This is an important aspect to demonstrate for accuracy of the computed solutions in applications that always require a discretization containing more than one element. For the formulations (a)–(c) we consider solutions of class $C^1(\bar{\Omega}^e)$. For the new beam element formulation (d) we consider solutions of class $C^{00}(\bar{\Omega}^e)$. We make the following remarks before we present the results.

Remarks

(1) In EBBT (used currently) ${}_s\sigma_{12} = 0$ and there is no concept of ${}_a\sigma_{12}$, hence transverse shear force is zero.

(2) In EBBT/NCCM $\sigma_{12} = {}_s\sigma_{12} + {}_a\sigma_{12}$ in which ${}_s\sigma_{12} = 0$ but ${}_a\sigma_{12} \neq 0$ which yields nonzero transverse shear force.

(3) The mathematical models in (1) and (2) when expressed as two equations in displacements u_1 and u_2 are identical but are derived using different physics as explained earlier. Thus, the displacement u_1, u_2 and the quantities based on their differentiation will be identical in EBBT and EBBT/NCCM (except shear strain for EBBT). However, we recall that EBBT/NCCM is thermodynamically consistent, but EBBT is not.

(4) In TBT ${}_s\sigma_{12} \neq 0$, hence transverse shear force is non-zero and ${}_s\sigma_{12}$ also contributes to strain energy; hence, this model will produce additional transverse displacement due to shear deformation compared to EBBT in which shear deformation is zero. This is significant and important in beams that are not slender.

(5) The new formulation based on CCM (formulation in (d)) when converged is really theory of elasticity solution when the integrated sum of the squares of the residuals approach zero, but the solution is computed numerically. In all beam models that are not based on continuum mechanics conservation and balance laws, the Poisson's ratio only appears as shear modulus. This is obviously non-physical for slender as well as deep beams. However, in the new formulation the Poisson's effect is present correctly through constitutive relations for slender as well as non-slender beams.

Model problem solutions

For formulations (a)–(c) (i.e. EBBT, EBBT/NCCM, TBT) we present results for solutions of class $C^1(\bar{\Omega}^e)$ at p-level of 5, even though solutions for p-level of 3–5 are almost identical. In case of new formulation (d) we have presented results for $p_\xi = p_\eta = 2, 3, \ldots, 9$ to show weak convergence of C^0 solutions to C^1. However, in Figure 5.2 only the converged solution at $p_\xi = p_\eta \geq 5$ are presented.

Figures 5.2(a)–(c) show plots of displacement u_2 versus x_1 of the centerline of the beam for $h \times b = 0.25" \times 0.25"$, $5" \times 1"$ and $8" \times 1"$ for EBBT, EBBT/NCCM, TBT and the new formulation. For the slender beam ($h \times b = 0.25" \times 0.25"$) all four formulations (a)–(d) yield almost identical results (Figure 5.2(a)). For such slender beam the shear deformation is not significant, hence TBT and the new formulation results are almost identical to EBBT and EBBT/NCCM. For $h \times b = 5" \times 1"$ the shear deformation is significant compared to the slender beam ($h \times b = 0.25" \times 0.25"$), hence TBT yields higher values of displacement u_2 compared to EBBT and EBBT/NCCM. The solution from the new formulation yields even higher u_2 compared to TBT due to presence of complete two dimensional elasticity in the new formulation. As h increases, the shear deformation becomes more significant. In Figure 5.2(c) for $h \times b = 8" \times 1"$ we observe even a larger deviation of u_2 versus x_1 for TBT compared to u_2 versus x_1 for EBBT and EBBT/NCCM. Likewise we also observe larger deviation of u_2 versus x_1 obtained from the new formulation when compared to TBT. We clearly observe larger difference between new formulation and TBT for $h \times b = 8" \times 1"$

compared to $h \times b = 5" \times 1"$. We remark that the computed solution from the new formulation (and others as well) are converged solutions with L_2-norm of the residual functional approaching zero, hence these solutions are of the same accuracy as the theoretical solutions.

Figures 5.3(a)–(c) show plots of axial displacement u_1 versus x_2 at $x_1 = 6.0"$ for $h \times b = 0.25" \times 0.25"$, $5" \times 1"$ and $8" \times 1"$ respectively for formulations (a)–(d). In case of slender beam plane section of beam remains plane after deformation in all formulations. In formulations (a)–(c) the beam cross-section remains plane regardless of $h \times b$ (as expected). However, the solutions from the new formulation show that as h increases, the beam cross-section does not remain plane. An important and significant aspect of the new formulation presented here is that the deformation of the cross-section is not assumed a priori as done in current beam theories through kinematic assumptions. Progressively increasing p-levels automatically simulate the deformation physics specific to the application (h and b values in the model problem).

Graphs of axial stress σ_{11} versus x_2 at $x_1 = 6.0"$ using formulations (a)–(d) for $h \times b = 0.25" \times 0.25"$, $5" \times 1"$ and $8" \times 1"$ are shown in Figures 5.4(a)–(c). For each value of h, σ_{11} versus x_2 is linear and is exactly same for formulations (a)–(c). From Figure 5.4(a) we observe that for $h = 0.25"$ σ_{11} versus x_2 from formulation (d) shows inter element discontinuity at p-level of two due to local approximation of class C^{00} for u_1 and u_2, but for p-levels of three and higher σ_{11} versus x_2 matches with formulations (a)–(c) perfectly. Due to slender beam the cross-section of the beam at $x_2 = 6.0"$ remains plane. From 5.4(b) for $h = 5"$ we note that σ_{11} versus x_2 from formulation (d) is un-converged at p-level of two but p-levels of three and higher yield converged solution of σ_{11}. We note that in this case σ_{11} versus x_2 is not linear any more which is in agreement with Figure 5.3(b) showing that for this case the cross-section of the beam is not plane anymore. In Figure 5.4(c) for $h = 8"$ for p-levels of four and higher (yielding converged behavior) σ_{11} versus x_2 obtained from formulation (d) is quite non-linear implying that the beam cross-section does not remain plane (Figure 5.3(c)).

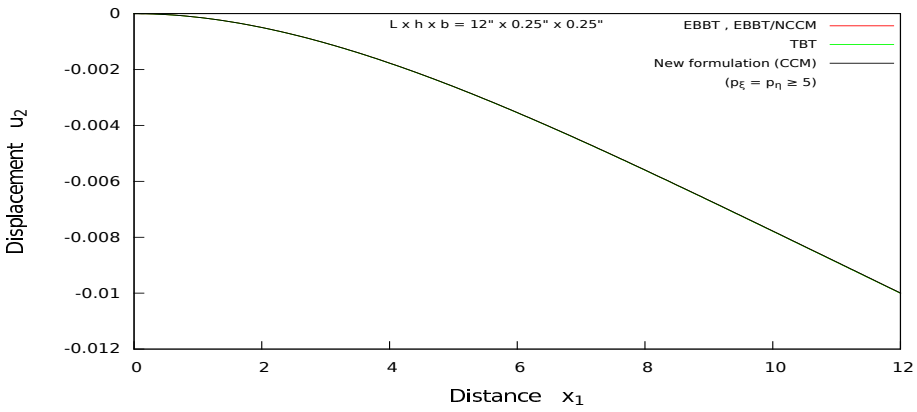

(a) Displacement u_2 versus x_1 ($h \times b = 0.25" \times 0.25"$)

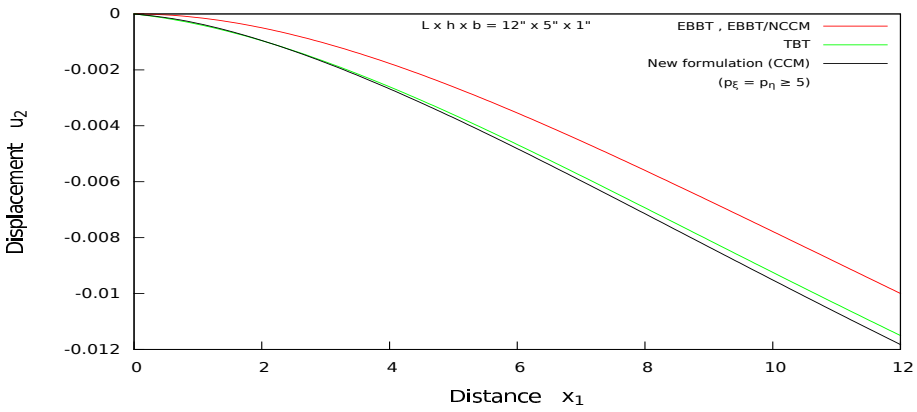

(b) Displacement u_2 versus x_1 ($h \times b = 5" \times 1"$)

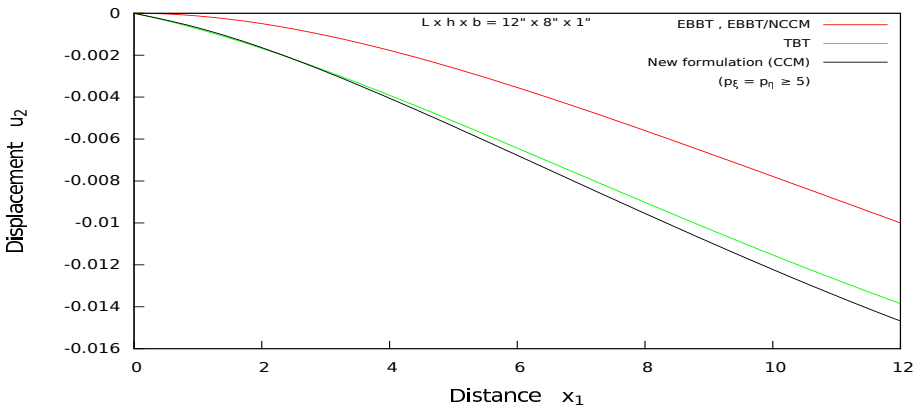

(c) Displacement u_2 versus x_1 ($h \times b = 8" \times 1"$)

Figure 5.2: Displacement u_2 of the centerline versus axial distance x_1 for $h = 0.25", 5", 8"$

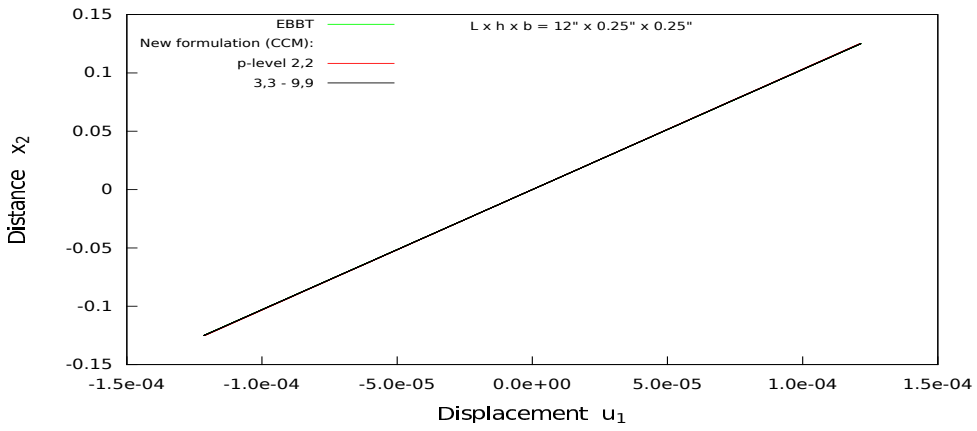

(a) Displacement u_1 versus x_2 at $x = 6.0$” ($h \times b = 0.25$” $\times\ 0.25$”)

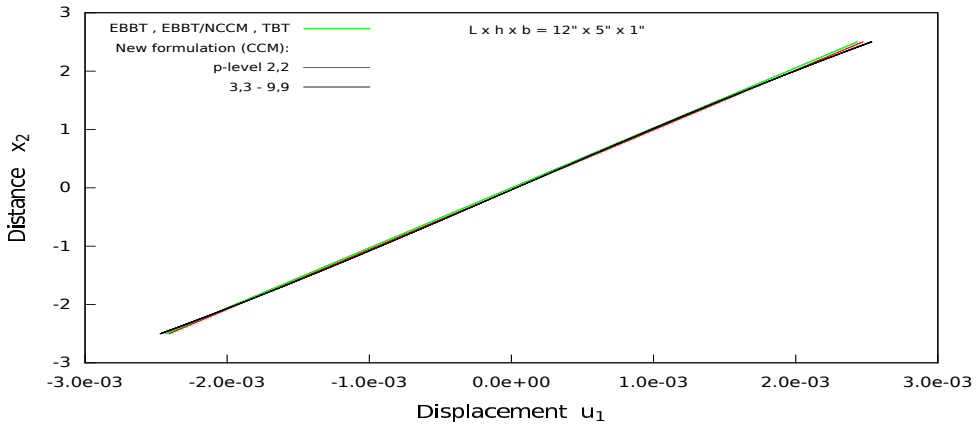

(b) Displacement u_1 versus x_2 at $x = 6.0$” ($h \times b = 5$” $\times\ 1$”)

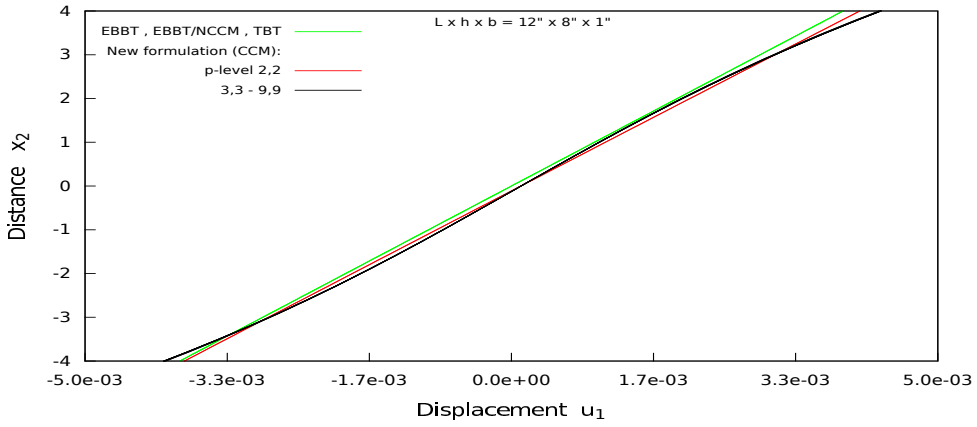

(c) Displacement u_1 versus x_2 at $x = 6.0$” ($h \times b = 8$” $\times\ 1$”)

Figure 5.3: Axial displacement u_1 versus distance x_2 at $x_1 = 6.0$” for $h = 0.25”, 5”, 8”$

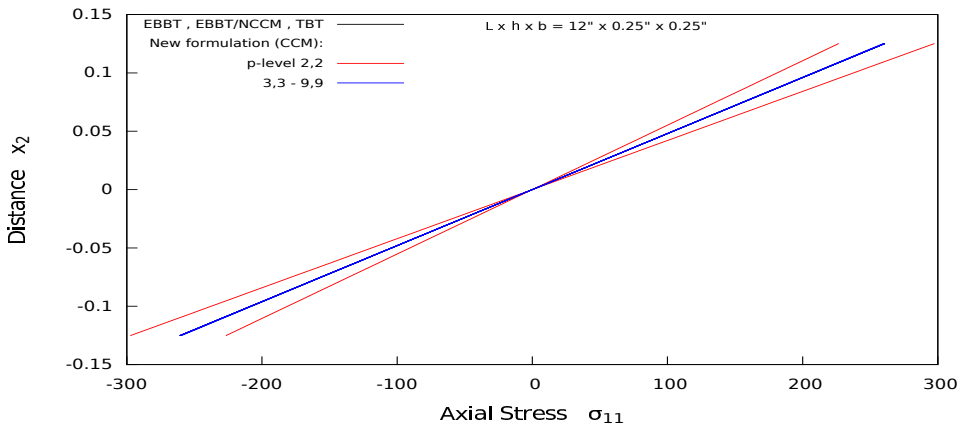

(a) Axial stress σ_{11} versus x_2 at $x = 6.0$" ($h \times b = 0.25" \times 0.25"$)

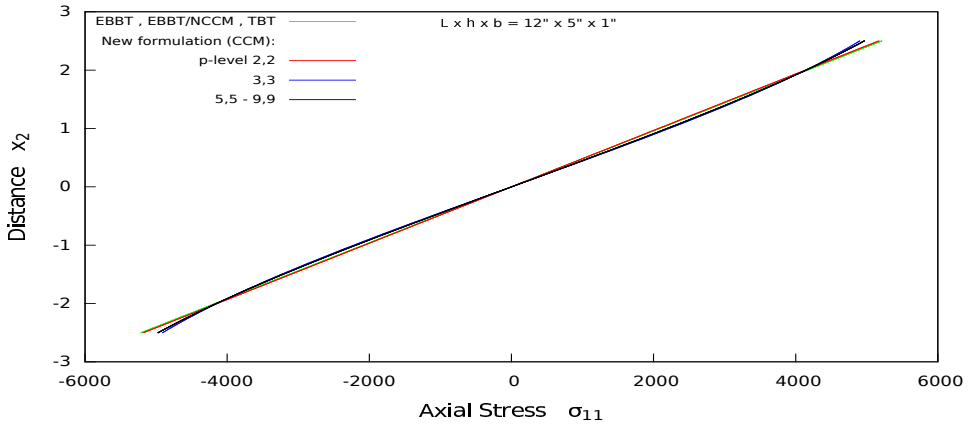

(b) Axial stress σ_{11} versus x_2 at $x = 6.0$" ($h \times b = 5" \times 1"$)

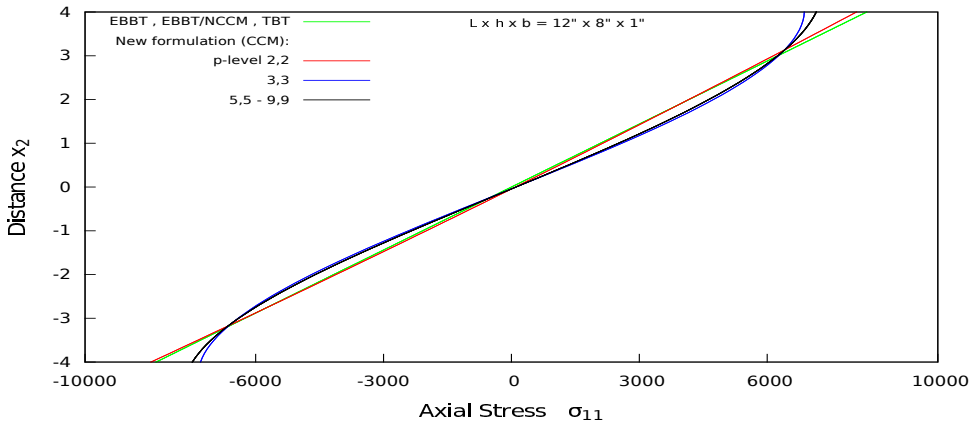

(c) Axial stress σ_{11} versus x_2 at $x = 6.0$" ($h \times b = 8" \times 1"$)

Figure 5.4: Axial stress σ_{11} versus distance x_2 at $x_1 = 6.0$" for $h = 0.25", 5", 8"$

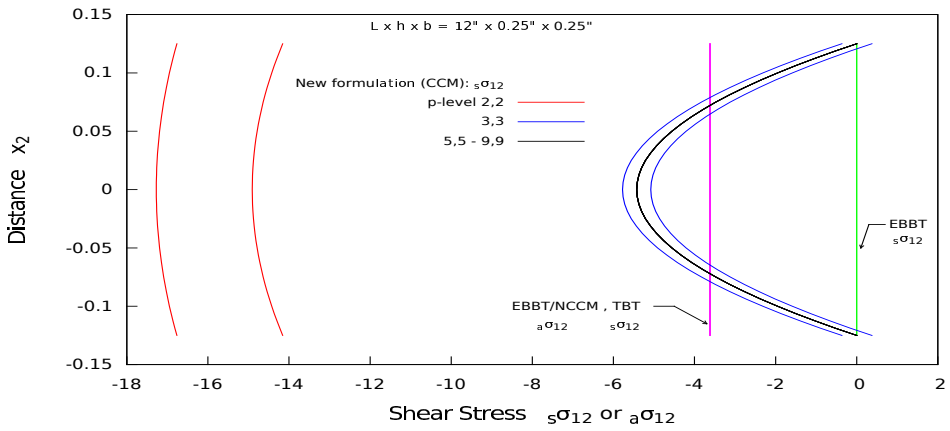

(a) Shear stress ${}_s\sigma_{12}$ or ${}_a\sigma_{21}$ versus x_2 at $x = 6.0$" ($h \times b = 0.25" \times 0.25"$)

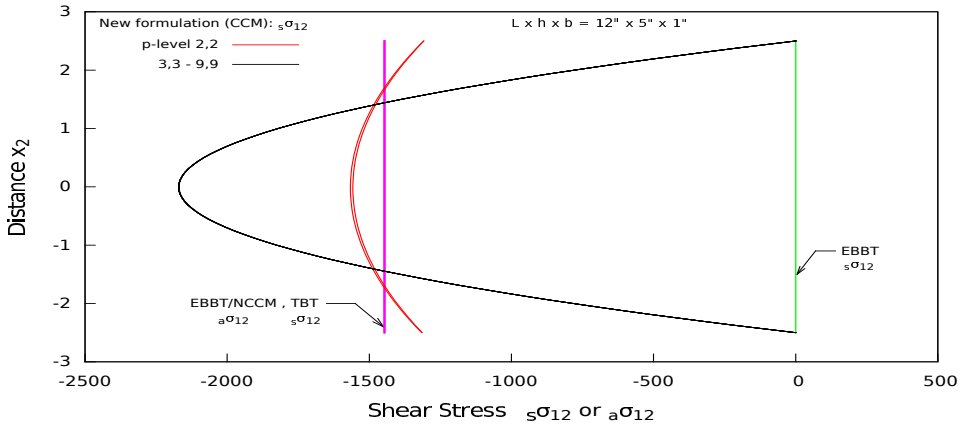

(b) Shear stress ${}_s\sigma_{12}$ or ${}_a\sigma_{21}$ versus x_2 at $x = 6.0$" ($h \times b = 5" \times 1"$)

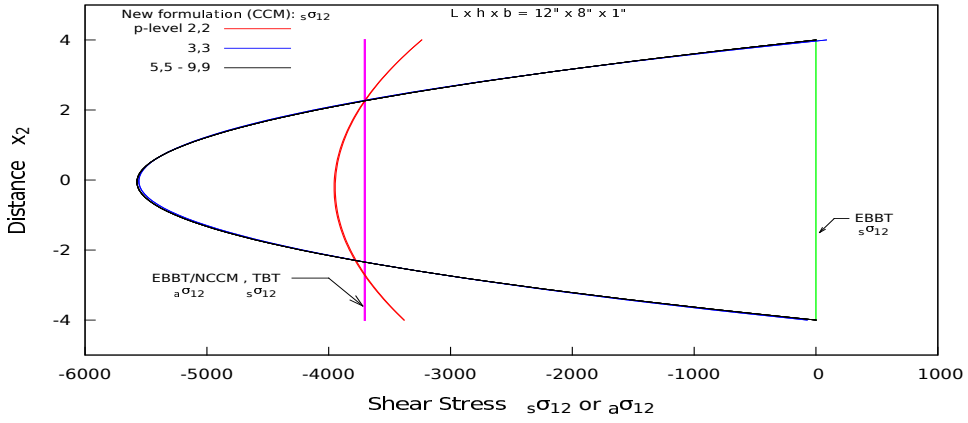

(c) Shear stress ${}_s\sigma_{12}$ or ${}_a\sigma_{21}$ versus x_2 at $x = 6.0$" ($h \times b = 8" \times 1"$)

Figure 5.5: Shear stress ${}_s\sigma_{12}$ or ${}_a\sigma_{21}$ versus distance x_2 at $x_1 = 6.0$" for $h = 0.25", 5", 8"$

Figures 5.5(a)–(c) show plots of ${}_s\sigma_{12}$ or ${}_a\sigma_{12}$ versus x_2 at $x_1 = 6.0$" obtained using formulations (a)–(d) for $h \times b = 0.25" \times 0.25"$, $5" \times 1"$ and $8" \times 1"$ respectively. In EBBT (used currently), ${}_s\sigma_{12} = 0$ and ${}_a\sigma_{12}$ does not exist. ${}_a\sigma_{12}$ from EBBT/NCCM is exactly same in magnitude and direction as ${}_s\sigma_{12}$ from TBT for all three values of h implying that for this model problem the transverse shear force in EBBT/NCCM and TBT is exactly same for three values of h. In Figure 5.5(a) we note that ${}_s\sigma_{12}$ from formulation (d) exhibits inter element discontinuity at $x_1 = 6.0$" for p-level of two and the values of ${}_s\sigma_{12}$ are in error as well. At p-level of three ${}_s\sigma_{12}$ is quadratic with zero values at $x_2 = -0.25$" and 0.25" (shear free surfaces) but the solution for ${}_s\sigma_{12}$ still exhibits inter element discontinuity. At p-level of five and beyond ${}_s\sigma_{12}$ is converged. Distribution of ${}_s\sigma_{12}$ is perfectly quadratic along the depth of the beam with zero values at $x_2 = -0.25$" and 0.25". In Figure 5.5(b) for $h = 5$" the ${}_s\sigma_{12}$ versus x_2 at $x_1 = 6.0$" is not converged at p-level of two but for p-level of three and beyond correct solution of ${}_s\sigma_{12}$ is obtained. The same observations as described for $h = 5$" (Figure 5.5(b)) hold for ${}_s\sigma_{12}$ versus x_2 at $x_1 = 6.0$" shown in Figure 5.5(c) for $h = 8$". We remind that ${}_a\sigma_{12} = 0$ in the new formulation as it is based on CCM in which Cauchy stress tensor is symmetric.

5.2 Thermoviscoelastic solids without memory

The finite element formulations used in computations are based on space-time decoupled formulation using GM/WF in space, this results in a system of ODEs in time. The system of ODEs in time contain the mass matrix $[M]$, stiffness matrix $[K]$, and the damping matrix $[C]$. We consider the following studies here

(i) Normal modes of vibration.

(ii) Normal mode synthesis for transient dynamic response.

(iii) Time response using Wilson's θ time integration method.

- Both undamped and damped time responses are considered.

The dimensionless forms of the mathematical models are used in computations. Following reference quantities and dimensionless variables are used:

Reference length $L_0 = 1$", reference density $(\rho_0)_{ref} = 0.289018\,\text{lbm/in}^3$, reference modulus E_0 (or stress) $= 30 \times 10^6$ psi, reference velocity $v_0 = \sqrt{E_0/\rho_0}$, reference time $t_0 = L_0/v_0$.

We choose modulus of elasticity of 30×10^6 psi, Poisson's ratio ν of 0.3, density of $0.289018\,\text{lbm/in}^3$. We consider a clamped-clamped (fixed-fixed) beam of length 60" with area of cross-section $h\times b =$ $1" \times 1"$ (slender beam), and $12" \times 1"$ (deep beam). The origin of the coordinate system is at the left end ($x_1 = 0$). x_1x_2 is the plane of bending, and x_1 is the axis of the beam (Figure 5.6).

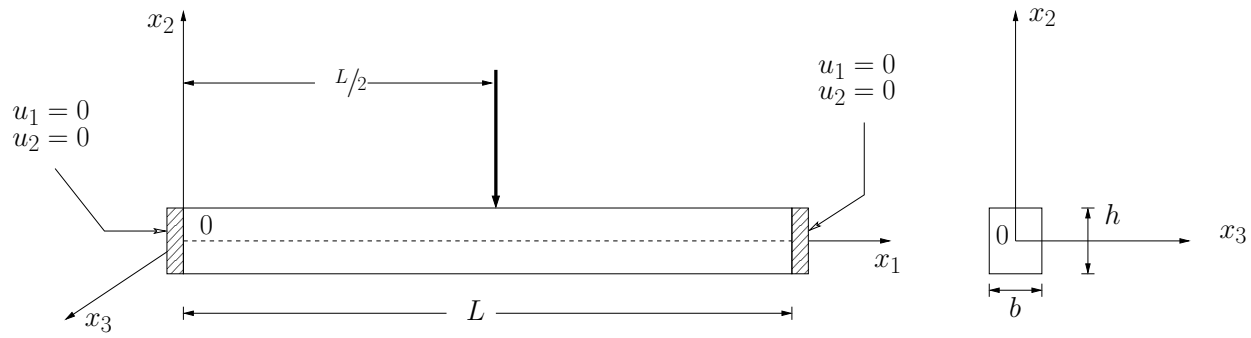

Figure 5.6: Schematic of a clamped-clamped (CC) beam with boundary conditions in x_1x_2 plane.

The loading consists of a point load acting at the midspan (at $x_1 = L/2 = 30"$) of the beam in the negative x_2 direction. The magnitude of the load for each value of h and b is chosen in such a way that the Euler-Bernoulli beam model produces a maximum static displacement (at $x_1 = 30"$) of $-0.4"$ under the load. This gives 0.000029629 and 0.0512 as the magnitude of the non-dimensionalized point load for $h \times b = 1" \times 1"$ and $h \times b = 12" \times 1"$ beam dimensions, respectively.

In the studies presented here we consider a four element uniform discretization, with solutions of class C^1 in ξ direction (along the axis of the beam), and with an equal degree of $p_\xi = p_\eta = p = 5$.

5.2.1 Normal modes of vibrations

The natural modes of vibrations are calculated using the mass matrix $[M]$ and the stiffness matrix $[K]$ for both the slender and deep beam. The calculated frequency is compared with the theoretical value of the frequency, and the mode shapes are plotted for the first six modes. The theoretical value of the frequencies (${}^t\omega_i$) is evaluated using the Euler-Bernoulli beam theory for a clamped-clamped beam, Blevins [94, 95] and given by.

$$ {}^t\omega_i = \frac{\lambda_i^2}{2\pi L^2}\sqrt{\frac{EI}{m}} \quad ; \; i = 1, 2, \ldots, \; hz \tag{5.1} $$

Where, E is the modulus of elasticity, I is the second moment of area about the neutral axis, m is the mass of the beam per unit length, and λ_i is the i^{th} solution of the transcendental equation.

$$ \cos\lambda \cosh\lambda = 1 \tag{5.2} $$

Figure 5.7 and 5.8 show the first six bending mode shapes, along with the calculated and theoretical natural frequencies for both the slender beam ($h = 1$") and the deep beam ($h = 12$").

For all the six modes, we see that the calculated value and the theoretical value natural frequency agree closely for slender beam. For the deep beam, the calculated natural frequency is lower than the theoretical value for all the six modes. This is due to the fact that stiffness in the new formulation is lower compared to EBBT for the same mass.

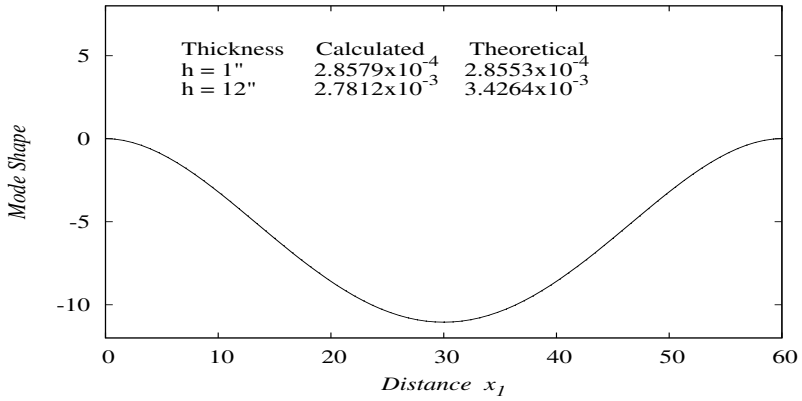

(a) First mode shape

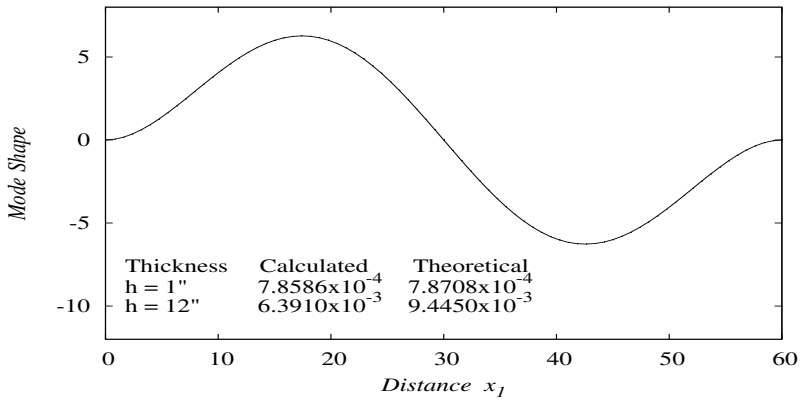

(b) Second mode shape

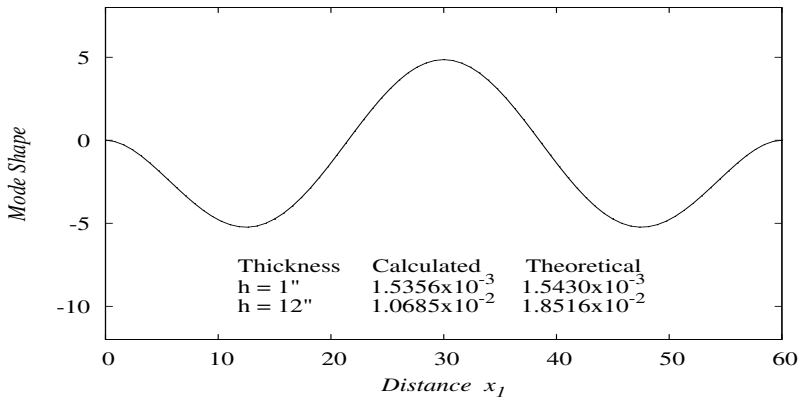

(c) Third mode shape

Figure 5.7: Mode shapes of the first three modes of a clamped-clamped beam.

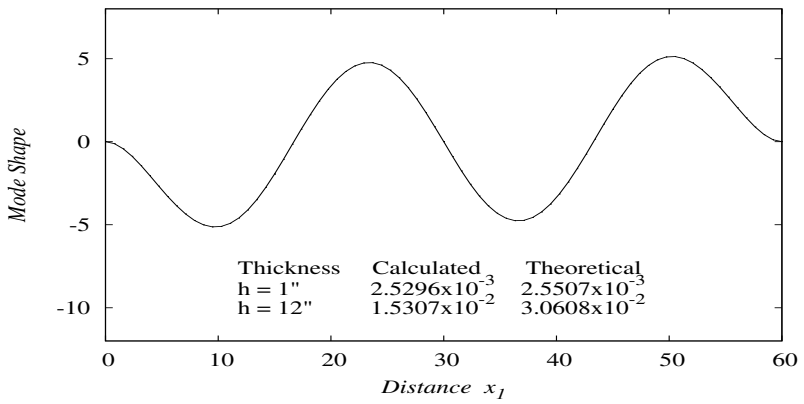

(a) Fourth mode shape

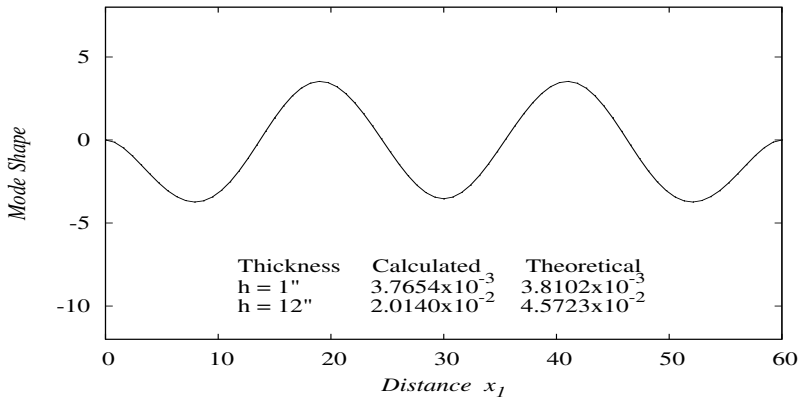

(b) Fifth mode shape

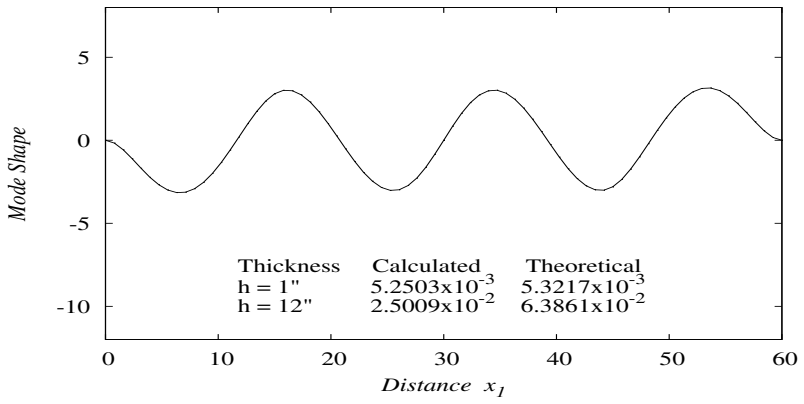

(c) Sixth mode shape

Figure 5.8: Mode shapes of the fourth to sixth mode of a clamped-clamped beam.

5.2.2 Normal Mode Synthesis

The time response is calculated using normal mode synthesis for the undamped beam and for the damped beam with a damping ratios of $\zeta = 0.2, 0.8$. We consider same dimensionless damping ratio for all modes. The time response is calculated by using (i) only the first mode as well as using (ii) the first three modes of vibration. Theoretical solutions of the decoupled ODEs are used [9]. Both set of calculations produce identical results.

Figures 5.9 – 5.12 show plots of displacement u_2 vs x_1 of the centerline of the beam for undamped beam and damped beam with $\zeta = 0.2$ and $\zeta = 0.8$, for both slender and deep beam, for a time corresponding to one and a half cycle of the undamped beam.

The following observations hold for both slender and deep beams.

(i) The undamped beam shows the largest maximum deflection or amplitude (displacement u_2 of the beam centerline at the midspan). For undamped beam this deformation cycle is repeated without amplitude decay as time elapses.

(ii) Time response of damped beam shows progressive amplitude decay as cycle repeats. As expected, we observe more pronounced amplitude decay with a faster rate for higher value of damping ratios.

(iii) For large value of time the undamped beam would continue to oscillate without any amplitude decay due to the fact that in this case there is no energy dissipation mechanism. Where as in case of damped response beyond a certain time the beam reaches stationary state as seen in figure 5.10(c) for $\zeta = 0.8$ for slender beam and figure 5.12(c) for deep beam. For $\zeta = 0.2$ this stationary state is reached after a time corresponding to six cycles of undamped beam.

(iv) Irrespective of the value of the damping coefficient, the steady state deflection profile is the same. Moreover, the value of this steady state deflection profile is slightly larger than that of the static loading case. This is shown in figure 5.13(a) for slender beam and 5.13(b) for deep beam.

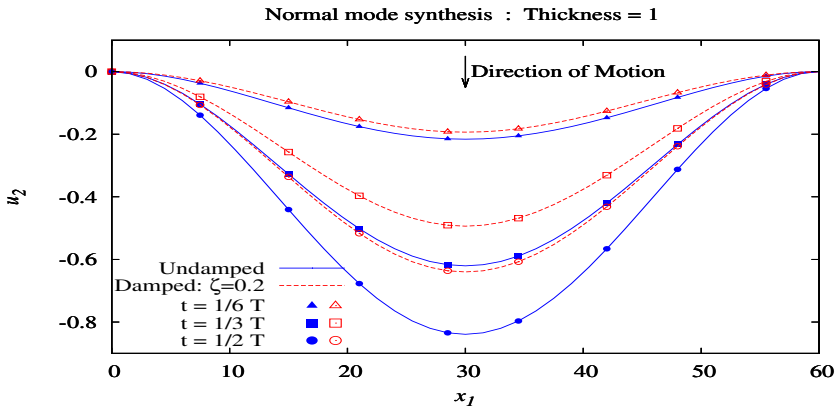

(a) Displacement u_2 versus x_1 for the first one-third of the time period

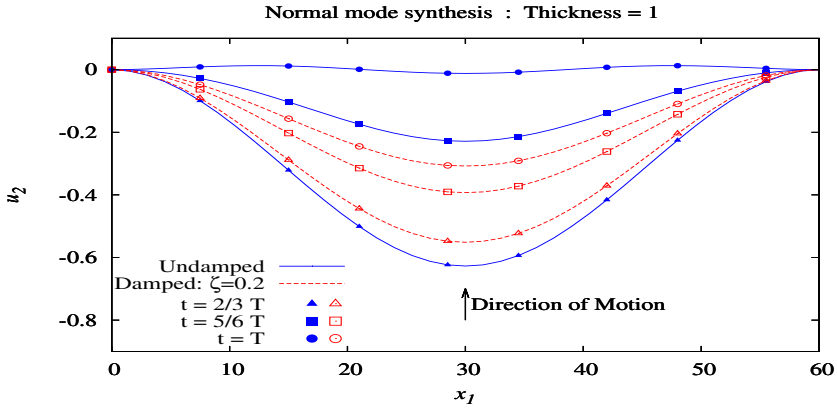

(b) Displacement u_2 versus x_1 for the second one-third of the time period

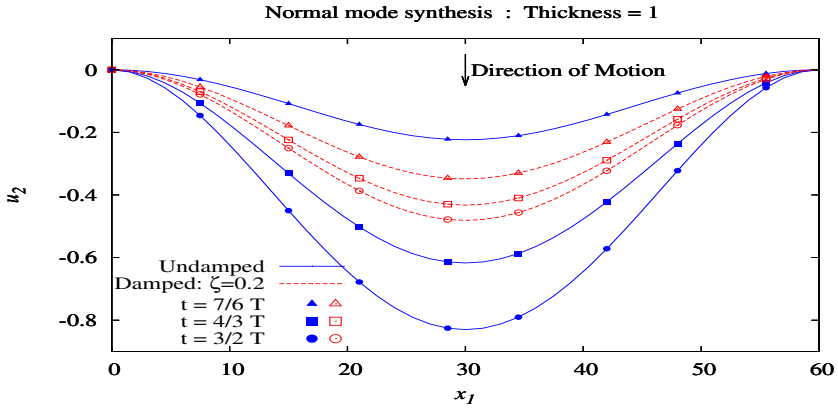

(c) Displacement u_2 versus x_1 for the third one-third of the time period

Figure 5.9: Displacement u_2 of the centerline versus x_1 for undamped vs. damped beam with $\zeta = 0.2$ using normal mode synthesis; number of modes used: 1 to 3. Time period of undamped beam T = 3499.07

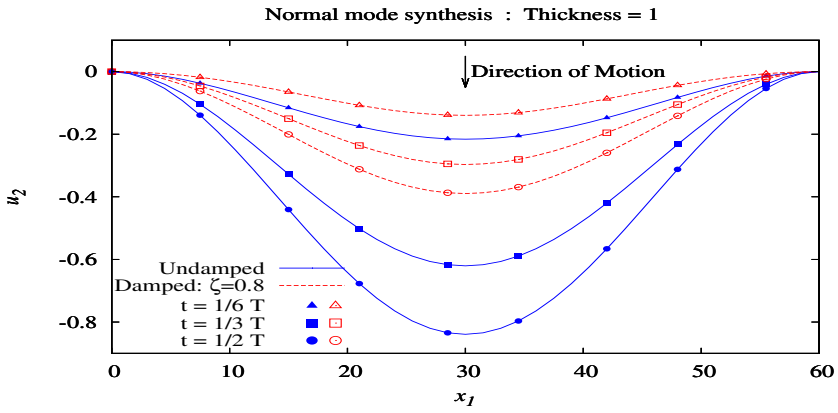

(a) Displacement u_2 versus x_1 for the first one-third of the time period

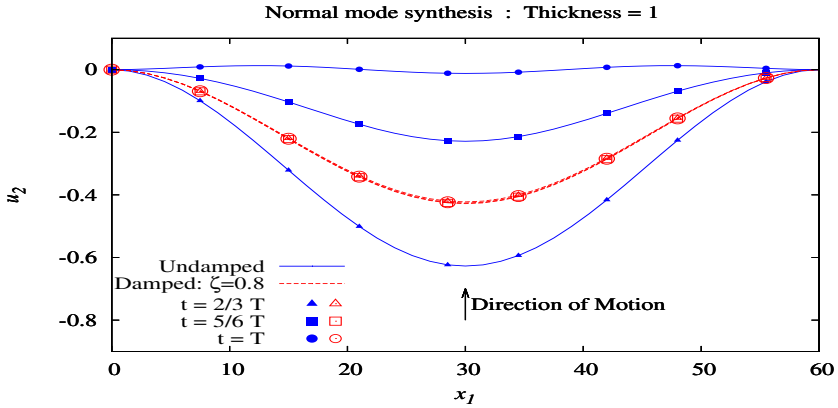

(b) Displacement u_2 versus x_1 for the second one-third of the time period

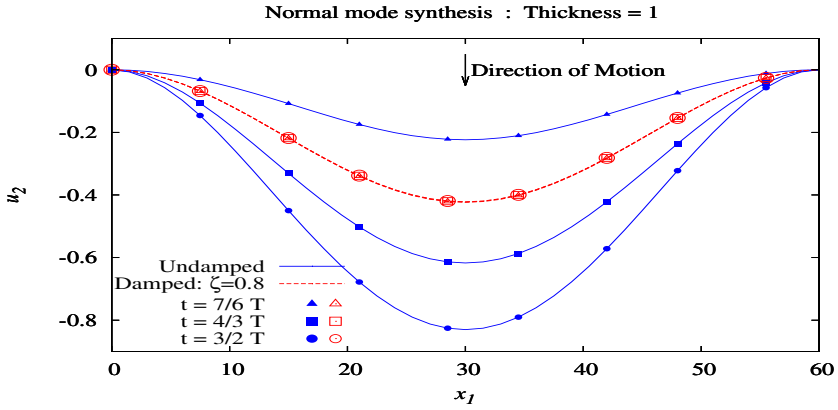

(c) Displacement u_2 versus x_1 for the third one-third of the time period

Figure 5.10: Displacement u_2 of the centerline versus x_1 for undamped vs. damped beam with $\zeta = 0.8$ using normal mode synthesis; number of modes used: 1 to 3. Time period of undamped beam T = 3499.07

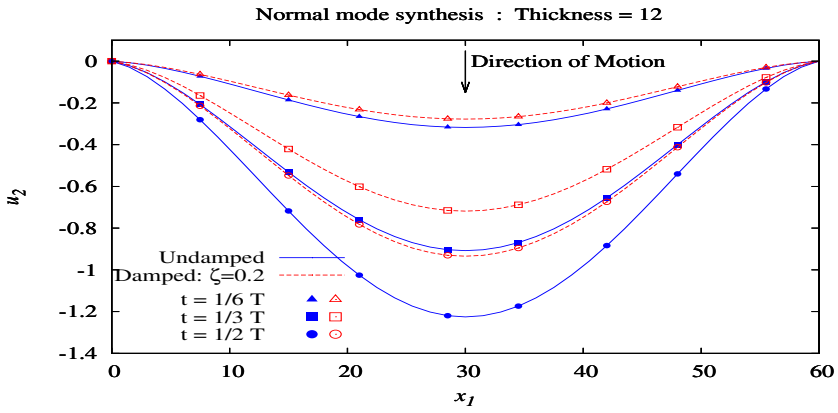

(a) Displacement u_2 versus x_1 for the first one-third of the time period

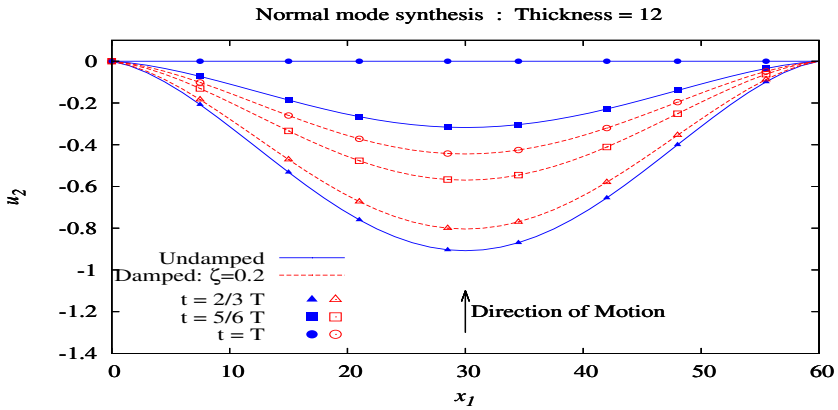

(b) Displacement u_2 versus x_1 for the second one-third of the time period

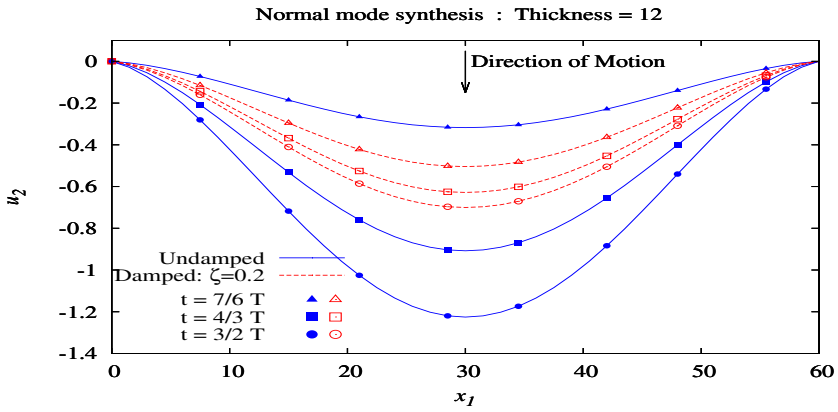

(c) Displacement u_2 versus x_1 for the third one-third of the time period

Figure 5.11: Displacement u_2 of the centerline versus x_1 for undamped vs. damped beam with $\zeta = 0.2$ using normal mode synthesis; number of modes used: 1 to 3. Time period of undamped beam T = 359.56

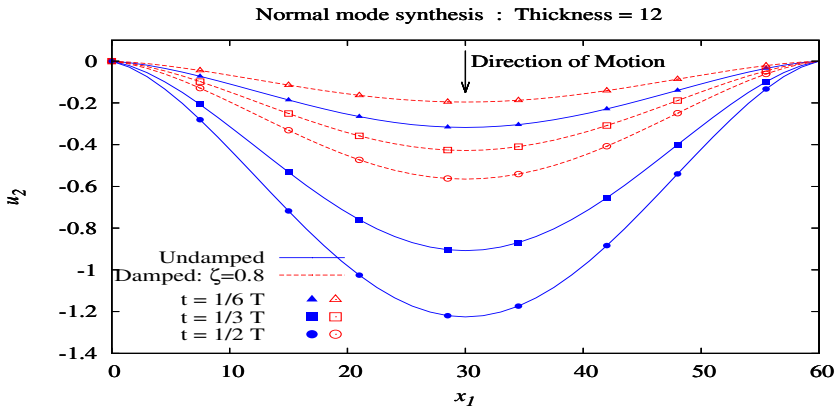

(a) Displacement u_2 versus x_1 for the first one-third of the time period

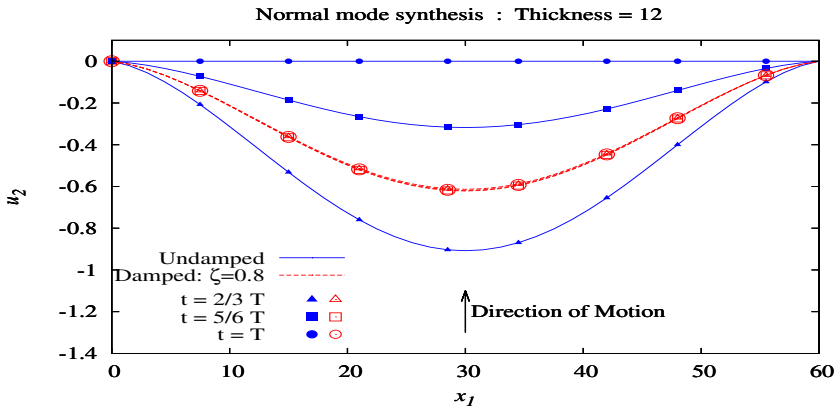

(b) Displacement u_2 versus x_1 for the second one-third of the time period

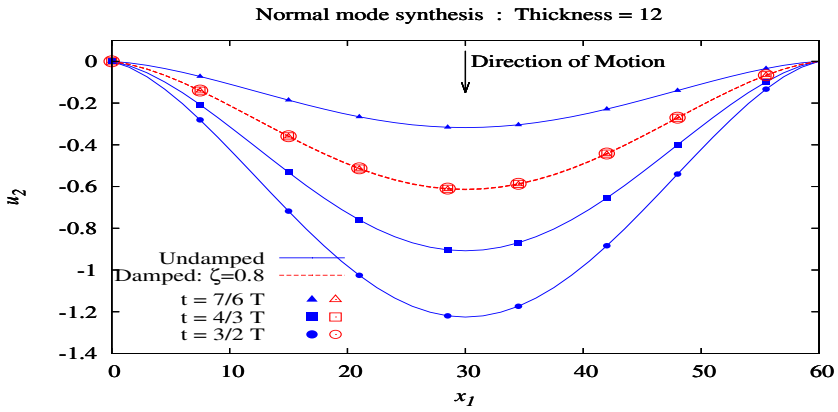

(c) Displacement u_2 versus x_1 for the third one-third of the time period

Figure 5.12: Displacement u_2 of the centerline versus x_1 for undamped vs. damped beam with $\zeta = 0.8$ using normal mode synthesis; number of modes used: 1 to 3. Time period of undamped beam T = 359.56

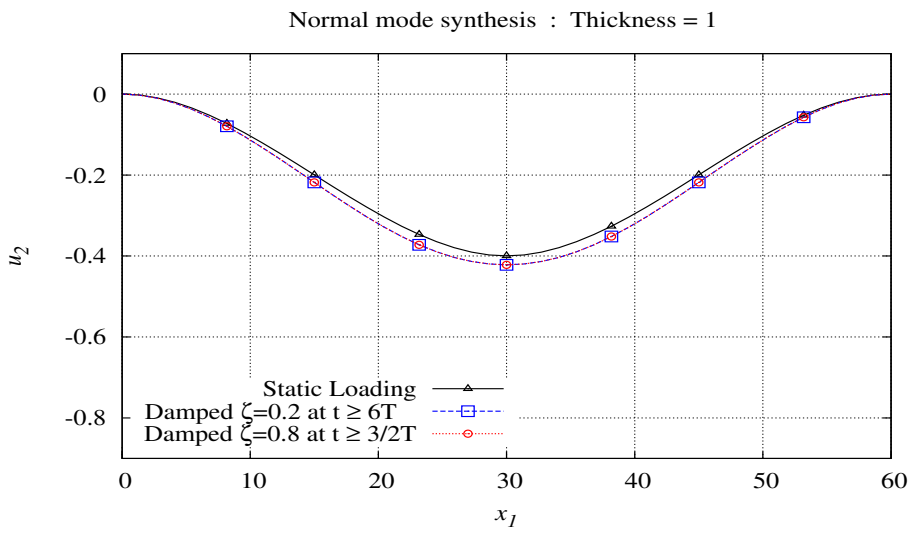

(a) Displacement u_2 versus x_1 for the slender beam. Time period of the undamped beam T = 3499.07

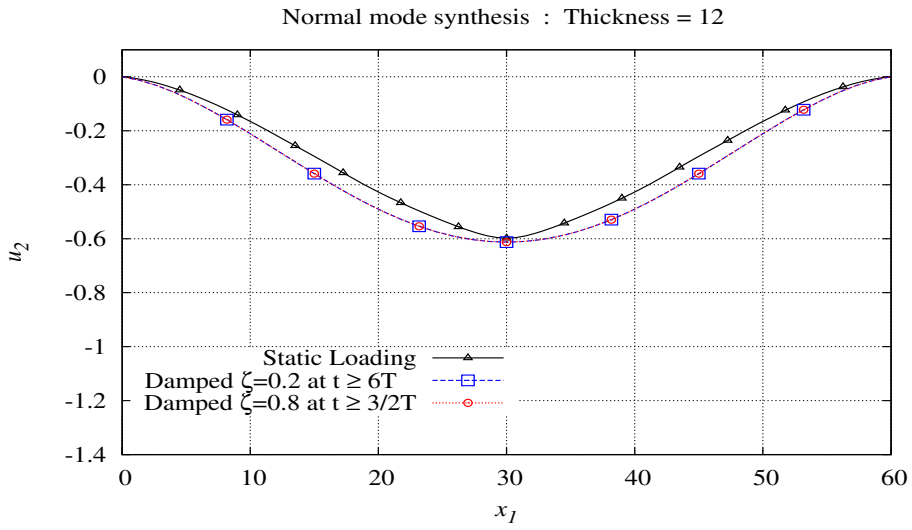

(b) Displacement u_2 versus x_1 for the deep beam. Time period of the undamped beam T = 359.56

Figure 5.13: Displacement u_2 of the centerline versus x_1 for static loading vs. damped beam with $\zeta = 0.2$ and $\zeta = 0.8$ after reaching steady state, using normal mode synthesis; number of modes used: 1 to 3.

(v) The difference between the steady state deflection profile and the static load deflection profile is because the damping matrix is altered when we make the assumption that it is proportional

to the mass and stiffness matrix (Rayleigh damping).

5.2.3 Wilson's θ method

The time response is also calculated using Wilson's θ method with linear acceleration for undamped as well as damped cases. Time response is calculated using $\underset{\sim}{\mu} = 100\mu$ and $\underset{\sim}{\lambda} = 100\lambda$ as the values of the material coefficients. Time increment of $\Delta t = {}^{T}/_{100}$ was chosen with $\theta = 1.4$ [9], T being the time period of the undamped beam.

Figures 5.14 – 5.15 show plots of displacement u_2 vs x_1 of the centerline of the beam for undamped and damped cases, for both slender and deep beams, for time t corresponding to one and a half cycles of the undamped beam. $C = 100$ is the factor by which μ and λ are multiplied by to get $\underset{\sim}{\mu}$ and $\underset{\sim}{\lambda}$, respectively.

Remarks made for mode superposition technique for time response hold precisely here as well for the calculated time response. Except, the value of the steady state deflection profile calculated using Wilson's θ method is same as that of the static loading case. This is shown in figure 5.16(a) for slender beam and 5.16(b) for deep beam.

5.3 Summary

In the following we present a brief summary of the work presented in this chapter.

(1) For all four formulations (EBBT, EBBT/NCCM, TBT, and new formulation), the plots of displacement u_2 versus x_1 of the centerline of the beam for slender beam yield almost identical results. As the depth of the beam increases ($h = 5$" and $h = 8$"), TBT yields higher shear deformation than EBBT and EBBT/NCCM. The converged solutions of the new formulation shows larger deviation of u_2 versus x_1 than the TBT since the solutions are of the same accuracy as the theoretical solutions.

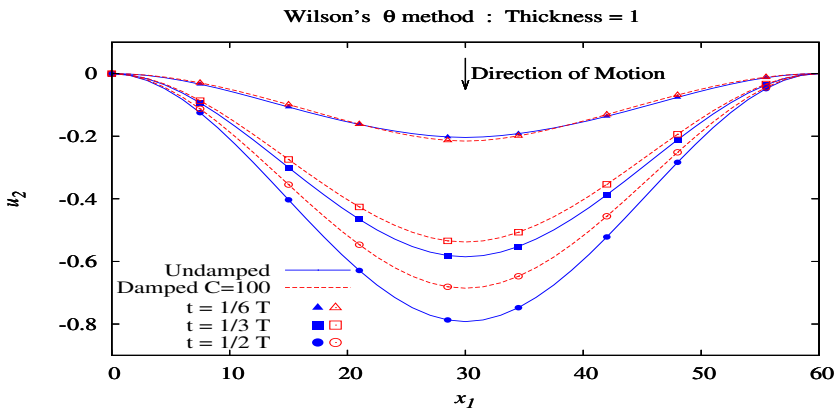

(a) Displacement u_2 versus x_1 for the first one-third of the time period

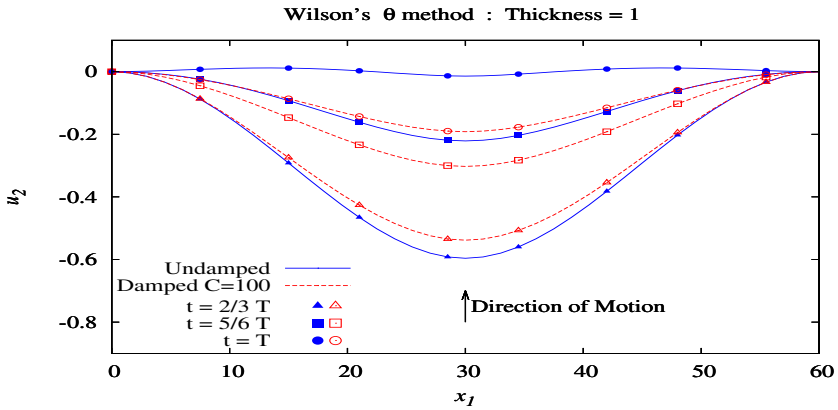

(b) Displacement u_2 versus x_1 for the second one-third of the time period

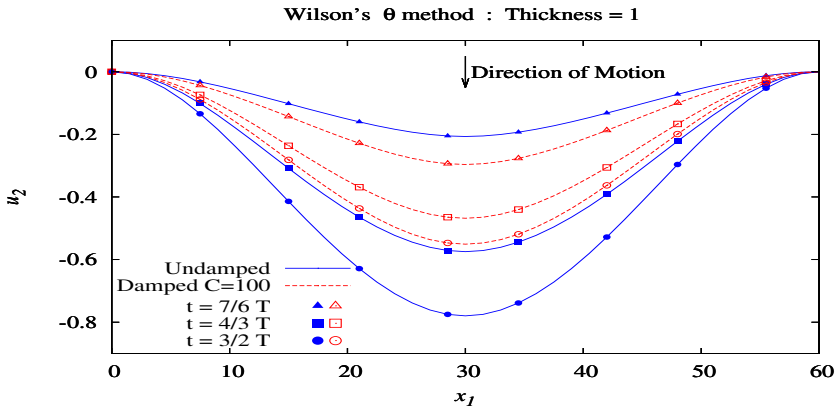

(c) Displacement u_2 versus x_1 for the third one-third of the time period

Figure 5.14: Displacement u_2 of the centerline versus x_1 for undamped vs. damped beam with $C = 100$ using Wilson's θ method. Time period of undamped beam T = 3499.07

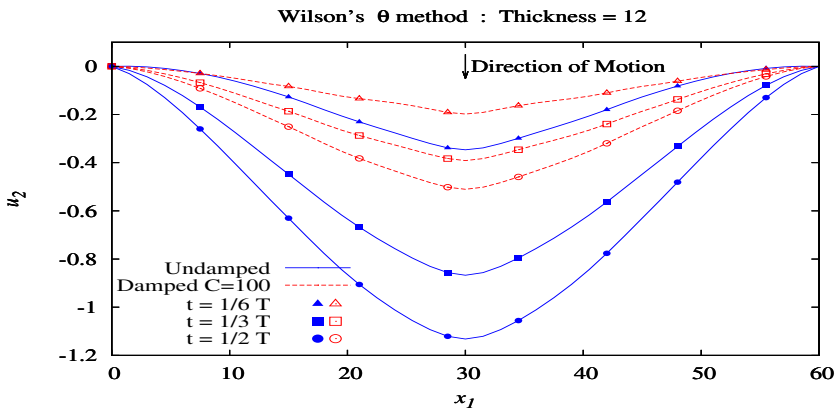

(a) Displacement u_2 versus x_1 for the first one-third of the time period

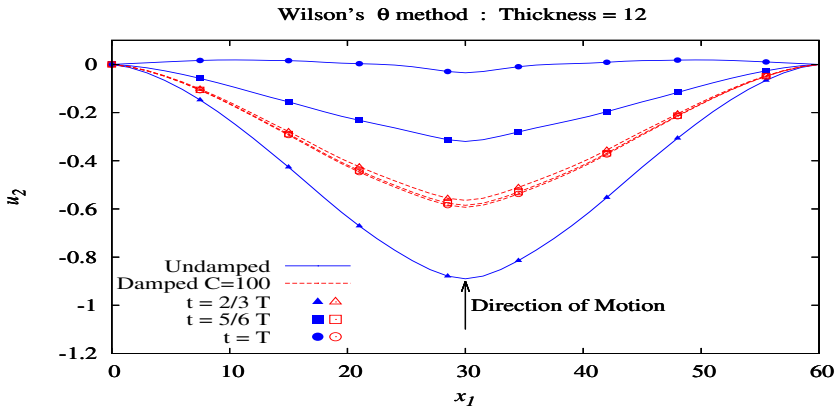

(b) Displacement u_2 versus x_1 for the second one-third of the time period

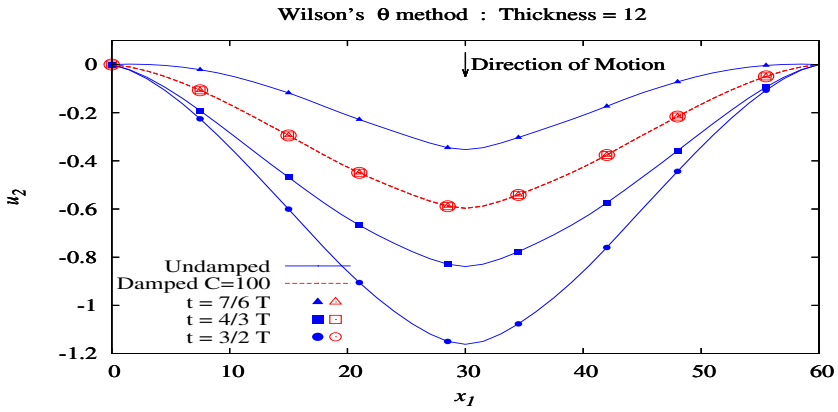

(c) Displacement u_2 versus x_1 for the third one-third of the time period

Figure 5.15: Displacement u_2 of the centerline versus x_1 for undamped vs. damped beam with $C = 100$ using Wilson's θ method. Time period of undamped beam T = 359.56

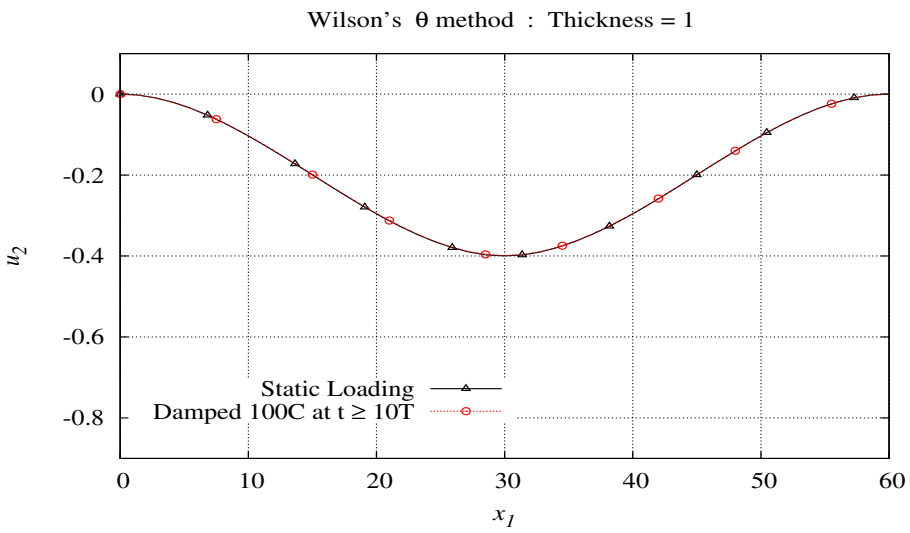

(a) Displacement u_2 versus x_1 for the slender beam. Time period of the undamped beam T = 3499.07

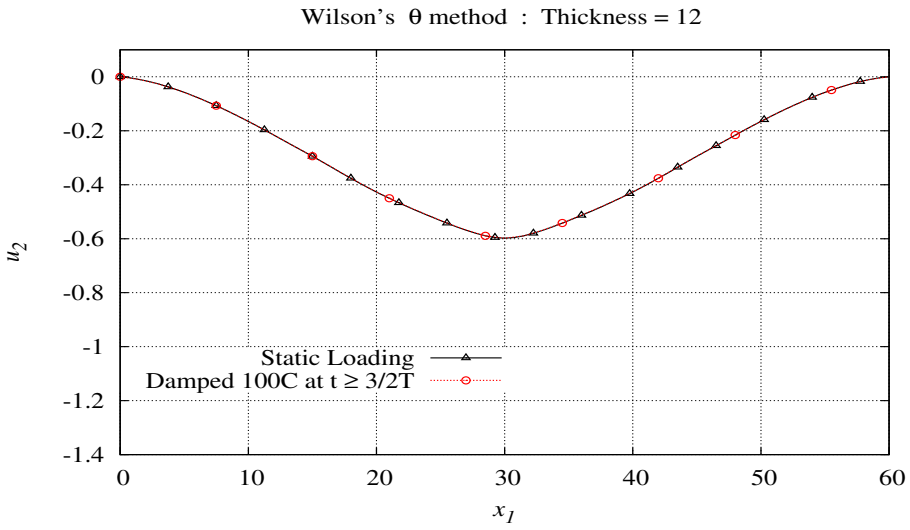

(b) Displacement u_2 versus x_1 for the deep beam. Time period of the undamped beam T = 359.56

Figure 5.16: Displacement u_2 of the centerline versus x_1 for static loading vs. damped beam with $100C$ after reaching steady state, using Wilson's θ method.

(2) The plots of axial displacement u_1 versus x_2 at $x_1 = 6.0$" for slender beams shows that the cross section remains plane after deformation for all four formulations. As the depth of

the beam increases ($h = 5$" and $h = 8$"), the converged solutions of the new formulation shows that the cross-section does not remain plane. This is because the deformation of the cross-section is not assumed a priori as done in currently used beam theories (EBBT and TBT). While the cross-section of the other three mathematical models (EBBT, TBT, and EBBT/TBT) all remain plane even for deeper beams, and also yield almost identical results.

(3) The plots of axial stress σ_{11} versus x_2 at $x_1 = 6.0$" for slender beams yield identical results for all four formulations, if we consider the converged solution for the new formulation. As the depth of the beam increases ($h = 5$" and $h = 8$"), the axial stress shows non-linear behavior across the beam cross-section for the converged solution of the new formulation because the cross-section is does not remain plane. While the axial stress of the other three mathematical models (EBBT, TBT, and EBBT/TBT) show linear behavior along x_2 even for deeper beams, and also yield almost identical results.

(4) The plots of transverse shear stress versus x_2 at $x_1 = 6.0$" shows that for EBBT the shear stress is zero (${}_s\sigma_{12} = 0$ and ${}_a\sigma_{12}$ does not exist) for both slender and deep beams. Both TBT and EBBT/NCCM yield the same magnitude (a constant value across the cross-section) and direction of shear stress. For EBBT/NCCM the shear stress due to ${}_s\sigma_{12}$ is zero and thus the non-zero shear stress is only due to ${}_a\sigma_{12}$. The shear stress from the converged solutions of the new formulation is perfectly quadratic along the beam cross-section for both the slender and deep beams.

(5) For all the six modes,the calculated value and the theoretical value of the natural frequency agree closely for the slender beam. For the deep beam, the calculated natural frequency is lower than the theoretical value for all the six modes. This is due to the fact that stiffness in the new formulation is lower compared to EBBT for the same mass.

(6) The undamped beam shows the largest maximum deflection or amplitude (displacement u_2 of the beam centerline at the midspan). For undamped beam this deformation cycle is repeated without amplitude decay as time elapses.

(7) Time response of damped beam shows progressive amplitude decay as cycle repeats. As expected, we observe more pronounced amplitude decay with a faster rate for higher value of damping ratios.

(8) For large value of time the undamped beam would continue to oscillate without any amplitude decay due to the fact that in this case there is no energy dissipation mechanism. Where as in case of damped response beyond a certain time the beam reaches stationary state

(9) Irrespective of the value of the damping coefficient, the steady state deflection profile is the same. For the time response calculated using normal mode synthesis, the value of this steady state deflection profile is slightly larger than that of the static loading case. But for the time response calculated using Wilson's θ method, the value of the steady state deflection profile is same as that of the static loading case.

(10) The difference between the steady state deflection profile and the static load deflection profile for the time response calculated using normal mode synthesis is because the damping matrix is altered when we make the assumption that it is proportional to the mass and stiffness matrix (Rayleigh damping).

Chapter 6

Summary and Conclusions

The mathematical models for the currently used EBBT and TBT have been used as representative mathematical models for the currently used beam theories to investigate their thermodynamic consistency based on conservation and the balance laws of classical or non-classical continuum mechanics. The EBBT utilizes internal rotation due to displacement gradient tensor in the kinematic assumption while the TBT uses Cosserat rotation in the kinematic assumption, but the derivation of the mathematical model requires both internal and Cosserat rotations. Use of internal and/or Cosserat rotations in the kinematic assumption is typical of all beam theories. Thus, the findings and conclusions reported here for EBBT and TBT hold for all beam theories used presently.

It is shown that the mathematical models for EBBT and TBT derived (for IVPs as well as BVPs) using energy functional or principle of virtual work cannot be derived using the conservation and the balance laws of classical continuum mechanics or non-classical continuum mechanics based on internal rotations or internal and Cosserat rotations. Thus, based on the fact that EBBT and TBT contain features of all currently used beam models, we conclude that all currently used beam mathematical models are thermodynamically inconsistent i.e. the deformation resulting from the solutions of these mathematical models violates thermodynamic equilibrium based on classical as well as non-classical continuum mechanics.

We have shown that using the kinematic assumption of EBBT it is possible to derive a thermo-

dynamically consistent mathematical model using NCCM based on internal rotations. When this mathematical model (balance of linear momenta) is cast purely in terms of displacements u_1 and u_2 only for BVPs, it is exactly same as EBBT mathematical model for BVPs except that in case of EBBT ${}_s\sigma_{12} = 0$ and ${}_a\sigma_{12}$ does not exist, but in case of EBBT/NCCM ${}_s\sigma_{12} = 0$ and ${}_a\sigma_{12} \neq 0$. Thus, the solutions obtained using EBBT and EBBT/NCCM for BVPs will be same in all aspects except the transverse shear. We have shown that the meanings of the individual terms in the balance of linear momenta in EBBT/NCCM mathematical model are consistent with balance laws. We clearly see that currently used EBBT model for IVPs is completely different from the model derived here using NCCM with internal rotations.

Since the currently used beam models are derived using energy functional or principle of virtual work, only reversible processes can be described using this approach. Inclusion of dissipation and memory in these models is only possible using phenomenological approach in $\mathbb{R}^1$ without energy equation and entropy inequality. This approach cannot be extended to $\mathbb{R}^2$ and $\mathbb{R}^3$. It is shown that due to the presence of internal rotations arising from the displacement gradients and/or the Cosserat rotation in the kinematic assumption used in all beam theories, the currently used mathematical models with these kinematic assumptions cannot be derived using classical continuum mechanics or the non-classical continuum mechanics.

A new formulation to study bending of beams in $\mathbb{R}^2$ using conservation and balance laws of classical continuum mechanics and construction of beam finite element formulation using hpk framework with variationally consistent integral form is presented. In this approach the mathematical model consist of true conservation and balance laws and the choice of local approximations for the beam finite elements facilitates incorporation of desired kinematic behavior. This approach is free of the a priori assumptions of kinematic relations, computations are unconditionally stable, local approximations can be higher degree (p) and higher order (k). This approach addresses slender as well as deep beam physics and provides true measure of error through residual functional based on the calculated solutions for the model problems. The generality and versatility of this approach permits consideration of beam bending behavior based on classical continuum mechanics balance

laws with assurance of thermodynamic consistency of the solutions and permitting greater flexibility in describing the deformation physics. This approach permits consideration of reversible as well as irreversible deformation physics. We have shown that damping and rheology mechanisms consistent with energy equation and entropy inequality can be derived.

Beam formulation in chapter 2 has been extended in chapter 3 to include mechanism of damping. Complete derivation of the mathematical model based on conservation and balance laws of CCM is presented in chapter 3.

In chapter 4, the formulation of chapter 3 has been extended to include fading memory mechanism. The mechanism of damping in chapter 3 and 4 is based on ordered rate theory. The memory mechanism in the formulation in chapter 4 is also based on ordered rate theory.

Model problem studies are presented in chapter 5 for bending of thermoelastic and thermoviscoelastic beams without memory (dissipation).

Bibliography

[1] Ballarini, R. (April 18, 2003). The Da Vinci-Euler-Bernoulli Beam Theory? *(https://web.archive.org/web/20060623063248/http://www.memagazine.org/contents/current/webonly/webex418.html). Mechanical Engineering Magazine Online.* , Archived from the original (http://www.memagazine.org/contents/current/webonly/webex418.html), on July 23, 2006. Retrieved 2006-07-22.

[2] Witmer, E. A. Elementary bernoulli-euler beam theory. *MIT Unified Engineering Course Notes*, pages 5–114 to 5–164, 1991-1992.

[3] Caresta, M. Vibrations of a free-free beam. *(https://www.colorado.edu/physics/phys1240/phys1240_fa15/homelabs/Beam_vibration_Mauro%20Caresta_UNSW/.pdf) (PDF)*, Retrieved 2016-08-01.

[4] Han, S. M. Benaroya, H. and Wei, T. (March 22, 1999). Dynamics of Transversely Vibrating Beams using four Engineering Theories. *(https://web.archive.org/web/20060623063248/http://www.memagazine.org/contents/current/webonly/webex418.html) (PDF). final version. Academic Press.* , Retrieved 2006-04-15.

[5] Timoshenko, S. P. *History of strength of materials*. McGraw-Hill New York, 1953.

[6] Truesdell, C. A. *The rational mechanics of flexible or elastic bodies 1638-1788, Introduction to Vol. X and XI*. Venditioni Exponunt Orell Fussli Turici, 1960.

[7] Gelfand, I.M. and Fomin, S.V. *Calculus of variations*. Dover Publications Inc New York, 2000.

[8] Surana, K. S. and Reddy, J. N. *The Finite Element Method for Boundary Value Problems: Mathematics and Computations*. CRC/Taylor and Francis, 2017.

[9] Surana, K. S. and Reddy, J. N. *The Finite Element Method for Initial Value Problems*. CRC/Taylor and Francis, 2017.

[10] Reddy, J. N. *An Introduction to the Finite Element Method*. 3rd ed., McGraw-Hill, New York, 2006.

[11] Levinson, M. A new rectangular beam theory. *Journal of Sound and Vibration*, 74(1):81–87, 01 1981.

[12] Reddy, J. N. A simple higher-order theory for laminated composite plates. *Journal of Applied Mechanics, Transactions ASME*, 51(4):745–752, 12 1984.

[13] Heyliger, P.R. and Reddy, J.N. A higher-order beam finite element for bending and vibration problem. *Journal of Sound and Vibration*, 126(2):309–326, 10 1988.

[14] Hutchinson, J. R. Shear coefficients for timoshenko beam theory. *Journal of Applied Mechanics*, 68(1):87–98, 01 2001.

[15] Reddy, J. N. Nonlocal Theories for Bending, Buckling and Vibration of Beams. *International Journal of Engineering Science*, 45(2-8):288–307, 2007.

[16] Reddy, J. N. and Pang, S. D. Nonlocal continuum theories of beams for the analysis of carbon nanotubes. *Journal of Applied Physics*, 103(2):023511–1 to 023511–16, 02 2008.

[17] Reddy, J. N. and Arbind, A. Bending relationship between the modified couple stress-based functionally graded timoshenko beams and homogeneous bernoulli-euler beams. *Ann. Solid Struc. Mech.*, 3:15–26, 2012.

[18] Ma, H.M. and Gao, X-L and Reddy, J.N. A microstructure-dependent Timoshenko beam model based on a modified couple stress theory. *Journal of the Mechanics and Physics of Solids*, 56(12):3379–3391, 2008.

[19] Ma, H.M. and Gao, Xin-Lin and Reddy, J.N. A nonclassical Reddy-Levinson beam model based on a modified couple stress theory. *International Journal for Multiscale Computational Engineering*, 8(2):167–180, 2010.

[20] Reddy, J. N. Nonlocal nonlinear formulations for bending of classical and shear deformation theories of beams and plates. *International Journal of Engineering Science*, 48(11):1507–1518, 11 2010.

[21] Reddy, J.N. Microstructure-dependent couple stress theories of functionally graded beams. *Journal of the Mechanics and Physics of Solids*, 59(11):2382–2399, 2011.

[22] Del Piero, G. A rational approach to cosserat continua, with application to plate and beam theories. *Mechanics Research Communications*, 58:97–104, 2014.

[23] Hjelmstad, K. D. . *Fundamentals of structural mechanics*. Upper Saddle River, N.J. : Prentice Hall, 1997.

[24] Surana, K.S. *Advanced Mechanics of Continua*. CRC/Taylor and Francis, Boca Raton, FL, 2015.

[25] Surana, K. S. and Nunez D. and Reddy, J. N. and Romkes, A. Rate Constitutive Theory for Ordered Thermoelastic Solids. *Annals of Solid and Structural Mechanics*, 3:27–54, 2012.

[26] Surana, K. S. and Moody, T. C. and Reddy, J. N. Ordered Rate Constitutive Theories in Lagrangian Description for Thermoviscoelastic Solids without Memory. *Acta Mechanica*, 224(11):2785–2816, 2013.

[27] Surana, K. S., Reddy J. N. and Nunez, D. Ordered Rate Constitutive Theories for Thermoviscoelastic Solids without Memory in Lagrangian Description using Gibbs Potential. *Continuum Mechanics and Thermodynamics*, 27(3):409–431, 2014.

[28] Bird, R. B. and Armstrong, R. C. and Hassager, O. *Dynamics of Polymeric Liquids, Volume 1, Fluid Mechanics, Second Edition*. John Wiley and Sons, 1987.

[29] Surana, K. S. and Moody, T. C. and Reddy, J. N. Ordered Rate Constitutive Theories in Lagrangian Description for Thermoviscoelastic Solids with Memory. *Acta Mechanica*, 226(1):157–178, 2014.

[30] Surana, K. S. and Powell, M. J. and Reddy, J. N. A More Complete Thermodynamic Framework for Solid Continua. *Journal of Thermal Engineering*, 1(1):1–13, 2015.

[31] Surana, K. S. and Reddy, J. N. and Nunez, D. and Powell, M. J. A Polar Continuum Theory for Solid Continua. *International Journal of Engineering Research and Industrial Applications*, 8(2):77–106, 2015.

[32] Surana, K. S. and Powell, M. J. and Reddy, J. N. A More Complete Thermodynamic Framework for Fluent Continua. *Journal of Thermal Engineering*, 1(1):14–30, 2015.

[33] Surana, K. S. and Powell, M. J. and Reddy, J. N. A Polar Continuum Theory for Fluent Continua. *International Journal of Engineering Research and Industrial Applications*, 8(2):107–146, 2015.

[34] Surana, K. S. and Powell, M. J. and Reddy, J. N. Constitutive Theories for Internal Polar Thermoelastic Solid Continua. *Journal of Pure and Applied Mathematics: Advances and Applications*, 14(2):89–150, 2015.

[35] Surana, K. S. and Powell, M. J. and Reddy, J. N. Ordered Rate Constitutive Theories for Internal Polar Thermofluids. *International Journal of Mathematics, Science, and Engineering Applications*, 9(3):51–116, 2015.

[36] Surana, K. S. and Mohammadi, F. and Reddy, J. N. and Dalkilic A. S. Ordered Rate Constitutive Theories for Non-Classical Internal Polar Without Memory. *International Journal of Mathematics, Science, and Engineering Applications (IJMSEA)*, 10(2):99–131, 8 2016.

[37] Surana, K. S. and Joy, A. D. and Reddy, J. N. A finite deformation, finite strain non-classical internal polar continuum theory for solids. *Mechanics of Advanced Materials and Structures*, (published online), 2017.

[38] Surana, K. S. and Joy, A. D. and Reddy, J. N. A non-classical internal polar continuum theory for finite deformation and finite strain in solids. *International Journal of Pure and Applied Mathematics*, 4:59–97, 2016.

[39] Surana, K. S. and Joy, A. D. and Reddy, J. N. A non-classical internal polar continuum theory for finite deformation of solids using first Piola-Kirchhoff stress tensor. *Journal of Pure and Applied Mathematics: Advances and Applications*, 16(1):1–41, 2016.

[40] Surana, K. S. and Long, S. W. and Reddy, J. N. Rate Constitutive Theories of Orders n and ${}^1n$ for Internal Polar Non-Classical Thermofluids without Memory. *Applied Mathematics,*, 7(16):2033–2077, 2016.

[41] Surana, K. S. and Joy, A. D. and Reddy, J. N. A non-classical continuum theory for fluids incorporating internal and cosserat rotation rates. *Continuum Mechanics and Thermodynamics*, 29:1249–1289, 2017.

[42] Surana, K. S. and Joy, A. D. and Reddy, J. N. A non-classical continuum theory for solids incorporating internal rotations and rotations of cosserat theories. *Continuum Mechanics and Thermodynamics*, 29:665–698, 2017.

[43] Surana, K. S. and Joy, A. D. and Reddy, J. N. Ordered rate constitutive theories for non-classical thermoviscoelastic solids with memory incorporating internal and cosserat rotations. *Continuum Mechanics and Thermodynamics*, (in press) DOI: https://doi.org/10.1007/s00161-018-0697-8, July 2018.

[44] Surana, K. S. and Joy, A. D. and Reddy, J. N. Non-classical continuum theory and the constitutive theories for thermoviscoelastic solids without memory incorporating internal and cosserat rotations. *Acta Mechanica*, (in print), 2018.

[45] Surana, K. S. and Joy, A. D. and Reddy, J. N. Ordered rate constitutive theories for non-classical thermoviscoelastic fluids incorporating internal and cosserat rotation rates. *Internal Journal of Applied Mechanics*, (in print), 2018.

[46] Voigt, W. Theoretische Studien über die Wissenschaften zu Elastizitätsverhältnisse der Krystalle. *Abhandl. Ges. Göttingen*, 34, 1887.

[47] Voigt, W. Über Medien ohne innere Kräfte und eine durch sie gelieferte mechanische Deutung der Maxwell-Hertzschen Gleichungen. *Göttingen Abhandl.*, pages 72–79, 1894.

[48] Cosserat, E. and Cosserat, F. *Théorie des Corps Déformables*. Hermann, Paris, 1909.

[49] Günther, W. Zur Statik und Kinematik des Cosseratschen Kontinuums. *Abhandl. Braunschweig. Wiss. Ges.*, 10:195–213, 1958.

[50] Grioli, G. Elasticità Asimmetrica. *Annali di Matematica Pura ed Applicata*, 50(1):389–417, 1960.

[51] Aero, E. L. and Kuvshinskii, E. V. Fundamental Equations of the Theory of Elastic Media with Rotationally Interacting Particles. *Soviet Physics, Solid State*, 2:1272–1281, 1961.

[52] Schäfer, H. Versuch einer Elastizitätstheorie des Zweidimensionalen Ebenen Cosserat-Kontinuums. *Miszellaneen der Angewandten Mechanik*, pages 277–292, 1962.

[53] Truesdell, C. A. and Toupin, R. A. The Classical Field Theories of Mechanics. In S. Flügge, editor, *Handbuch der Physik*, volume 3. Springer-Verlag, Berlin, 1960.

[54] Mindlin, R. D. and Tiersten, H. F. Effects of Couple-stresses in Linear Elasticity. *Archive for Rational Mechanics and Analysis*, 11(1):415–448, 1962.

[55] Toupin, R. A. Elastic Materials with Couple-stresses. *Archive for Rational Mechanics and Analysis*, 11(1):385–414, 1962.

[56] Koiter, W. T. Couple Stresses in the Theory of Elasticity, I and II. *Proceedings Series B, Koninklijke Nederlandse Akademie van Wetenschappen*, 67:17–44, 1964.

[57] Eringen, A. C. *Nonlinear Theory of Continuous Media*. McGraw-Hill, 1962.

[58] Eringen, A. C. and Suhubi, E. S. Nonlinear Theory of Simple Micro-Elastic Solids – I. *International Journal of Engineering Science*, 2(2):189–203, 1964.

[59] Eringen, A. C. and Suhubi, E. S. Nonlinear Theory of Simple Micro-Elastic Solids – II. *International Journal of Engineering Science*, 2(2):389–404, 1964.

[60] Eringen, A. C. Simple Microfluids. *International Journal of Engineering Science*, 2(2):205–217, 1964.

[61] Eringen, A. C. Mechanics of Micromorphic Materials. *H. Gortler (ed.) Proc. 11th Intern. Congress. Appl. Mech.*, pages 131–138, 1964a.

[62] Mindlin, R. D. Micro-Structure in Linear Elasticity. *Archive for Rational Mechanics and Analysis*, 16:51–78, 1964.

[63] Green, A.E. and Rivlin, R.S. Multipolar continuum mechanics. *Archive for Rational Mechanics and Analysis*, 17(2):113–147, 1964.

[64] Mindlin, R. D. Stress Functions for a Cosserat Continuum. *International Journal of Solids and Structures*, 1:265–271, 1965.

[65] Brand, M. and Rubin, M. B. A Constrained Theory of a Cosserat Point for the Numerical Solution of Dynamic Problems of Non-Linear Elastic Rods with Rigid Cross-Sections. *International Journal of Non-Linear Mechanics*, 42:216–232, 2007.

[66] Cao, D. Q. and Tucker, R. W. Nonlinear Dynamics of Elastic Rods using the Cosserat Theory: Modelling and Simulation. *International Journal of Solids and Structures*, 45:460–477, 2008.

[67] Riahi, A. and Curran, J. H. Full 3D Finite Element Cosserat Formulation with Application in Layered Structures. *Applied Mathematical Modelling*, 33:3450–3464, 2009.

[68] Sansour, C. A Unified Concept of Elastic Viscoplastic Cosserat and Micromorphic Continua. *J. Phys. IV France*, 8:341–348, 1998.

[69] Sansour, C. and Skatulla, S. A Strain Gradient Generalized Continuum Approach for Modelling Elastic Scale Effects. *Computer Methods in Applied Mechanics and Engineering*, 198:1401–1412, 2009.

[70] Sansour, C. and Skatulla, S. and Zbib, H. A Formulation for the Micromorphic Continuum at Finite Inelastic Strains. *International Journal of Solids and Structures*, 47:1546–1554, 2010.

[71] Varygina, M. P. and Sadovskaya, O. V. and Sadovskii, V. M. Resonant Properties of Moment Cosserat Continuum. *Journal of Applied Mechanics and Technical Physics*, 51(3):405–413, 2010.

[72] Nikabadze, M. U. Relation Between the Stress and Couple-Stress Tensors in the Microcontinuum Theory of Elasticity. *Moscow University Mechanics Bulletin*, 66(6):141–143, 2011.

[73] Ieşan, D. Deformation of Porous Cosserat Elastic Bars. *International Journal of Solids and Structures*, 48:573–583, 2011.

[74] Jung, P. and Leyendecker, S. and Linn, J. and Ortiz, M. A Discrete Mechanics Approach to the Cosserat Rod Theory – Part 1: Static Equilibria. *International Journal for Numerical Methods in Engineering*, 85:31–60, 2010.

[75] Alonso-Marroquín, F. Static Equations of the Cosserat Continuum Derived from Intra-Granular Stresses. *Granular Matter*, 13:189–196, 2011.

[76] Chiriţă, S. and Ghiba, I. D. Rayleigh Waves in Cosserat Elastic Materials. *International Journal of Engineering Science*, 54:117–127, 2012.

[77] Cao, D. Q. and Song, M. T. and Tucker, R. W. and Zhu, W. D. and Liu, D. S. and Huang, W. H. Dynamic Equations of Thermoelastic Cosserat Rods. *Communications in Nonlinear Science and Numerical Simulations*, 18:1880–1887, 2013.

[78] Addessi, D. and De Bellis, M. L. and Sacco, E. Micromechanical Analysis of Heterogeneous Materials Subjected to Overall Cosserat Strains. *Mechanics Research Communications*, 54:27–34, 2013.

[79] Cialdea, A. and Dolce, E. and Malaspina, A. and Nanni, V. On an Integral Equation of the First Kind Arising in the Theory of Cosserat. *International Journal of Mathematics*, 24(5), 2013.

[80] Skatull, S. and Sansour, C. A Formulation of a Cosserat-like Continuum with Multiple Scale Effects. *Computational Materials Science*, 67:113–122, 2013.

[81] Liu, Q. Hill's lemma for the average-field theory of cosserat continuum. *Acta Mechanica*, 224:851–866, 2013.

[82] Genovese, D. A two-director cosserat rod model using unconstrained quaternions. *European Journal of Mechanics A/Solids*, 43:44–57, 2014.

[83] Huang, W. and Sloan, S. W. and Sheng, D. Analysis of Plane Couette Shear Test of Granular Media in a Cosserat Continuum Approach. *Mechanics of Materials*, 69:106–115, 2014.

[84] Eringen, A. C. *Mechanics of Continua*. John Wiley and Sons, 1967.

[85] Yang, F.A.C.M. and Chong, A.C.M. and Lam, D.C.C. and Tong, P. Couple stress based strain gradient theory for elasticity. *International Journal of Solids and Structures*, 39(10):2731–2743, 2002.

[86] Surana, K. S. and Long, S. W. and Reddy, J. N. Necessity of law of balance/equilibrium of moment of moments in non-classical continuum theories for fluent continua. *Acta Mechanica*, 22(7):2801–2833, July 2018.

[87] Surana, K. S. and Shanbhag, R. S. and Reddy, J. N. Necessity of law of balance of moment of moments in non-classical continuum theories for solid continua. *Meccanica*, 53(11):2939–2972, September 2018.

[88] Surana, K. S. and Nguyen, S. H. Higher-order shear-deformable two-dimensional hierarchical beam elements for laminated composites. *Mathematical and Computer Modelling*, 14, DOI: https://doi.org/10.1016/0895-7177(90)90310-J:893–898, 1990.

[89] Surana, K. S. and Nguyen, S. H. p-version hierarchical two dimensional curved beam element for elastostatics. *Computers & Structures*, 37(6), DOI: https://doi.org/10.1016/0045-7949(90)90013-R:1013–1029, 1990.

[90] Surana, K. S. and Nguyen, S. H. Two-dimensional curved beam element with higher-order hierarchical transverse approximation for laminated composites. *Computers & Structures*, 36(3), DOI: https://doi.org/10.1016/0045-7949(90)90284-9:499 – 511, 1990.

[91] Surana, K. S. and Nguyen, S. H. Hierarchical three dimensional curved beam element based on p-version. *Computational Mechanics*, 7(4), DOI: https://doi.org/10.1007/BF00370042:289–298, 1991.

[92] Surana, K. S. and Nguyen, S. H. Completely hierarchical two-dimensional curved beam element for dynamics. *Computers & Structures*, 40(4), DOI: https://doi.org/10.1016/0045-7949(91)90326-H:957–967, 1991.

[93] Surana, K. S. and Nguyen, S. H. Three-dimensional curved beam element based on p-version for dynamics. *Computers & Structures*, 41(5), DOI: https://doi.org/10.1016/0045-7949(91)90281-P:887–895, 1991.

[94] Blevins, R.D. *Formulas for natural frequency and mode shape*. Van Nostrand Reinhold Company, New York, 1979.

[95] Blevins, R.D. *Formulas for Dynamics, Acoustics and Vibration*. John Wiley & Sons, 2015.